2020

Diverse Kappa Opioid Receptor Agonists: Relationships Between Signaling and Behavior

Amelia Dunn

DIVERSE KAPPA OPIOID RECEPTOR AGONISTS: RELATIONSHIPS BETWEEN SIGNALING AND BEHAVIOR

A Thesis Presented to the Faculty of

The Rockefeller University

in Partial Fulfillment of the Requirements for

the degree of Doctor of Philosophy

by

Amelia Dunn

June 2020

Diverse Kappa Opioid Receptor Agonists: Relationships Between Signaling and Behavior

Amelia Dunn, Ph.D.

The Rockefeller University 2020

The opioid system, comprised mainly of the three opioid receptors (kappa, mu and delta) and their endogenous neuropeptide ligands (dynorphin, endorphin and enkephalin, respectively), mediates mood and reward. Activation of the mu opioid receptor is associated with positive reward and euphoria, while activation of the kappa opioid receptor (KOR) has the opposite effect. Activation of the KOR causes a decrease in dopamine levels in reward-related regions of the brain, and can block the rewarding effects of various drugs of abuse, making it a potential drug target for addictive diseases. KOR agonists are of particular interest for the treatment of cocaine and other psychostimulant addictions, because there are currently no available medications for these diseases. Studies in humans and animals, however, have shown that activation of the KOR also causes negative side effects such as hallucinations, aversion and sedation.

Several strategies are currently being employed to develop KOR agonists that block the rewarding effects of drugs of abuse with fewer side effects, including KOR agonists with unique pharmacology. The goal of the research presented here was to profile the signaling pathways activated by KOR agonists and to investigate relationships between unique pharmacology and animal models of KOR-mediated behaviors, in order to better understand how to target the KOR for therapeutic use.

First, we quantified the effects of KOR agonists at both G-protein and β-arrestin-2 signaling pathways to compare to a variety of downstream effects, including sedation behavior.

We found that β-arrestin-2, but not G-protein, efficacy strongly correlated with sedation in mice. We found that there was no apparent relationship between either G-protein or β-arrestin-2 signaling pathways with other investigated downstream signaling pathways, such as ERK1/2 and mTOR, however. We also investigated the effects of KOR activation on protein-receptor interactions, to identify other potential mediators of KOR effects.

Finally, we compared the effects of several unique KOR agonists on addiction-related behaviors in mice. We found that nalfurafine, which is approved for human use in Japan, very potent KOR agonist, was able to modulate the rewarding effects of cocaine at very low doses that did not cause sedation or aversion. We also found that the commonly-used, full KOR agonist U50,488 had a similar effect, suggesting that this "therapeutic window" could be a property of the KOR system in general. Overall, this work suggests that KOR agonists at very low doses, that show very little β-arrestin-2 signaling activity, may be able to modulate the rewarding effects of cocaine while causing fewer negative side effects.

ACKNOWLEDGMENTS

First and foremost, I want to thank my advisor Dr. Mary Jeanne Kreek. Her science has helped so many people, and I feel incredibly lucky for the opportunity to learn from her and her example of both scientific rigor and passion for her work. I'm so grateful for the support and guidance I've received during my time here. Dr. Kreek – thank you for everything.

This work, of course, also belongs to many members of the Kreek lab. I'm forever grateful for the mentorship of Dr. Brian Reed, who was there for every single step of my PhD. Brian, I'll strive to follow your example of going where the data leads, while always keeping the bigger picture, and the people you're trying to help, in mind. Thank you for teaching me so much, and for the opportunity to contribute to this project. I'm lucky to have had so many wonderful mentors in the Kreek lab, including Drs. Yong Zhang and Eduardo Butelman. Eduardo, thank you for so many helpful suggestions and encouragement. Yong, thank you your many kind words and telling me to go home on the weekends.

I'm incredibly grateful to Dr. Kyle Windisch for being a mentor, friend, and role model. Thank you for showing me how to be a careful and critical scientist, as well as a thoughtful and generous lab citizen. And of course, for the endless hours teaching and helping with surgeries. Finally, I want to thank the students and research assistants that I've been lucky enough to work with over the years, in particular, Josh, Catherine, Ali, Jose, Ariel and Phil. Thank you for making the endless hours in the CBC and the GTPγS room not only bearable, but sometimes even fun. I'm so lucky to have been a part of Team Kappa with you.

I've received a great deal of support and mentoring from my thesis committee, Drs. Vanessa Ruta, Tom Sakmar and Brian Chait, as well. Your encouragement and thoughtful contributions to my project, both during and outside of my committee meetings, were incredibly helpful and

essential for this work. Thank you to the Sakmar lab in particular for crucial technical help early on in my project, as well as welcoming me into their scientific community. And of course, the Chait lab was where I started my Rockefeller career in 2012. I'm grateful to Brian, and entire Chait lab, both for that opportunity and for the continued help, guidance and collaboration in the years since. In particular, I'd like to thank Dr. Wenzhu Zhang for so much patient technical help preparing and running the mass spectrometry samples, and Dr. Paul Olinares for always lending a helpful hand and kind ear.

It has been such a privilege to be part of the Rockefeller community. I'm incredibly grateful to the Dean's Office – Sid Strickland, Emily Harms, Cris Rosario, Stephanie Fernandez, Kristen Cullen, Andrea Morris, Marta Delgado – for their support through the graduate program, and their commitment to providing opportunities for students to get involved in research. Participating in the SURF program started me on this path, and teaching for the Summer Neuroscience Program here has been a highlight of my grad school career. A huge thank you to my fellow SNP directors, and especially to all of the incredible high school students, who made the last two weeks of August the craziest and most fun time of the year.

Thank you to all of my friends that have made the past five years, the best five years. Your encouragement and support have meant the world to me, and you've made NYC home. And finally, I'm forever grateful for the endless support of my family and Ananth – I couldn't have done it without you.

TABLE OF CONTENTS

LIST OF FIGURES

LIST OF TABLES

LIST OF ABBREVIATIONS

GPCR (G-protein coupled receptor)

KOR (kappa opioid receptor)

MOR (mu opioid receptor)

DOR (delta opioid receptor)

MAPK (mitogen-activated protein kinase)

EFC (enzyme fragment complementation)

ERK1/2 (extracellular-related kinases 1 and 2)

mTOR (mammalian target of rapamycin)

Rps6 (ribosomal protein S6)

GAPDH (glyceraldehyde 3-phosphate dehydrogenase)

RAi (intrinsic relative activity)

LC-MS/MS (liquid chromatography with tandem mass spectrometry)

PEP (posterior error probability)

SILAC (stable isotope labeling by amino acids in cell culture)

GFP (green fluorescent protein)

ANOVA (analysis of variance)

CPP (conditioned place preference)

IVSA (intravenous self-administration)

norBNI (nor-Binaltorphimine)

BRET (bioluminescence resonance energy transfer)

FRET (fluorescence resonance energy transfer)

GRK2 (G-protein coupled receptor kinase 2)

CHAPTER 1. BACKGROUND AND GOALS

1.1 Opioid receptors mediate mood and reward, including addiction

With the rise of the "opiate epidemic" in recent years, addictions have come to the forefront of the national conversation on health. Research has led to better understanding of some factors that contribute to specific addictive diseases, leading to improved treatment options for some. Addiction to opiate drugs like heroin, that target the mu opioid receptor, can be treated effectively with medication-assisted therapy with drugs such as methadone and buprenorphine.[6] Fewer effective options are available for those addicted to alcohol, however, and there are currently no medication-assisted therapies for addiction to cocaine, methamphetamine and other psychostimulants, which affect over 1 million people in the United States alone.[1] Understanding more about the different systems in the brain and body that are involved in addictive diseases, such as the opioid system, can lead to better understanding of the disease, and better treatment options.

Humans have used drugs that target opioid receptors for centuries for medicinal, and later recreational, purposes, although the targets themselves weren't discovered until the 1970's. Scientists used the displacement of radiolabeled naloxone in homogenized rodent brain tissue to prove the existence of opioid receptors as specific and saturable binding sites for opioid drugs in 1973.[2–4] It had long been hypothesized that there were several different opioid receptor subtypes, based on the varying pharmacological properties of the different opioid drugs available to test in human and animal models.[5] Before they were definitively proven, two of these receptors were named for the actions of different opioid drugs – the mu opioid receptor for its binding of morphine and the kappa opioid receptor for its binding of the benzomorphan drug ketocyclazocine.[6] These opioid drugs with distinct pharmacological properties were eventually

used to identify receptor subtypes. For example, a tritiated benzomorphan compound was used to identify binding sites that were consistent with the pharmacological properties of this putative kappa opioid receptor in guinea pig cerebellum.[7] The delta opioid receptor was named later, when it was found to be enriched in mouse vas deferens tissue.[8] By the early 1990's, scientists had identified and cloned the three main opioid receptor subtypes.[9–13]

The three main opioid receptors (KOR, MOR and DOR) and their endogenous peptide ligands (dynorphins, endorphins and enkephalins) are now recognized as crucial mediators of mood and reward, as well as pain and other sensations. Genetic and pharmacological studies have shown that the MOR system is necessary for the rewarding and euphoria-inducing properties of many drugs of abuse, including MOR agonists like morphine and drugs of abuse with different mechanisms of action, such as alcohol (reviewed in Darcq and Kieffer, 2018).[14] The DOR system is thought to mediate mood, as DOR agonists are anxiolytic and cause anti-depressant like behavior in animal models and DOR knock-out mice have increased anxiety and depressive-like behavior.[15] The KOR system, on the other hand, appears to negatively regulate both mood and reward (Figure 1.1).

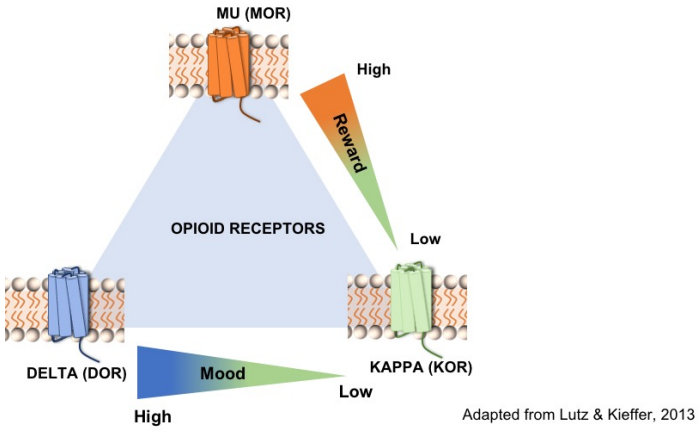

Figure 1.1. Opioid receptor systems differentially mediate mood and reward

1.2 The KOR system negatively regulates reward

In addition to causing the antinociceptive effects characteristic of most opioid agonists, KOR agonists have been shown repeatedly to be aversive and dysphoric in both animal and human studies. Early studies in rats found that the activation of KORs and MORs by small molecules had opposing effects on dopamine release in reward-related regions of the brain; while MOR agonists stimulated dopamine release, KOR agonists decreased dopamine release.[16] Activation of KORs by the endogenous peptide ligand dynorphin A (1-17) also led to a decrease in dopamine release. [17] This is thought to be the mechanism through which the KOR system mediates negative affect naturally. In animal models, for example, stressful experiences lead to negative affect, as demonstrated by depressive and anxiety-like behaviors, and this process is mediated by the KOR system.[18,19] Both KOR and dynorphin expression appear to be upregulated following administration of drugs such as morphine and cocaine in animal models,[20–22] as well as after cocaine overdose in humans,[23] suggesting that the KOR system may also be involved in the development of negative affective states in the addiction process.

Because of its anti-reward properties and role in addiction, many groups have investigated the KOR as a potential therapeutic target for the treatment of addictive diseases. KOR agonists have been shown to block the rewarding and reinforcing effects of several different drugs of abuse in animal models such as self-administration and conditioned-place preference (reviewed in Banks 2019).[24] These drugs include cocaine, ethanol, and MOR agonists such as morphine. Further, work from Yong Zhang has shown that activation of the KOR by dynorphin A (1-17) can block the dopaminergic surge caused by cocaine in mice, suggesting a mechanism for this reward blockade.[17]

In models of stress-induced reinstatement of drug seeking, however, the KOR system appears to potentiate reinstatement.[19,25] Additionally, there have been studies demonstrating that KOR agonists potentiate drug reward under certain circumstances in animal models.[24] It is clear that the KOR plays an important and complex role in the regulation of drug reward, and research is ongoing to determine the best way to therapeutically target this receptor for the treatment of addictive diseases. KOR agonists are particularly interesting for the treatment of cocaine and other psychostimulant addictions, as there are currently no available medications for these diseases.

1.3 Many KOR agonists have negative side effects in humans

Human studies have revealed negative side effects of KOR agonists that have hampered drug development. In the 90's and early 2000's, the KOR-selective arylacetamide agonists spiradoline (U69,066E) and enadoline were tested for analgesic efficacy in humans. Two studies of enadoline in 1996 for post-operative and dental pain showed no effect of the KOR agonist on analgesia overall.[26,27] While the highest dose of enadoline tested did decrease some reports of post-operative pain, the study had to be terminated early because of "neuropsychiatric events", including psychotomimetic effects and hallucinations.[27] Studies of spiradoline similarly found that this compound caused significant sedation in humans, as well as dysphoria, and that it could not replace MOR analgesics because of these side effects (reviewed in Wadenburg 2003).[28]

Shortly after these clinical studies, scientists also identified the KOR as the target for the main psychoactive compound in the plant *Salvia divinorum*.[29,30] Leaves from this plant have been used for centuries by the Mazatec people of Oaxaca, Mexico as part of their spiritual rituals and practices, and more recently as a recreational hallucinogen in parts of Mexico and the United States. The active compound, salvinorin A, was isolated in the 1980's and its molecular target

was identified as the kappa opioid receptor by Bryan Roth in the early 2000's. [29] The potent hallucinogenic properties of salvinorin A, as well as reports of sedation and dysphoria in *Salvia divinorum* users, helped to confirm the effects of KOR agonist activity in humans, in addition to providing a new scaffold for the development of unique kappa opioid compounds.[31]

Despite the adverse effects displayed by KOR agonists, there are some compounds currently in clinical use that target the KOR. Nalmefene is currently approved to treat alcohol addiction in Europe, and naltrexone is approved in the US for the treatment of opioid and alcohol addiction. Nalmefene and naltrexone are both MOR antagonists that have recently been shown to have partial KOR agonism for signaling through G-proteins.[32–34] Neither drug appears to cause the psychotomimetic, sedative or dysphoric side effects that are common to KOR agonists, however, suggesting that their partial agonism or signaling profile at the KOR may be beneficial for therapeutic development.

The only KOR-selective agonist that is used in humans is the compound nalfurafine, approved in Japan to treat pruritus in 2009. It is extremely potent, with a daily oral dose of 2.5μg for adults. While the reported KOR-mediated signaling properties of nalfurafine vary among studies, likely due to differences in assays and cell lines, it has been shown to have full efficacy at the KOR for almost all signaling pathways.[35,36] Post-marketing studies have demonstrated very few of the side effects expected with KOR agonism.[37] Additional studies in animals have examined the "therapeutic window" for nalfurafine dosing, between the doses that cause the desired antinociceptive and antipruritic therapeutic effects and the doses that cause negative side effects like sedation, and generally found that nalfurafine does not cause negative side effects at therapeutic doses. Other KOR agonists such as salvinorin A and the well-characterized arylacetamide agonist U50,488 tested in the same studies, however, caused negative side effects

at the same doses needed for therapeutic effects in these antinociceptive and antipruritic assays.[35,38,39] Initial studies have demonstrated that nalfurafine modulates the rewarding effects of drugs of abuse as well, although it is unclear how this effect compares with other KOR agonists.

Finally, KOR antagonists have been tested preclinically for different therapeutic indications including anti-depressant and anti-addictive properties.[40] Limited human studies so far have not demonstrated KOR blockade to be an effective treatment for depression or addictions. [41,42] However the short-acting KOR antagonists that are currently under investigation have also not shown any negative side effects.[41,42]

Together, the preclinical and clinical data suggest that KOR agonists with modified pharmacological properties, such as partial agonists, or agonists like nalfurafine with unique properties, could be potential therapeutics for treating addictive diseases, and particularly cocaine and other stimulant addiction.[43]

1.4 KOR agonists activate multiple signaling pathways

Additionally, there is a large effort to make and test agonists that selectively activate only certain pathways downstream of the KOR in order to confer therapeutic properties without causing negative side effects. The KOR, along with the other opioid receptors, is an inhibitory G-protein coupled receptor (GPCR). Upon receptor activation, heterotrimeric G-protein activation leads to inhibition of cyclic AMP production and hyperpolarization via ion channel interactions. Phosphorylation of the receptor also leads to the recruitment of β-arrestin-2, which leads to receptor internalization. This receptor-arrestin complex also confers its own set of signaling responses that may be independent of G-protein signaling (Figure 1.2). There have been recent

discoveries of downstream signaling pathways of KORs that are both G-protein-dependent and G-protein-independent (β-arrestin-dependent), including certain mitogen-activated protein kinases (MAPKs) and, more recently, the mTOR signaling pathway (mammalian target of rapamycin) (Figure 1.2).

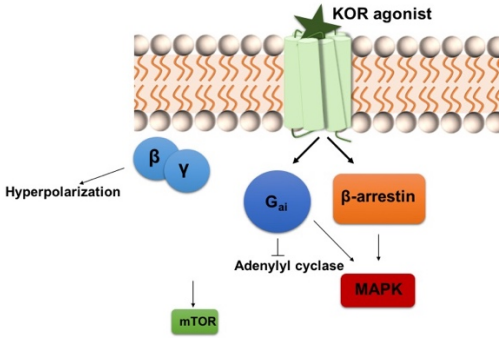

Figure 1.2. G-protein coupled receptors signal through diverse pathways

Studies of genetic knockout animals have suggested that certain downstream effects in vivo may require specific activation of these G-protein or β-arrestin signaling pathways. Specifically, in arrestin-knockout mice, activation of the mu opioid receptor still caused analgesia, but did not cause respiratory depression, suggesting that this side effect of MOR agonists required β-arrestin signaling.[44] This offers exciting possibilities for therapeutic development, as agonists that activate only one pathway could be used to elicit only a specific subset of downstream consequences, while excluding possible adverse effects (Figure 1.3). These "biased" or "functionally-selective" MOR agonists are currently being developed for pain relief based in part on studies from the Bohn laboratory and others reporting that G-protein biased MOR agonists were anti-nociceptive, but did not induce respiratory depression, in rodent

models.[45–47] This hypothesis is still being tested in humans with the G-protein biased MOR agonist TRV 130 (Oliceridine).[48,49]

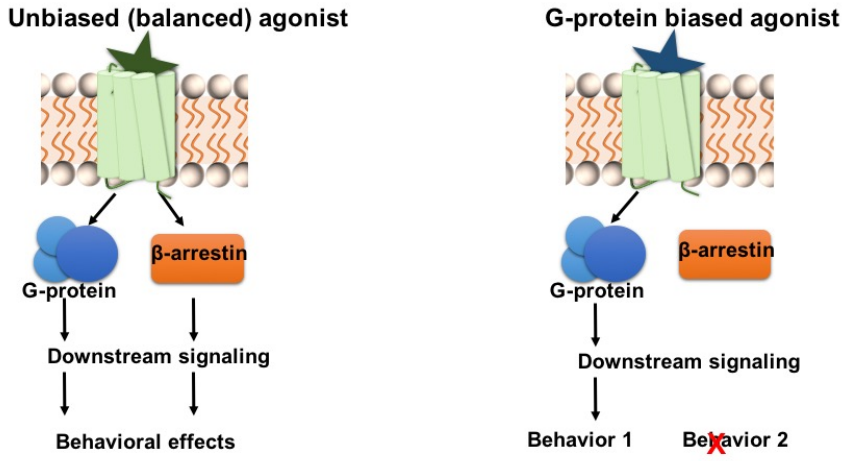

Figure 1.3. Biased agonists may be able to selectively induce downstream effects

Efforts have also been made to characterize KOR agonist pharmacology and determine which behaviors involve, or even require, G-protein or β-arrestin signaling (reviewed in Mores 2019).[50] RB-64, among the first biased KOR agonists, is an analog of salvinorin A that preferentially activates G-protein signaling over β-arrestin-2 signaling. In animal studies, this compound was antinociceptive, however it did not cause the sedative effects caused by the unbiased KOR agonists U50,488 and salvinorin A.[51] Later studies of a novel series of G-protein biased triazole compounds also suggested that β-arrestin signaling was necessary for the sedative properties of KOR agonists, but not antipruritic or antinociceptive effects.[52]

There are also efforts to characterize additional novel KOR agonists, as well as previously-described opioid compounds, for their G-protein versus arrestin bias at the kappa opioid receptor. [53–55] Many of these compounds have been previously characterized in animal

models, and some even in humans, and understanding more about their pharmacology could help improve understanding of the relationships between signaling pathways and behaviors downstream of the KOR. These efforts, however, have highlighted some of the technical difficulties in assigning an agonist the label of "biased".

To measure ligand bias, the activities of a compound in two different signaling pathways are compared. This requires selecting assays and endpoints for measuring activity, as well as a reference agonist to designate "full" activity in each pathway, which can vary between studies. Bias is most commonly quantified using the operational model of partial agonism first described by Black and Leff in the 1980's.[56,57] By definition, all quantifications of ligand bias are specific to the assays and reference agonists chosen.

In addition to these experimental details that can vary between labs, it has been shown that agonist activity downstream of a receptor can vary depending on what cellular components are available, meaning that measurements of ligand bias can vary between cell lines and tissues. This makes it difficult to compare measurements of bias between studies, and also suggests that in vitro measurements of ligand bias may not be indicative of signaling in disease-relevant tissue. Despite these concerns, a recent 2017 study from the Bohn laboratory demonstrated that an in vitro measurement of "Bias Factor" did in fact correlate significantly with the "therapeutic window", between antinociceptive and respiratory depression effects, in mice.[46] While there are many difficulties to measuring ligand bias, or understanding what signaling pathways are activated in the disease-relevant tissue, this study demonstrated that these in vitro measurements can be useful tools for guiding drug development efforts.

1.5 Additional signaling pathways may be involved in opioid receptor signaling

In addition to investigating G-protein and β-arrestin signaling pathways, studies have identified other signaling proteins that may be involved in opioid receptor effects. Several proteins of the MAPK family, for example, have been implicated in KOR-mediated behavior. The β-arrestin-dependent activation of the MAPK p38 has been shown to be important for mediating the aversive effects of KOR agonists.[58,59] Additionally, blockade of the KOR with long acting antagonists has been shown to activate JNK (c-Jun N-terminal kinase) as well, another MAPK protein.[60] ERK1/2 (extracellular related kinases 1 and 2) proteins have been shown to be phosphorylated after KOR activation by many different KOR agonists, and a study with salvinorin A suggested that ERK1/2 activation is necessary for the blockade of dopamine release by KOR agonists.[61] An important study from the Bohn laboratory also demonstrated that ERK1/2 phosphorylation downstream of the KOR could be independent of G-protein or β-arrestin activation, highlighting the importance of examining these additional signaling pathways.[62]

A recent phosphoproteomic study compared signaling protein activation (via phosphorylation patterns) in particular brain regions of mice treated with different KOR agonists.[39] This study identified that certain KOR agonists, at doses that caused aversion, led to increased mTOR signaling compared to non-aversive KOR agonists. Follow-up studies indicated that mTOR activation was necessary for KOR-mediated aversion, but not sedation, suggesting that this signaling pathway may also be important to consider for the development of KOR agonists with fewer side effects.[36]

New techniques in biochemistry and structural biology are also being developed to investigate the molecular basis of opioid receptor signaling, particularly the differential

activation of opioid receptors by biased ligands. For example, using nanobodies that selectively bind the active conformation of the MOR, the Von Zastrow laboratory has identified differences in the subcellular localization of active MORs after treatment of cells with the endogenous β-endorphin peptide versus small molecule agonists.[63] Strategies like these could help to identify key relationships between drug action at the molecular level and the behavioral level, that could in turn aid drive drug discovery efforts.

1.6 Research goals

Data from preclinical and clinical studies of KOR ligands suggest that modified pharmacology, such as partial agonists or unique signaling pathway activation, could help lead to KOR agonists with fewer side effects. Recent advances in GPCR research also suggest that biased agonists, that selectively activate only certain pathways downstream of the receptor, could also improve side effect profiles of different compounds. Here, we have explored several different strategies to investigate the relationships between KOR signaling and behavior, including exploring biased agonists, identifying other downstream signaling pathways and testing compounds that have already proven to be safe in humans in preclinical mouse models of cocaine reward.

In **Chapter 3**, 21 structurally-diverse KOR agonists were pharmacologically profiled for both G-protein and β-arrestin-2 signaling, and their ligand bias in this context was quantified. We then examined the relationships between these early G-protein and arrestin signaling pathways and KOR-mediated sedation in mice, as measured by the rotarod assay.

In **Chapter 4**, we examined the ability of KOR agonists to activate additional signaling pathways that have been more recently implicated in KOR-mediated behaviors, including

ERK1/2 phosphorylation and mTOR activation. We also investigated novel pathways that may be involved in KOR-signaling for future study.

Finally, in **Chapter 5**, we examined preclinical mouse models of KOR-mediated behaviors using several different types of KOR agonists, including a G-protein biased agonist and the clinically-utilized agonist nalfurafine. We compared the effective doses of different KOR agonists for negative side effects, as well as models of cocaine reward and reinforcement. Together, the goal of this work is to better understand the different pharmacological strategies that could be used to develop KOR ligands for therapeutic use in the future.

CHAPTER 2. MATERIALS AND METHODS

2.1. Chemical compounds

Dynorphin A(1-17) (YGGFLRIRPKLKWDNQ) was obtained from BACHEM. GR89686 (4-[(3,4-Dichlorophenyl)acetyl]-3-(1-pyrrolidinylmethyl)-1-piperazinecarboxylic acid methyl ester fumarate) was obtained from Tocris. Nor-Binaltorphimine was obtained from Abcam (Cambridge, UK). Salvinorin A and Mesyl Salvinorin B were given by Dr. Tom Prisinzano (University of Kansas). Nalmefene was obtained from Baker Norton Pharmaceuticals (Miami, FL, USA). Nalfurafine was obtained from Adooq Bioscience (Irvine, CA, USA). N-substituted-[N-[2-phenylethyl]-N-[2-(3-hydroxyphenyl)ethyl]-amines (where substitutions = N-butyl for BPHA, cyclopropyl for HS666, methylcyclobutyl for MCBPHA and methylcyclopentyl for MCPPHA) were synthesized by a contract research organization, WuXi Apptech (Shanghai, China), using methods reported previously by the group of Schmidhammer.[64] WMS 0610 (1-{4-Benzyl-8 – pyrrolidine-1-yl-perhydroquinoxalinyl}-2-(3,4- dichlorophenyl)ethen one) and WMS 0611(2-(3,4-Dichlorophenyl)-1-(-8- pyrrolidine-1-yl-perhydroquinoxalinyl)- ethanone) were also synthesized by WuXi Apptech, using methods previously reported by the group of Wunsch.[65] For these synthesized compounds, mass spectrometric and NMR signals were in agreement with previous publications. LY2444296 [(*S*)-3-fluoro-4-(4-((2-(3-fluorophenyl) pyrrolidin-1-yl) methyl)phenoxy)benzamide] was also synthesized by WuXi, with a small portion generously donated by Eli Lilly (Indianapolis, IN), which was used to confirm that the WuXi synthesized compound was molecularly identical (as determined by reversed-phase high-performance liquid chromatography retention time). Remaining compounds were obtained from Sigma (St. Louis, MO, USA). This includes U69,593[(-)-(5α,7α,8β)-N-Methyl-N-[7-(1-pyrrolidinyl)-1-oxaspiro[4.5]dec-8-yl]-benzeneacetamide], U50,488 [trans-(±)-3,4-Dichloro-N-

methyl-N-[2-(1-pyrrolidinyl)cyclohexyl]benzeneacetamide], U62,066E [(±)-(5α,7α,8β)-3,4-Dichloro-N-methyl-N-[7-(1-pyrrolidinyl)-1-oxaspiro[4.5]dec-8-yl]benzeneacetamide], and ICI204448[(RS)-[3-[1-[[(3,4-Dichloro phenyl)acetyl]methylamino]-2-(1-pyrrolidinyl)ethyl]phenoxy] acetic acid]. [^{3}H]U69,593, and [^{35}S]GTPγS were procured from Perkin Elmer (Waltham, MA, USA). 3G1 and 3G2 were novel compounds synthesized by WuXi Apptech, using methods adapted from those previously reported.[64]

2.2 In vitro signaling studies

2.2.1 β-arrestin-2 enzyme fragment complementation (ECF)

Experiments were conducted using the PathHunter Detection Kit obtained from DiscoveRx. Cells stably expressing human kappa opioid receptors (PathHunter U2OS hOPRK1 β-arrestin-2 cell line, DiscoveRx, Fremont, CA, USA) were plated in 96- or 384-well plates. Cells were stimulated with the compounds for 90 minutes at 37°C followed by incubation for 60 minutes in the presence of galactosidase substrate, yielding chemiluminescent product. All concentrations were tested in quadruplicate for each experiment, and had an N of 3 experiments total. Each 384-well plate also had 32 additional replicates of 10μM U69,593 that were used for normalization. Chemiluminescence was measured using a Synergy Neo microplate reader (BioTek, Winooski, VT, USA). Antagonism assays were done in the same manner, in the presence of 300nM U69,593.

2.2.2 [^{35}S]GTPγS Binding with U2OS cell membranes

Membranes from U2OS cells (PathHunter U2OS hOPRK1) stably expressing human KORs were used. Cells were scraped from tissue culture plates, homogenized with a Tissue Tearor homogenizer in membrane buffer (10mM Tris-HCl, 100mM NaCl, and 1mM EDTA; pH 7.4), and centrifuged at 20,000 g for 30 minutes at 4°C and frozen at -80°C until use. Prior to use, the

pellets were resuspended in assay buffer (50mM Tris-HCl, 100mM NaCl, 5mM $MgCl_2$, and 1mM EDTA; pH 7.4) and homogenized with a dounce homogenizer and 50 μg incubated with 0.1nM [^{35}S]GTPγS, 10nM GDP, and the appropriate concentration of agonist for 20 minutes at 30°C. All concentrations were tested in quadruplicate for each experiment, and had an N of 3 experiments total. Membranes with bound [^{35}S]GTPγS were collected on Whatman GF/B filter paper (Brandel, Gaithersburg, MD, USA) utilizing a Brandel harvester. Bound [^{35}S]GTPγS was quantified using a TriCarb-2900TR scintillation counter (Packard, Downers Grove, IL, USA) following addition of 4 mL ReadySafe scintillation fluid (Beckman Coulter, Indianapolis, IN, USA).

2.2.3 [^{35}S]GTPγS Binding with mouse striatum tissue

Mice were euthanized by cervical dislocation, in a manner approved by The Rockefeller University Institutional Animal Care and Use Committee. Ventral striatum tissue, corresponding to the caudate putamen and nucleus accumbens regions, was removed immediately after sacrifice and tissue was frozen in liquid nitrogen. Tissue samples were then stored at -80°C until further use. Homogenization and assay protocol were adapted from Bohn, Zhou and Ho 2015[66] and described below.

Striatum samples were homogenized in homogenization buffer (10mM Tris-HCl, pH 7.4, 100mM NaCl, 1mM EDTA, 1mM DTT added immediately prior to use) by a Tissue Tearor homogenizor on ice, dounced in a dounce homogenizor and passed through a 26 gauge needle for homogenization. The tissue was then centrifuged at 20,000 g for 30 minutes at 4°C, rinsed with homogenization buffer and spun down again. Pellets were resuspended in assay buffer (50mM Tris-HCl, pH 7.4, 100mM NaCl, 5mM $MgCl_2$, 1mM EDTA, 1mM DTT added immediately prior to use) and incubated with 0.1nM [^{35}S]GTPγS, 20 nM GDP, and the

appropriate concentration of agonist for 1 hour at RT. All concentrations were tested in quadruplicate. Membranes with bound [^{35}S]GTPγS were collected on Whatman GF/B filter paper (Brandel, Gaithersburg, MD, USA) utilizing a Brandel harvester. Bound [^{35}S]GTPγS was quantified using a TriCarb-2900TR scintillation counter (Packard, Downers Grove, IL, USA) following addition of 4 mL ReadySafe scintillation fluid (Beckman Coulter, Indianapolis, IN, USA).

2.2.4 In-cell western blots for ERK1/2 phosphorylation

HEK293 cells stably expressing a FLAG (DYKDDDDK) -tagged mouse KOR were plated in a 96-well plate and stimulated with compound for 5 minutes after 1 hour of serum starvation. All concentrations were tested in triplicate. Cells were then prepared for immunofluorescent staining with phosphorylated ERK1/2 (Phospho-p44/p42 MAPK, 1:100, Cell Signaling Technology, Danvers, MA, USA) and GAPDH (GAPDH (0411), 1:100, Santa Cruz Biotechnology, Dallas, TX, USA) primary antibodies, and near-infrared secondary antibodies (IRDye 680CW and IRDye 800CW, 1:500, LiCor Biosciences, Lincoln, NE, USA). Plates were imaged on the Li-Cor Odyssey CLx Imaging System (LiCor Biosciences, Lincoln, NE, USA).

2.2.5 Western blots for Rps6 phosphorylation

U2OS cells (PathHunter U2OS hOPRK1) stably expressing human KORs were plated in a 96wwell plate and stimulated with compound for 1 hour after 14-16 hours of serum starvation. All concentrations were run in triplicate. Cells were lysed with radioimmunoprecipitation (RIPA) buffer (Thermo Fisher Scientific, Waltham, MA, USA). Samples were run on SDS PAGE gels, and multiple gels trimmed and transferred to a single western blot ("multistrip" western blot).[67] Blots were probed with phosphorylated Rps6 (P-S6 Ribosomal Protein (Ser240/244), 1:1000, Cell Signaling Technology, Danvers, MA, USA) and GAPDH (GAPDH (0411), 1:1000, Santa Cruz

Biotechnology, Dallas, TX, USA) primary antibodies, and near-infrared secondary antibodies (IRDye 680CW and IRDye 800CW, 1:500, LiCor Biosciences, Lincoln, NE, USA). Blots were imaged on the Li-Cor Odyssey CLx Imaging System (LiCor Biosciences, Lincoln, NE, USA) and quantified using ImageJ (US National Institutes of Health, Bethesda, MD, USA).

2.2.6 LogRAi bias calculations

For all in vitro assays described here, data was normalized to the maximal response of 10μM reference agonist U69,593 run at the same time. For [^{35}S]GTPγS, β-arrestin-2, and ERK1/2 phosphorylation assays, dose response curves were determined using nonlinear regression in Graphpad Prism 7 (GraphPad Software, San Diego, CA, USA) and EC_{50} and E_{max} values are presented with standard error. LogRAi values were calculated as described in Ehlert, 2005[68] and 2008[69] [reviewed with other methods of bias analysis in Kenakin and Christopoulos 2013],[70] as the LogRAi = $\log(E_{max}/EC_{50})$. This value is analogous to the transduction factor calculated from the operational model of partial agonism,[57] as long as the slope factor of the dose-response curve is 1.

In certain instances of very low maximal efficacy, competitive model analysis was performed as described in Stahl et al., 2015 in Graphpad Prism 7[71]. These cases are shown in Figures 3.3 and 4.2. Normal dose-response data was used for each test compound, as well as dose-response data from the test compound in competition with 300nM U69,593. The dose-response curve of U69,593 was used for reference agonist data.

For each of these specific instances, the data was fit to the equations below. Here, "Bottom" and "Top" refer to the minimum and maximum stimulation in the data set, as a percentage of maximal U69,593 stimulation. This is the same units as the output, Y. The LogK value is the dissociation constant of the ligand, either reference or test. LogR is the transduction

coefficient of the reference ligand. [57] LogRA is the ratio of transduction coefficients of the test ligand and the reference ligand. In these equations, X is the concentration of the test ligand, while A is the concentration of the reference ligand (held constant in the assays where the test ligand is treated as an antagonist). Finally, n is the transducer slope factor which was held to 1 for analysis. For the β-arrestin-2 and ERK1/2 assays, the U69,593 curve was first fit to the reference ligand equation. These parameters were then used to fit the data from the test ligand both using the agonist and antagonist equations. Initial parameters and constraints were held as described in Stahl et al. 2015.[71]

Reference ligand:

$$Y = Bottom + \frac{Top - Bottom}{1 + (\frac{1 + 10^{(X - LogK_{ref})}}{10^{(X + LogK_{ref})}})^{n}}$$

Test ligand as an agonist:

$$Y = Bottom + \frac{Top - Bottom}{1 + (\frac{1 + 10^{(X - LogK_{test})}}{10^{(X + LogR + LogRA)}})^{n}}$$

Test ligand as an antagonist:

$$Y = Bottom + \frac{Top - Bottom}{1 + (\frac{1 + 10^{(A - LogK_{ref})} + 10^{(X - LogK_{test})}}{10^{(A + Log_{R})} + 10^{(X + LogR + LogRA)}})^{n}}$$

2.3 Biochemical studies and imaging

2.3.1 Stable-isotope labelling in cell culture (SILAC) and immunoprecipitation

HEK 293 cells expressing a KOR tagged with an N-terminal FLAG sequence (DYKDDDDK) were grown to confluence in 10cm dishes, in DMEM media containing light or heavy amino acids (^{15}N Lysine and Arginine) (all media from SILAC Protein Quantitation Kit (Trypsin), DMEM, ThermoFisher, Waltham, MA, USA). Cells were grown until cells in heavy media had at least 95% heavy amino acid incorporation. For immunoprecipitations, cells were lysed in lysis buffer (10% v/v glycerol, 75mM Tris pH 7.4, 2mM EDTA, 0.5% v/v digitonin) with PhosSTOP phosphotase inhibitor and cOmplete mini EDTA-free protease inhibitor cocktails (Sigma Aldrich, St Louis, MO, USA) and membranes lysed by passage through a 25 gauge needle and subsequent incubation and centrifugation. For SILAC experiments, cell lysates were mixed together and incubated with Anti-FLAG M2 agarose beads (Anti-FLAG M2 Affinity Gel, Sigma, St. Louis, MO, USA) overnight. Beads were washed with ice-cold lysis buffer (0.1% v/v digitonin) and proteins were eluted with 1X LDS sample buffer.

2.3.2 Mass spectrometry analysis

Samples were run on Bis-Tris protein gels and gel samples were subjected to in-gel tryptic digestion.[72] The resulting peptides were extracted and purified, analyzed by LCMS using a Thermo Orbitrap Fusion Lumos mass spectrometer, with a Thermo Easy-nLC 1200 HPLC and a Thermo Easy-Spray electrospray source (ThermoFisher, Waltham, MA, USA). Identification and quantification of proteins was performed by searching against a human protein sequence database with the MaxQuant software (version 1.2.2.5).[73]

2.3.3 Immunofluorescent sample preparation and imaging

Coverslips or plastic-bottomed 96-well plates were coated in poly-D-lysine, and HEK cells expressing a N-terminal GFP-tagged KOR were plated and grown to 80% confluence. Cells were then serum starved for 16-24 hours and cells were treated with the appropriate concentration of drug in serum-free media for 1 hour. Cells were fixed and permeabilized with ice-cold methanol, and blocked for at least 1 hour in Tris Licor Blocking Buffer (LiCor Biosceinces, Lincoln, NE, USA). Cells were stained with pan-14-3-3 primary (14-3-3 (pan) Antibody 8312, 1:50, Cell Signaling Technology, Danvers, MA) and Alexa-647 secondary (1:500, Thermo Fisher Scientific, Waltham, MA, USA) and subsequently with DAPI (Sigma Aldrich, St Louis, MO) for nuclear visualization. If coverslips were used, coverslips were mounted on slides using ProLong Diamond Antifade Mountant (Invitrogen, Eugene, OR, USA). Coverslip images (Figure 4.12) were taken using an Olymbus IX71 spinning disk microscope. 96-well plates were imaged using LSM 780 laser scanning confocal microscopy. Z-stacks from confocal microscopy were deconvoluted using Autoquant software (Media Cybernetics, Rockville, MD, USA) and nuclear localization was quantified using Imaris (Oxford Instruments, Abingdon, UK).

2.4 Animal studies

2.4.1 Animals

Male C57BL6 mice (9-13 weeks, 20-30g, Charles River Laboratories, Wilmington, MA, USA) were used in all studies. Mice were housed, four to a cage, in sound attenuated chambers with individual light controls, in stress-minimized rooms, with a reverse 12 hour light/dark cycle, and food and water were provided ad libitum. All animals were housed for at least one week, with daily handling, prior to studies. Animals were housed and euthanized in a manner approved by The Rockefeller University Institutional Animal Care and Use Committee.

2.4.2 Prolactin release

Mice were injected intraperitoneally with KOR agonists in saline (U50,488 and nalfurafine) or a vehicle of 10% v/v ethanol, 10% v/v Tween-80 and 80% distilled-deionized water (BPHA, MCBPHA, MCPPHA) 30 minutes prior to sampling. LY2444296 or vehicle pretreatment, if applicable, was given by intraperitoneal injection 60 minutes prior to sampling. Trunk blood was collected by rapid decapitation, followed within 2 hours by preparation of serum. Serum prolactin levels were determined using a commercially available enzyme-linked immunoassay (AbCam, Cambridge, UK) following dilution of serum 5-fold in assay buffer.

2.4.3 Rotarod Assay

Rotarod experiments were conducted with mice using a dedicated rodent rotarod apparatus, with up to five animals tested concurrently (IITC Life Science, Woodland Hills, CA, USA). Rotarod rotation rate began at 3 rotations per minute, and ramped to 30 rotations per minute over the course of 300 seconds, at which time the assay was terminated and animals returned to their home cage. Animals were acclimated to the rotarod on at least two occasions prior to the day of the test. On the day of the test, baseline times for each animal to fall off the rotarod were recorded. Animals that failed to remain on the rotarod for at least 150 seconds during baseline testing were removed from the analysis. Mice were then injected intraperitoneally with vehicle or compound, and rotarod measurements conducted, beginning 0-2 minutes after injection, and then subsequently at select time points thereafter. Rotarod performance was calculated as the percent of baseline time spent on the rotarod, and Pearson r correlation between rotarod performance and in vitro parameters was done using GraphPad Prism 7.0 (GraphPad Software, San Diego, CA, USA).

2.4.4 Conditioned-place preference and aversion assays

Mouse place preference chambers had three distinct compartments, separated by removable doors (ENV-3013; Med Associates, St. Albens, VT, USA). The central chamber had a solid grey floor and grey walls. The larger, black and white compartments had stainless steel rod and mesh floors, respectively. Experiments were performed in dimly-lit, sound attenuated chambers. All studies used a biased, counterbalanced design. During the pre-conditioning session, each animal was placed in the center compartment with the doors between chambers open. Time spent in each chamber was recorded for 30 minutes.

Conditioned-place aversion

For the conditioned-place aversion experiment with BPHA (Figure 5.7), animals were assigned their preferred compartment (black or white) from the pre-test as the drug paired chamber. Mice received 4 days of conditioning, with two conditioning sessions (AM and PM) per day. Mice were counterbalanced for AM or PM drug-paired conditioning sessions, and sessions were at least 3 hours apart. During each conditioning session, mice were pretreated with an intraperitoneal injection with BPHA (30mg/kg) or vehicle (10% ethanol, 10% Tween-80, 80% water). Then, mice were immediately placed in the appropriate chamber (with doors shut) for 30 minutes (Figure 2.1). After the four conditioning days, the post-test was performed in which mice were allowed free access to all chambers and time spent in each chamber was recorded for 30 minutes.

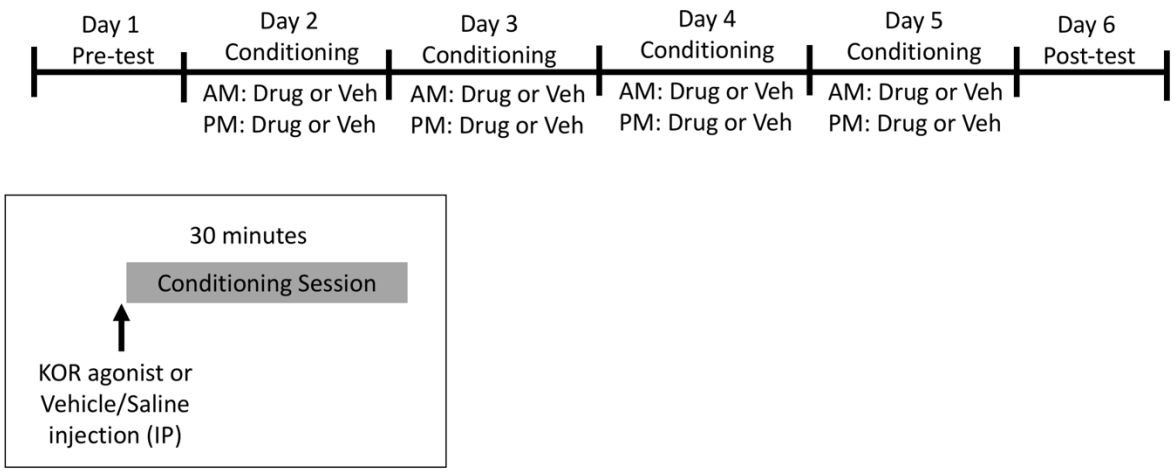

Figure 2.1. Conditioned place aversion assay set-up. Used for Figure 5.7, testing aversion with diphenethylamine compound BPHA.

Conditioned-place preference

For conditioned-place preference experiments (Figures 5.8 and 5.9), as well as aversion of nalfurafine and U50,488 (Figures 5.5 and 5.6), animals were assigned their non-preferred compartment (black or white) from the pre-test as the drug paired chamber. Mice received two days of conditioning, with two conditioning sessions (AM and PM) per day. Mice were counterbalanced for AM or PM drug-paired conditioning sessions, and sessions were at least 3 hours apart. During each conditioning session, mice were pretreated with an intraperitoneal injection with KOR agonist (U50,488, nalfurafine or saline) for 15 minutes, before saline or cocaine injection. Then, mice were immediately placed in the appropriate chamber (with doors shut) for 30 minutes (Figure 2.2). After the two conditioning days, the post-test was performed in which mice were allowed free access to all chambers and time spent in each chamber was recorded for 30 minutes.

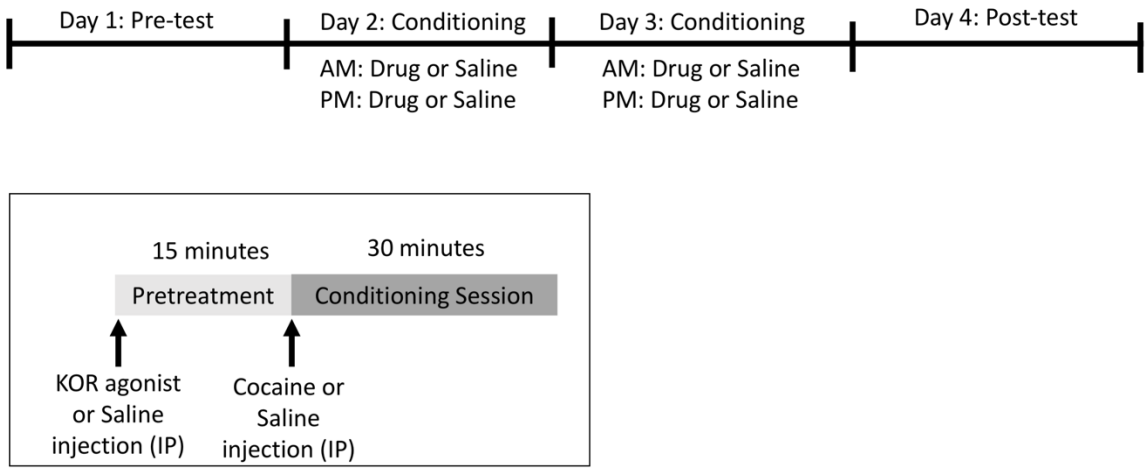

Figure 2.2. Conditioned-place preference assay set-up. Used to test the blockade of cocaine reward by KOR agonists U50,488 (Figure 5.8) and nalfurafine (Figure 5.9). Also used to test aversion caused by KOR agonists U50,488 (Figure 5.5) and nalfurafine (Figure 5.6).

2.4.5 Intravenous cocaine self-administration

Adult mice (8-10 weeks) were anesthetized with 5% vaporized isoflurane, and maintained on 2-3% isoflurane for the duration of the surgery. A catheter approximately 6 cm in length was inserted into the right jugular vein, up to a silicon ball placed 1.2-1.3 cm from the end of the catheter. Starting 48 hours after surgery, catheters were flushed with physiological saline containing heparin and the antibiotic gentamicin every other day to maintain catheter patency. For the IVSA experiments, mouse self-administration chambers were used inside sound attenuating boxes (ENV-307W; Med Associates, St. Albens, VT, USA). Each self-administration chamber contained a wall with two small holes, one defined as active and one defined as inactive. Mice were tested for 2 hours daily, with infusions of 0.5 mg/kg/infusion cocaine on an FR1 schedule following each active nose poke. During infusion, a cue light above the active hole was illuminated and then followed by a 20-second “time-out” period during which no infusions

could occur. Pretreatment experiments began when mice reached acquisition criteria, between 6-10 days after IVSA sessions began, depending on the animal. Acquisition criteria were: >70% of nose pokes in the active hole and <20% variation across two consecutive days. On each pretreatment day, mice were given IP injections of a KOR agonist (U50,488 or nalfurafine) or saline immediately before being placed in self-administration chambers. For the antagonist blockade experiment (Figure 5.11), mice were pretreated with 3mg/kg LY2444296 or vehicle by IP injection, and then given the KOR agonist or saline injections before being immediately placed in self-administration chambers (Figure 2.3). Catheter patency was checked weekly by infusion of ~30μL ketamine (5mg/mL), and only data from mice that passed this catheter patency test (defined as loss of muscle tone within a few seconds after ketamine infusion) were included in data analysis.

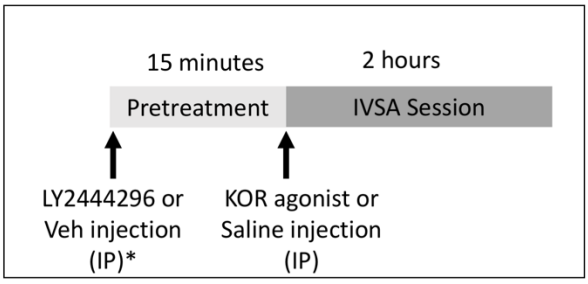

*Only in Figure 5.11

Figure 2.3. KOR agonist pretreatment set-up for cocaine IVSA

2.4.6 In vivo data analysis

Analysis of variance (ANOVA) tests were used to assess the effects of drug treatments on in vivo endpoints. Post-hoc multiple comparison tests were chosen based on relevant comparisons. Dunnett's post-hoc test was used to compare treatment groups to vehicle or saline control groups. Newman-Keuls post-hoc test was used to compare all treatment groups to each other, as

was often the case for antagonist pretreatment experiments for KOR specificity. Finally, Sidak's multiple comparison post-hoc test was used in the case of the intravenous self-administration experiments, in which there were repeated measures on time.

CHAPTER 3. G-PROTEIN VS ARRESTIN BIAS OF KOR LIGANDS

3.1 β-Arrestin-2 and G-protein signaling pathway activation by KOR ligands

While ligand bias can be measured between any signaling events or effectors downstream of an activated GPCR, "bias" most commonly refers to the difference between the receptor-proximal G-protein and β-arrestin signaling pathways.[74] Several studies have examined the ability of different KOR agonists to activate both of these signaling pathways, using a variety of different cell lines and endpoints. To measure G-protein recruitment to the receptor directly, bioluminescence resonance energy transfer (BRET) and radioligand binding assays ([^{35}S]GTPγS) are frequently used.[66] Importantly, the [^{35}S]GTPγS assay can be carried out in native tissue without genetic manipulations – this method has been optimized by the Bohn group to measure endogenous G-protein coupling in rodent striatum.[66] Second messengers downstream of G-protein activation, such as the inhibition of cAMP release and increased calcium release, are also used to measure G-protein activity downstream of the KOR. Finally, downstream signaling pathways such as ERK1/2 have also been used occasionally as proxies for G-protein activation.

In contrast to G-protein recruitment, heterologous cell lines must be used in BRET or enzyme fragment complementation assays to measure β-arrestin recruitment directly, with genetically modified versions of one of the isoforms of β-arrestin. Downstream responses such as internalization or p38 phosphorylation have also been used to measure arrestin recruitment indirectly.

In addition to the wide array of endpoints that have been used to measure these signaling pathways in the literature, it has also been shown that ligand bias is context-dependent, meaning the same ligand can differentially activate signaling pathways depending on the cell line or tissue

tested, for many GPCRs including the KOR.[75] These factors make it very difficult to compare across studies, and to draw any generalizations about the actions of biased ligands at the KOR.

The goal of this work, the majority of which was published in *ACS Chemical Neuroscience* in 2019,[34] was to compare the G-protein and β-arrestin-2 recruitment of 21, structurally diverse KOR ligands (Figure 3.1) in one cellular context. Here, we used the PathHunter U2OS hOPRK1 cell line, measuring G-protein signaling using the [^{35}S]GTPγS assay and β-arrestin-2 recruitment using the PathHunter DiscoverX enzyme fragment complementation assay. By using a single context, we could compare the activity of these ligands within their structural classes, and between structural classes.

3.1.1 Diverse KOR agonists tested for signaling properties

Most studies of the signaling properties of KOR agonists examine individual structural classes of ligands, with a few studies investigating larger sets of KOR ligands for specific signaling properties.[55] In this study, we aimed to examine a wide range of structurally diverse ligands for their early, receptor-proximal signaling properties at the KOR in a single cellular context. By using such a structurally diverse group of ligands, including the endogenous opioid neuropeptide dynorphin A (1-17), we could potentially draw more generalizable conclusions about the relationships between in vitro signaling properties and in vivo effects of KOR agonists.

First, the endogenous peptide ligand dynorphin A (1-17) was tested (Figure 3.1 A). Dynorphin peptides are cleaved from a precursor protein into several different lengths, with varying specificity for the opioid receptors. The form tested here, dynorphin A (1-17), is the most KOR-specific of the Dynorphin peptides and responsible for the majority of endogenous KOR activation.[76,77] In addition to dynorphin A (1-17), the other naturally-occurring compound

tested here was the natural product salvinorin A (Figure 3.1 A). Salvinorin A is a non-nitrogenous diterpene that is structurally unrelated to all other opioid ligands, and was recently characterized as a potent, selective KOR agonist.[30] Like many other KOR agonists, salvinorin A has considerable aversive, psychotomimetic and dysphoric properties in clinical and preclinical studies.[31,78] This discovery led to the development of salvinorin-based derivatives for KOR-targeted drug discovery. For example, the semi-synthetic analog mesyl salvinorin B, tested here as well, was previously characterized in vivo for its improved side-effect profile compared with the parent natural product salvinorin A (Figure 3.1 A).[79]

The most extensively-studied group of synthetic, selective KOR agonists are the arylacetamide compounds (Figure 3.1 C), based on the structure U50,488.[80] There has been extensive preclinical and in vitro pharmacology characterizing these compounds, however very few additional human studies have been conducted because of the negative side effects identified in early studies of arylacetamide agonists in humans, including spiradoline (U62,066E).[26–28]

While the naturally-occurring and arylacetamide groups of compounds are all relatively KOR-selective, we also tested several morphinan compounds that are better known for their activity at other opioid receptors (Figure 3.1 B). Nalmefene, naltrexone, buprenorphine and nalbuphine are all clinically-utilized compounds that are primarily recognized for their MOR activity. Nalmefene and naltrexone are MOR antagonists that have been previously studied for KOR partial agonism or antagonism.[32] Nalmefene is currently approved to treat alcoholism in Europe. Naltrexone is approved to treat opioid addiction and alcoholism in the US under the brand name Vivitrol, among others. Buprenorphine is also approved to treat opioid addiction, however it is a partial agonist at the MOR. Buprenorphine has also been reported to bind to the KOR, with reports of both partial agonism and antagonism.[81,82] Nalbuphine is also a MOR partial

agonist used to treat pain clinically, and has been shown to have partial KOR activity in certain signaling pathways.[83] All four of these morphinans have shown varying levels of KOR agonism for G-protein signaling, but very little activity in β-arrestin-2 recruitment or internalization assays previously.

The final morphinan compound studied was nalfurafine, which is clinically approved to treat pruritus in Japan under the name Remitch. Nalfurafine is a KOR agonist with some MOR activity, with ~2-10 fold binding selectivity for KOR over MOR.[35] Nalfurafine is notable for its very high potency at the KOR – the daily oral dose of Remitch for humans is 2.5μg. There have been reports of signaling at both the G-protein and β-arrestin-2 pathways, however measurements of ligand bias between the two pathways vary between studies.[35,36] One study, for example, used downstream signaling kinases ERK1/2 and p38 as readouts for G-protein and β-arrestin-2 signaling, respectively, to suggest that nalfurafine was biased for G-protein signaling over β-arrestin-2 signaling. Other groups have suggested that nalfurafine is unbiased because it shows full efficacy in assays for both signaling pathways.

In addition to these groups of well-characterized KOR ligands, we also tested two recently-described structural classes (Figure 3.1 D and E). The quinoxaline compounds WMS 0611 (which was first described as a peripherally-restricted KOR agonist) and 0610 by Bourgeois, et. al. 2014 and the diphenethylamine family of compounds first described by Spetea, et. al. 2012 were also tested. [64,84] BPHA (Compound 5 of Spetea et. al., 2012), MCBPHA (HS665 of Spetea et. al., 2012), MCPPHA (Compound 3 of Erli et. al., 2017) and HS666 (Spetea et. al., 2017) were further characterized in later studies for G-protein vs arrestin bias, as well as other KOR-mediated in vivo endpoints in mice.[85–87] Compounds 3G1 and 3G2, which were

novel to our 2019 *ACSCN* study, are structurally related to the diphenethylamines, and included in this class as well.[34]

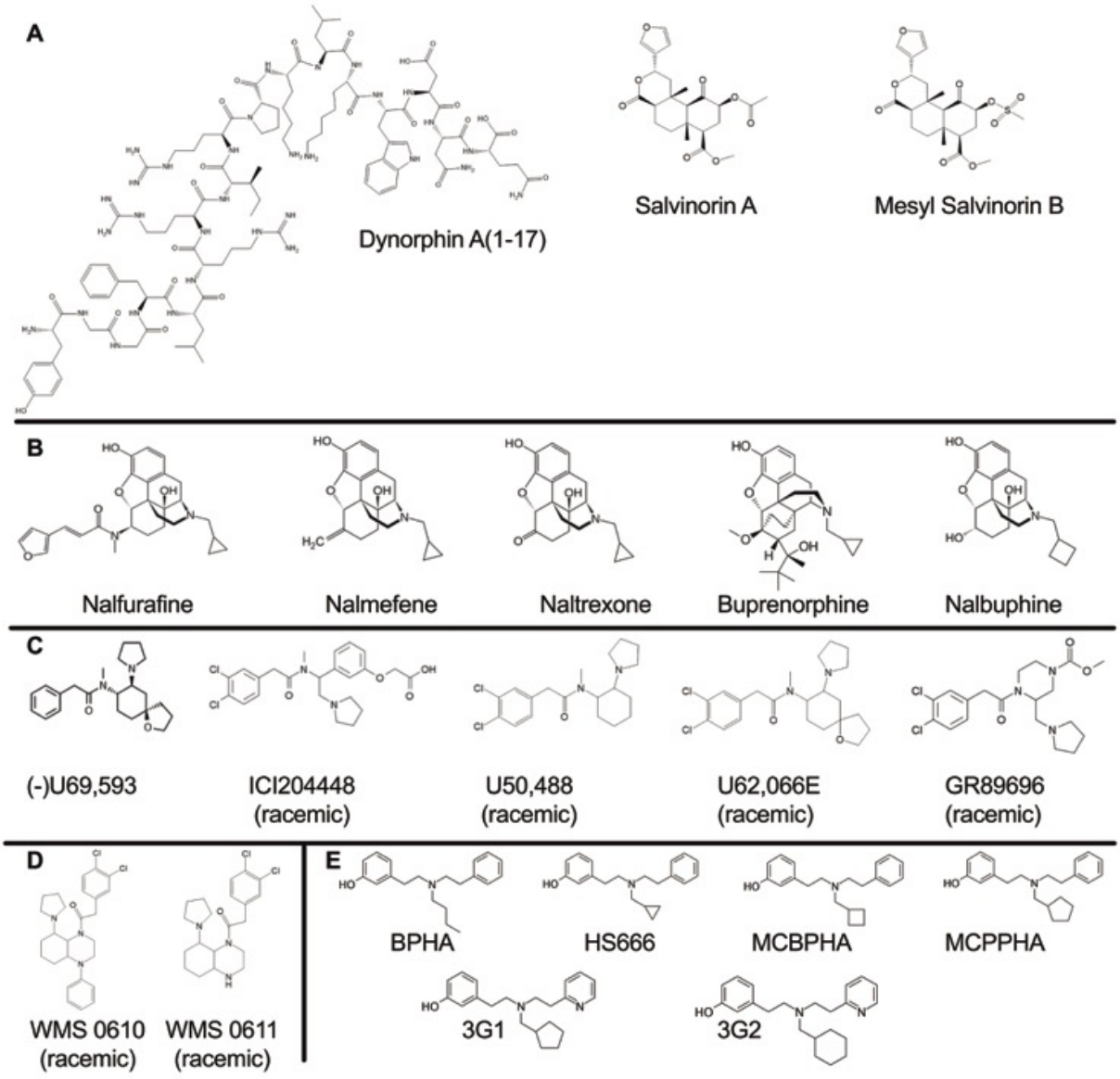

Figure 3.1. Structures of KOR agonists tested

Structures are arranged according to compound classes: A. the endogenous ligand dynorphin A(1-17), the natural product salvinorin A and the derivative mesyl salvinorin B; B. morphinan compounds; C. arylacetamide compounds; D. quinoxaline compounds; E. diphenethylamine compounds.

3.1.2 β-Arrestin-2 enzyme fragment complementation by KOR ligands in DiscoverX U2OS Cells

We tested each compound for β-arrestin-2 recruitment using the DiscoverX PathHunter enzyme fragment complementation (ECF) assay system. The DiscoverX PathHunter U2OS cell line used expressed an enzyme-fragment-linked human KOR, as well as an enzyme-fragment-linked β-arrestin-2, used for signal detection. All responses were blocked with KOR-selective antagonist nor-Binaltorphimine (norBNI) to determine KOR-selectivity. In Figure 3.2, potency (EC_{50}) and maximal efficacy (E_{max}) values are given as averages of 3 separate experiments, with 4 technical replicates per experiment alongside representative dose-response curves. The maximal efficacy of all other compounds was compared to the maximal efficacy of a concurrently run U69,593 dose-response curve, as U69,593 was used as the reference agonist in these experiments. The tables also include a $LogRAi_{Arr}$ value, described in further detail in Subsection 3.2.1, that compares activity of each ligand to the reference agonist U69,593.

In this assay, the reference agonist U69,593 robustly recruited β-arrestin-2, with a mean EC_{50} of 683nM (Figure 3.2). The endogenous ligand dynorphin A (1-17) was more potent than the reference agonist, as was the natural product salvinorin A. Mesyl salvinorin B, a derivate of salvinorin A, had similar activity to that of the reference agonist (Figure 3.2 A).

The other arylacetamide compounds, which are structurally related to the reference agonist U69,593 (Figure 3.1 C), all showed robust β-arrestin-2 recruitment with higher potencies and similar maximal efficacies compared with U69,593 (Figure 3.2). The compound GR89,696 was the most potent compound tested in this assay, with an average EC_{50} of 13.7nM.

The morphinan compounds, by contrast, overall showed very little β-arrestin-2 recruitment (Figure 3.2 B). Nalbuphine showed very modest β-arrestin-2 recruitment, with an

EC_{50} of over 4000nM and only 26% maximal efficacy. Nalmefene, naltrexone and buprenorphine did not demonstrate any measurable β-arrestin-2 recruitment in this assay (Figure 3.2 B). Dose-response curves of these compounds were tested against a steady concentration of 300nM U69,593 in this assay, in order to determine their ability to antagonize β-arrestin-2 recruitment by the reference agonist. In this paradigm, nalmefene, naltrexone and buprenorphine were potent antagonists of this signaling pathway (Figure 3.3). The exception in the morphinan class of compounds was nalfurafine, which had very robust β-arrestin-2 recruitment. Nalfurafine had a similar maximal efficacy to the reference agonist U69,593 and greater potency with a mean EC_{50} of 38.3nM (Figure 3.2 B).

Overall, the more recently described quinoxaline and diphenethylamine compounds did not show much β-arrestin-2 recruitment (Figure 3.2 D, E). WMS 0611 had more activity in this assay than the closely-related WMS 0610, with average EC_{50} values of 28μM and 4.3μM, respectively. The diphenethylamines HS666 and BPHA were antagonists in this assay (Figure 3.2 E), with full blockade but relatively large IC_{50} values (Figure 3.3). The remaining diphenethylamines (MCBPHA, MCPPHA, 3G1 and 3G2) were partial agonists for β-arrestin-2 recruitment (Figure 3.2 E).

A

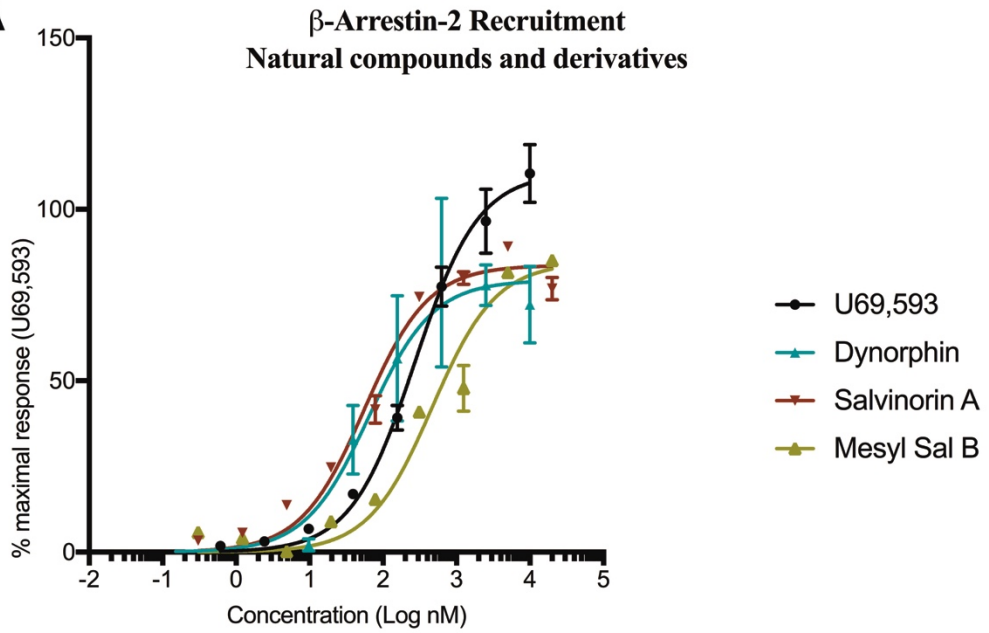

	EC50 (nM)	Emax (%max)	LogRAi$_{Arr}$
U69,593	683.2 (±200.3)	90.7 (±5.4)	0.0 (±0.1)
Dynorphin A (1-17)	77.1 (±27.9)	112.9 (±19.7)	1.0 (±0.2)
Salvinorin A	94.9 (±37.1)	84.7 (±9.2)	0.8 (±0.2)
Mesyl Sal B	704.9 (±102.4)	104.5 (±23.8)	0.0 (±0.1)

B

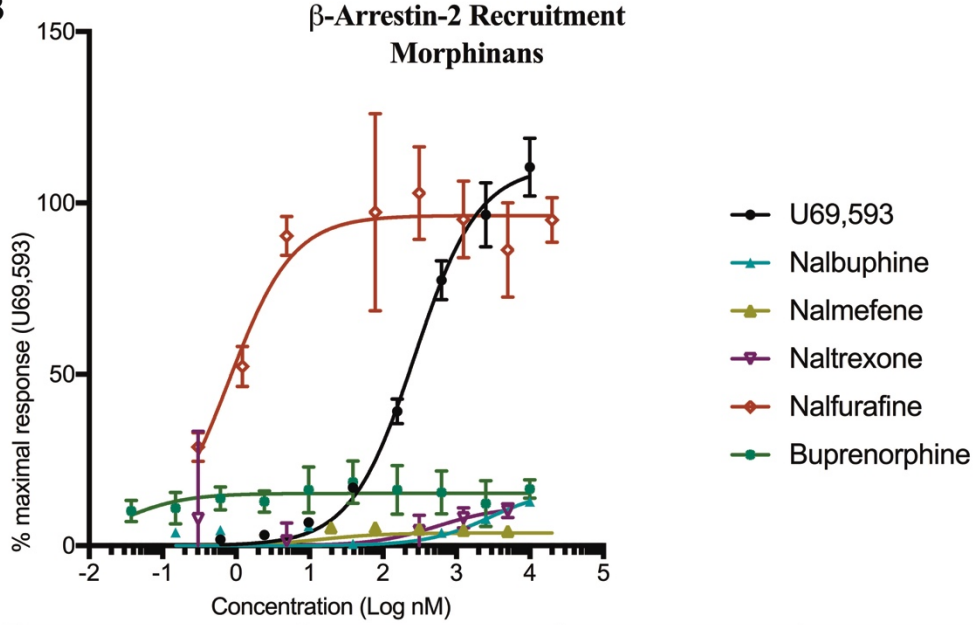

	EC50 (nM)	Emax (%max)	LogRAi$_{Arr}$
Nalbuphine	4370 (±3589)	26.3 (±13.4)	-1.3 (±0.4)
Nalmefene	No Fit	3.7% at 20μM	-2.0 (±0.2)*
Naltrexone	No Fit	11.5% at 20μM	-1.9 (±0.5)*
Nalfurafine	38.3 (±27.3)	106.5 (±9.5)	1.3 (±0.3)
Buprenorphine	No Fit	15.3% at 20μM	-2.7 (±1.3)*

C

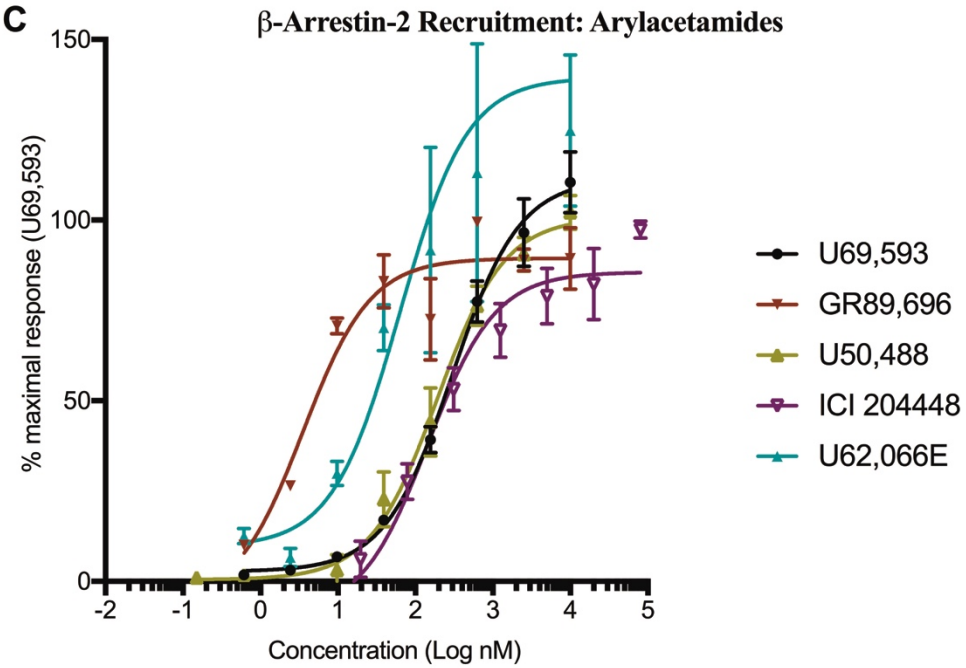

	EC50 (nM)	Emax (%max)	LogRAi$_{Arr}$
U62,066E	201.7 (±78.3)	119.1 (±11.9)	0.6 (±0.2)
GR89,696	13.7 (±4.6)	88.4 (±5.9)	1.7 (±0.1)
U50,488	413.7 (±106.6)	100.9 (±2.8)	0.3 (±0.1)
ICI 204448	97.3 (±28.8)	113.2 (±33.8)	0.9 (±0.2)

D

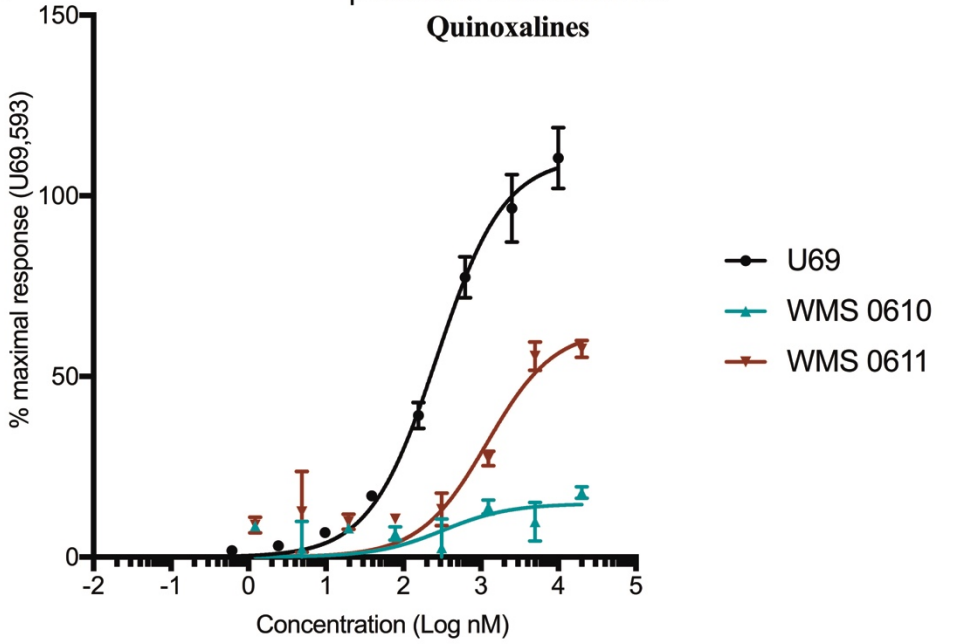

	EC50 (nM)	Emax (%max)	LogRAi$_{Arr}$
WMS 0610	28472 (±62220)	23.4 (±25.3)	-2.2 (±1.1)
WMS 0611	4272 (±2531)	73.1 (±12.5)	-0.9 (±0.3)

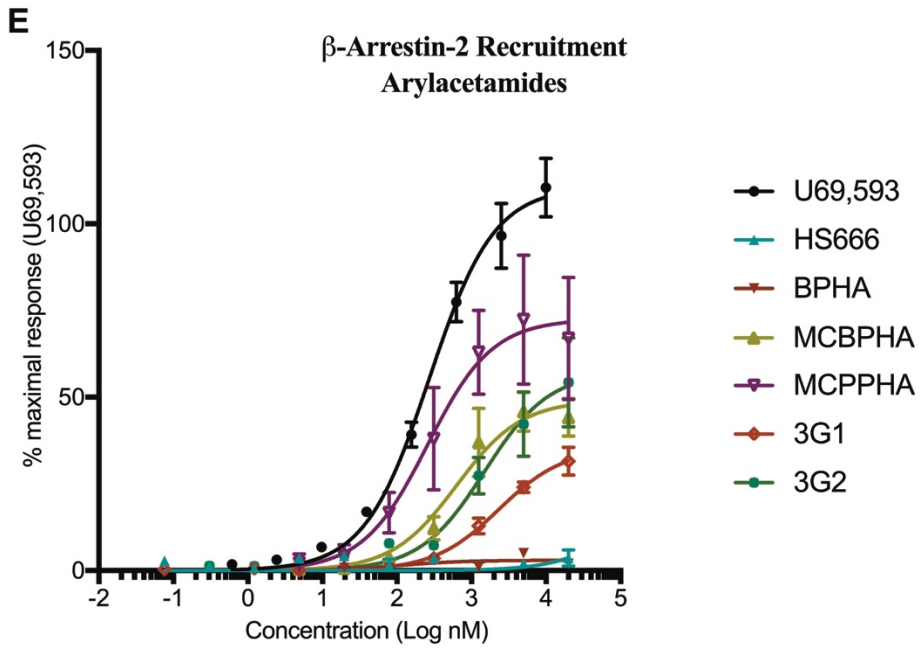

	EC50 (nM)	Emax (%max)	LogRAi$_{Arr}$
HS666	No Fit	28.4% at 20μM	-1.2 (±0.01)*
BPHA	No Fit	3.0% at 20μM	-2.0 (±0.4)*
MCBPHA	676.2 (±192.0)	49.4 (±6.5)	-0.3 (±0.1)
MCPPHA	261.9 (±58.6)	72.6 (±8.9)	0.3 (±0.1)
3G1	3956 (±2100)	61.2 (±11.0)	-0.9 (±0.2)
3G2	2082 (±558.6)	57.7 (±6.7)	-0.7 (±0.1)

Figure 3.2. β-Arrestin-2 EFC by KOR ligands and representative dose-response curves

Figures are arranged by structural class: (A) the endogenous ligand dynorphin A (1-17), the natural product salvinorin A and its derivative mesyl salvinorin B, (B) morphinan compounds, (C) arylacetamide compounds, (D) quinoxaline compounds and (E) diphenethylamine compounds. E_{max} values were calculated as the percentage of maximum U69,593 response from a concurrent U69,593 dose-response curve. Average EC_{50} and E_{max} values are represented as averages of 3 separate experiments with 4 replicates per experiment (±SEM). For compounds with low E_{max} values, data from the antagonist curves were fit to the operational model of partial agonism to calculate LogRAi values (*). Representative dose-response curves are shown alongside a representative U69,593 dose-response curve, in black in each graph. U69,593 stimulation was between 160 and 250% above baseline (800-2000 CUs).

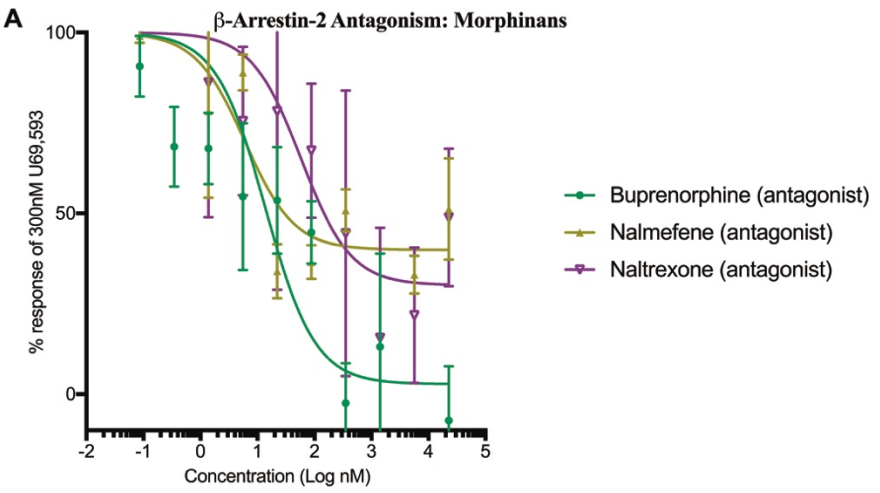

	IC50 (nM)	Max Inhibition (% 300nM U69)
Buprenorphine	7.2 (±6)	46.03 (±11.39)
Nalmefene	2.9 (±2)	41.36 (±4.68)
Naltrexone	21.9 (±18)	19.43 (±11.82)

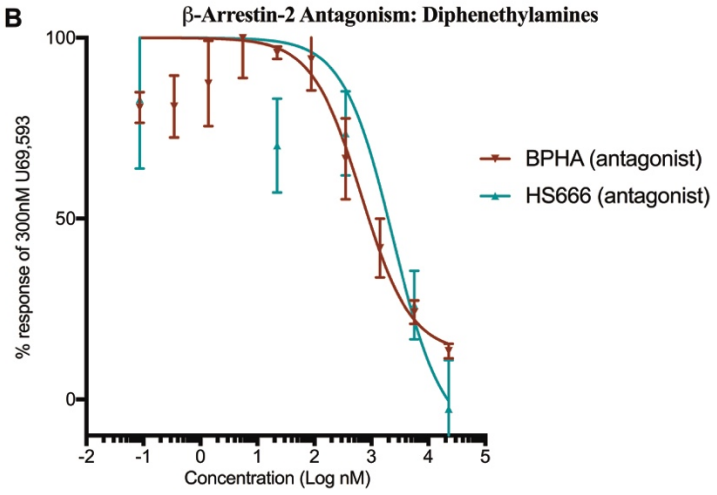

	IC50 (nM)	Max Inhibition (% 300nM U69)
HS666	7131 (±12815)	-14.27 (±64.94)
BPHA	1433 (±556)	4.40 (±8.92)

Figure 3.3. Blockade of U69,593-induced β-Arrestin-2 EFC by KOR ligands and representative dose-response curves. Compounds from (A) morphinan and (B) diphenethylamine classes of compounds with low E_{max} values were tested as antagonists to block arrestin enzyme fragment complementation by 300nM U69,593. Maximum inhibition values were calculated as the percentage of 300nM U60,593 response. Average IC_{50} and Max Inhibition values are represented as averages of 3 separate experiments with 4 replicates per experiment (±SEM).

3.1.3 [^{35}S]GTPγS binding by KOR ligands in DiscoverX U2OS cells

Each compound was tested for G-protein activation using the [^{35}S]GTPγS radioligand binding assay. This assay was done using membranes prepared from the same DiscoverX PathHunter U2OS cell line used for the β-arrestin-2 recruitment assay, in order to determine differential signaling mechanisms in the same context. All responses were antagonized with norBNI to determine KOR-selectivity, as this assay will measure any G-protein activity in the cell line. In Figure 3.4, potency (EC_{50}) and maximal efficacy (E_{max}) values are given as averages of 3 separate experiments, with 4 technical replicates per experiment alongside representative dose-response curves. The tables also include a $LogRAi_G$ value, described in further detail in Subsection 3.2.1, that compares activity of each ligand to the reference agonist U69,593.

The reference agonist U69,593 caused robust G-protein activation in this assay, with an average EC_{50} value of 3.3nM (Figure 3.4). Many compounds were more potent than U69,593 in this assay, however. Dynorphin A (1-17) was very potent for G-protein activation, with an average EC_{50} of 0.04nM (Figure 3.4 A). Both salvinorin A and mesyl salvinorin B were more potent than the reference agonist as well, however all of these compounds had maximal efficacies below 100%.

The arylacetamide compounds showed robust G-protein activation as well, with EC_{50} values ranging from 0.03nM to 0.6nM (Figure 3.4 C). The arylacetamide compound GR89,696 was the most potent compound tested in this assay, as it was in the β-arrestin-2 recruitment assay. The morphinan compounds also exhibited potent activity in this assay, and had maximal efficacy values ranging from 44.5% (nalbuphine) to 84.3% (nalfurafine) (Figure 3.4 B).

The quinoxaline and diphenethylamine compounds had variable G-protein activity downstream of the KOR, despite the structural similarity within groups (Figures 3.1 D, E). WMS

0611 was ~4-fold more potent than WMS 0610 for G-protein activation. EC_{50} values for the diphenethylamine series of compounds ranged from 0.5nM for MCPPHA to 22.7nM for HS666, with all compounds having similar maximal efficacies (75-87%) (Figure 3.4 E).

A

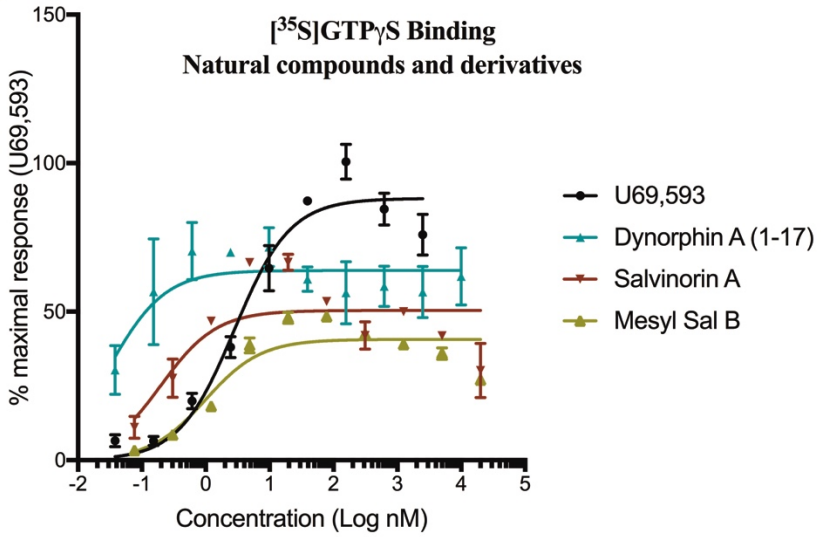

	EC50 (nM)	Emax (%max)	LogRAi$_G$
U69,593	3.3 (±0.6)	100.2 (±6.0)	0.0 (±0.1)
Dynorphin A (1-17)	0.04 (±0.03)	66.8 (±7.1)	1.7 (±0.3)
Salvinorin A	0.2 (±0.1)	80.3 (±3.4)	1.1 (±0.2)
Mesyl Sal B	1.0 (±0.2)	75.0 (±4.0)	0.4 (±0.1)

B

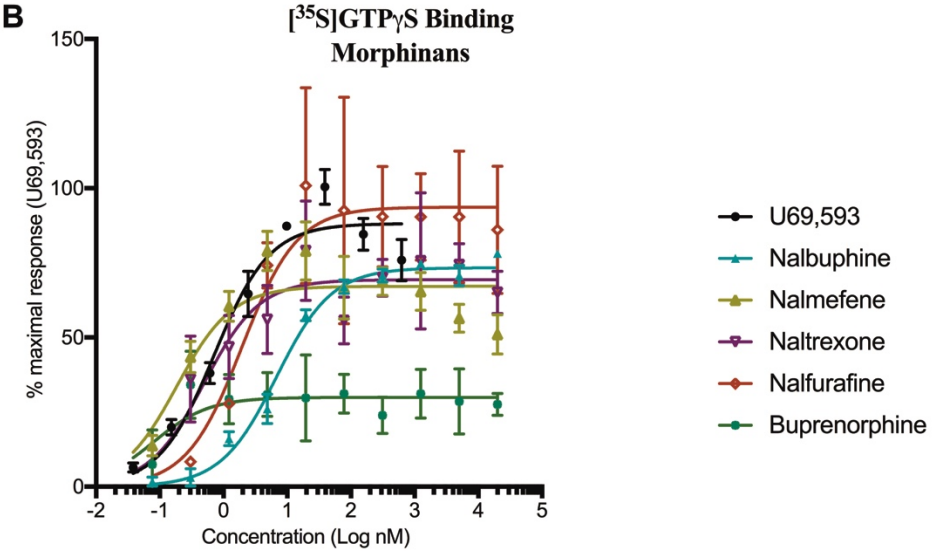

	EC50 (nM)	Emax (%max)	LogRAi$_G$
Nalbuphine	16.0 (±7.8)	66.2 (±8.1)	-0.9 (±0.2)
Nalmefene	0.2 (±0.1)	82.7 (±10.3)	1.1 (±0.2)
Naltrexone	0.6 (±0.3)	62.8 (±10.4)	0.5 (±0.2)
Nalfurafine	1.3 (±0.7)	84.3 (±11.6)	0.3 (±0.2)
Buprenorphine	0.2 (±0.1)	44.5 (±7.0)	0.9 (±0.2)

C

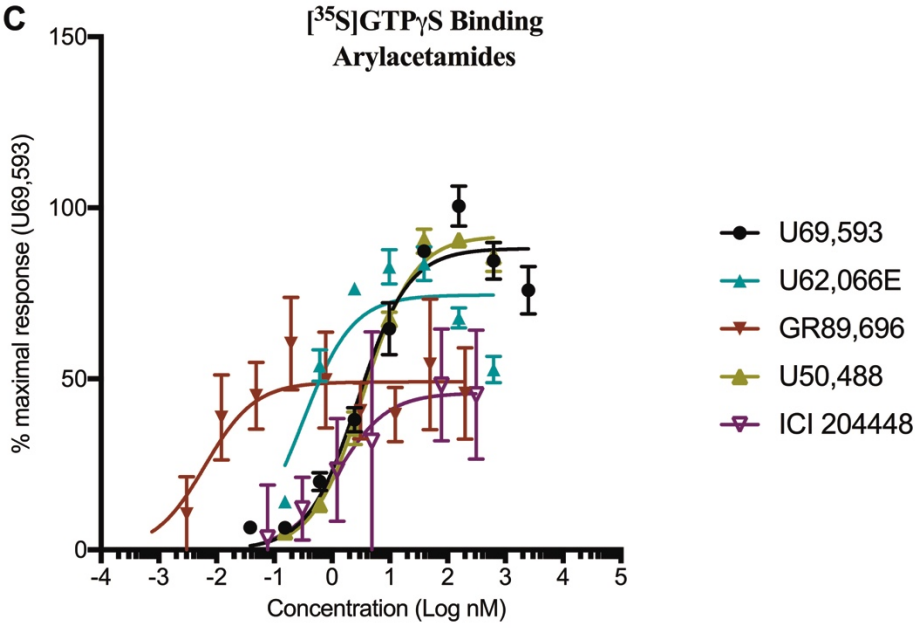

	EC50 (nM)	Emax (%max)	LogRAi$_G$
U62,066E	0.1 (±0.02)	85.4 (±13.1)	1.5 (±0.1)
GR89,696	0.02 (±0.01)	85.9 (±21.3)	2.2 (±0.2)
U50,488	0.6 (±0.2)	80.0 (±3.1)	0.6 (±0.1)
ICI 204448	0.1 (±0.02)	81.8 (±4.3)	1.4 (±0.1)

D

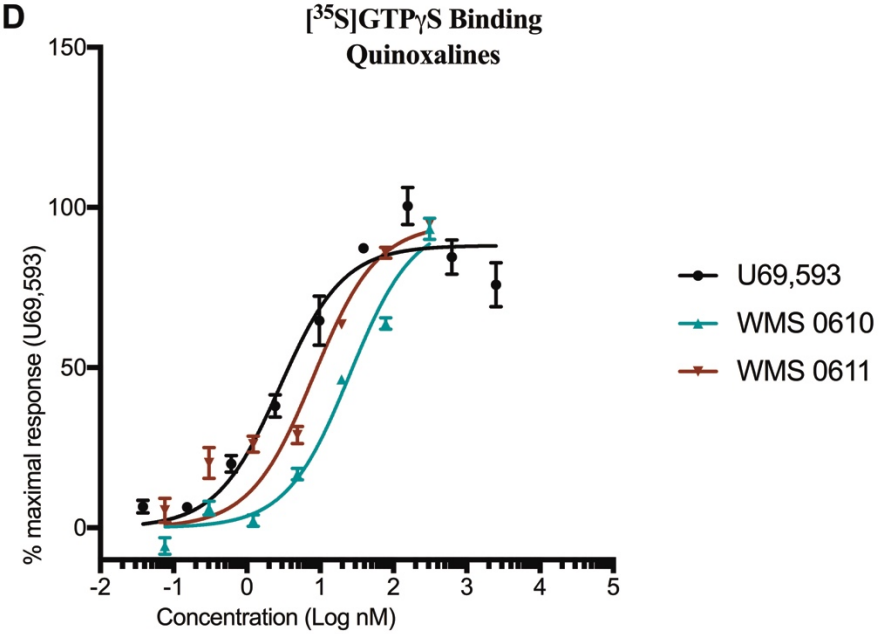

	EC50 (nM)	Emax (%max)	LogRAi$_G$
WMS 0610	20.1 (±5.1)	86.1 (±10.7)	-0.8 (±0.1)
WMS 0611	5.8 (±2.2)	77.2 (±13.0)	-0.4 (±0.2)

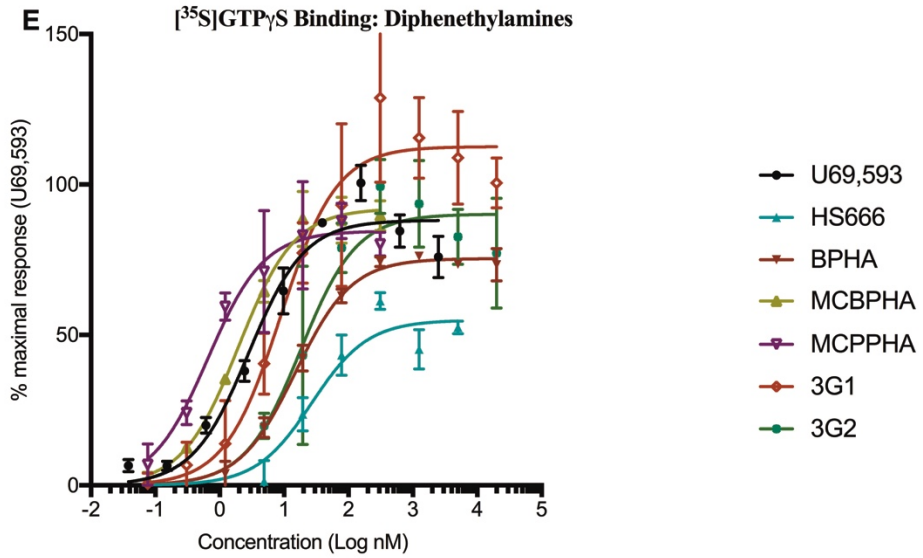

	EC50 (nM)	Emax (%max)	LogRAi$_G$
HS666	22.7 (±10.7)	75.3 (±11.0)	-1.0 (±0.2)
BPHA	14.3 (±6.7)	75.3 (±1.8)	-0.8 (±0.2)
MCBPHA	1.5 (±0.5)	84.9 (±4.8)	0.3 (±0.1)
MCPPHA	0.5 (±0.1)	79.0 (±5.0)	0.7 (±0.1)
3G1	8.2 (±2.4)	86.7 (±11.9)	-0.5 (±0.1)
3G2	11.8 (±3.8)	81.6 (±4.7)	-0.6 (±0.1)

Figure 3.4. [^{35}S]GTPγS binding by KOR ligands and representative dose-response curves

Figures are arranged by structural class: (A) the endogenous ligand dynorphin A (1-17), the natural product salvinorin A and derivative mesyl salvinorin B, (B) morphinan compounds, (C) arylacetamide compounds, (D) quinoxaline compounds and (E) diphenethylamine compounds. Average EC_{50} and E_{max} values are presented in tables as averages of 3 separate experiments with 4 replicates per experiment (±SEM). E_{max} values were calculated as the percentage of maximum U69,593 response from a concurrent U69,593 dose-response curve. LogRAi values were estimated from these average EC_{50} and E_{max} values. Representative dose-response curves are shown alongside a representative U69,593 dose-response curve, in black in each graph. U69,593 stimulation was between 35 and 70% above baseline (2000-8000 DPM).

3.1.4 GTPg35S binding by KOR ligands in mouse striatum tissue

While measuring arrestin recruitment directly requires heterologous cell lines, G-protein binding can be measured directly in native tissue. In order to examine G-protein signaling in a more physiologically-relevant context, we also investigated G-protein signaling in mouse striatal tissue, where there is dense KOR expression.[88] Mouse caudate putamen and nucleus accumbens were dissected and homogenized, and membranes were prepared for radioligand binding assays as described in Zhou, et. al. 2015.[66]

First, we optimized the preparation of the striatal membranes for KOR binding, and measured G-protein binding in the mouse striatum using the [^{35}S]GTPγS assay. The full reference agonist U69,593 robustly stimulated G-protein binding in the mouse striatum samples (Figure 3.5 A), and this effect was fully blocked by the KOR-selective antagonist norBNI (Figure 3.5 B). Nalmefene, which has been previously shown to be a partial agonist at the KOR, showed less than 50% G-protein binding compared to U69,593 in the mouse striatum (Figure 3.5 B). EC_{50} values for both compounds were higher than in U2OS cells, but consistent in their rank order (Figure 3.4 B, 3.6 A).

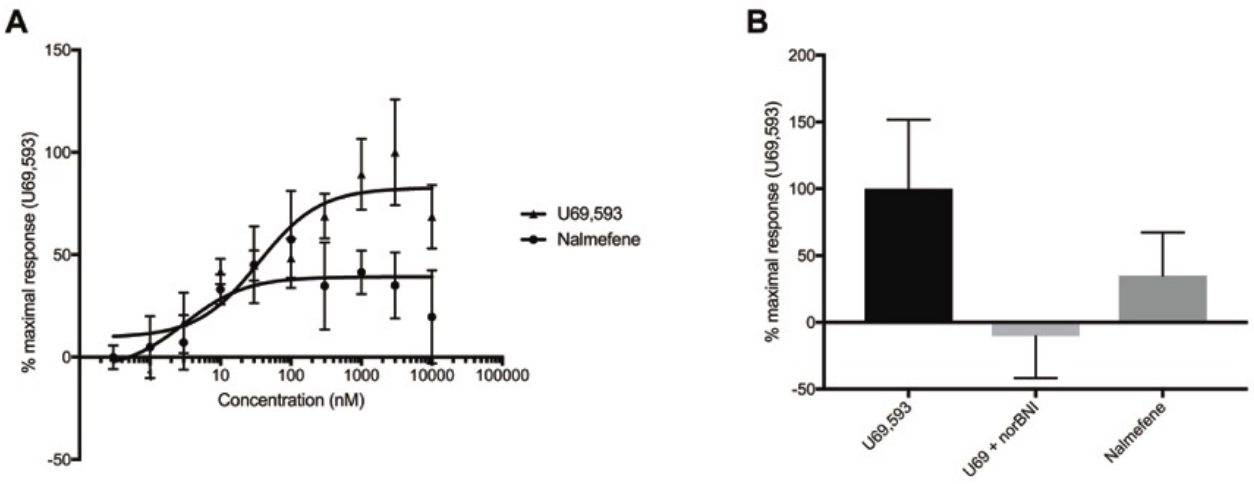

Figure 3.5. [^{35}S]GTPγS binding in mouse striatum tissue

Mouse striatum tissue was homogenized and incubated with 10nM [^{35}S]GTPγS and increasing concentrations of test compounds. E_{max} values are shown here as a percentage of max U69,593 response (2000-8000 DPM). (A) Dose-response curve for U6,593 had an EC_{50} of 34.7nM and nalmefene had an EC_{50} of 3.1nM. (B) E_{max} values alone are shown for co-treatment of tissue with 10μM U69,593 and 10μM antagonist norBNI and treatment of tissue with 20μM nalmefene.

3.1.5 Discussion

Many studies have pointed out the caveats of studying GPCR signaling pathways using heterologous cell systems. Unfortunately, it is currently necessary to use modified receptor and arrestin proteins in order to directly measure arrestin recruitment. In addition to the enzyme complementation assay used here, other methods of measuring arrestin recruitment also utilize fusion proteins, such as FRET and BRET. The less direct methods of measuring arrestin activity, such as internalization or p38 phosphorylation, do not require modified proteins, however, they do not account for the potential contributions of other signaling pathways.

In addition to the issue of modified protein structure and function, there is also recent evidence that GRK2 expression levels affect measurements of arrestin signaling at the mu opioid receptor,[89] including in the DiscoverX PathHunter assay.[45] Specifically lower levels of GRK2

expression were shown to mask partial agonism by decreasing overall signal. It is possible that the lack of GRK2 expression in the U2OS cells used here is leading us to underestimate the amount of arrestin recruitment caused by some agonists, such as the morphinan compounds that showed almost no measurable arrestin recruitment (Figure 3.2 B). However, our results are consistent with previous studies of morphinan compounds using other methods to assess arrestin activation. For example, nalbuphine was shown to cause minimal internalization,[54] and buprenorphine also demonstrated minimal arrestin recruitment in a BRET assay that included GRK2 co-expression.[81]

Using the U2OS DiscoverX PathHunter cell line for the [^{35}S]GTPγS assay, we found an unusually high level of G-protein coupling compared to previous studies. In particular, the morphinan series of compounds was found to have higher E_{max} values in the [^{35}S]GTPγS assay than expected – most published reports give maximal efficacy of less than 50% (compared to reference agonists) for compounds nalmefene, naltrexone and nalbuphine, where we demonstrated maximal efficacy between 70-80% compared to the full agonist U69,593 (Figure 3.4 B). This assay has been reported to be particularly susceptible to cellular context, because of different coupling levels for different G-proteins,[81] as well as a saturation effect if levels of receptor expression are too high. While the goal of this study was to investigate both signaling pathways within the same cell line, in future studies it would be beneficial to measure G-protein signaling directly in disease-relevant tissue.

To investigate G-protein activation in a more physiologically-relevant context, we tested several compounds for [^{35}S]GTPγS binding in mouse striatal tissue. This assay showed similar levels of [^{35}S]GTPγS binding for the reference agonist U69,593, and demonstrated lower efficacy agonism for the morphinan compound nalmefene that is more consistent with both

previous literature and known effects in humans (Figure 3.6 B). Previous studies have shown that nalmefene is a partial KOR agonist in humans, using the serum prolactin as a biomarker for KOR activation.[32] Additionally, data from humans in clinical trials and post-marketing data from the use of nalmefene to treat alcohol addiction indicates that nalmefene does not cause side effects like hallucinations or psychotomimesis,[90] while full KOR agonists tested in humans, such as spiradoline (U62,066E) and salvinorin A do.[28,31] Together with in vitro G-protein activation data from other cell lines and studies, these data indicate that nalmefene is likely acting as a partial KOR agonist in the therapeutically-relevant setting, and the data from the striatal tissue [^{35}S]GTPγS experiment more accurately models that setting than the [^{35}S]GTPγS data from the U2OS cells (Figures 3.4 B, 3.6 B). While this system is promising for measuring G-protein binding, it is still relatively inconsistent. Additional troubleshooting and optimization are required, and then additional compounds can be examined in the future.

3.2 KOR ligand bias and relationships between in vitro metrics and in vivo activity

In order to quantify ligand bias for these compounds in our U2OS cell system, we first needed to control for systemic factors. For example, directly comparing the EC_{50} of a compound in the [^{35}S]GTPγS assay and the β-arrestin-2 assay will not give a good measurement of bias because of differences in assay kinetics. To control for this kind of "system bias", we chose to use U69,593 as our reference ligand to run alongside all the other KOR agonists tested here. Each ligand could then be compared against the reference ligand, to control for assay-specific factors. All measurements of ligand bias are dependent on the reference agonist chosen, and this is another part of the "context" that is important to describe when describing a biased agonist.

For studies of the KOR, several different ligands have been used as the reference. Several groups have used dynorphin A (1-17), because it is the major endogenous neuropeptide.[54] We chose U69,593 as the reference agonist because it has been widely-characterized in many different labs as a full, unbiased agonist at the KOR with full activation of both the G-protein and β-arrestin-2 signaling pathways using several different assays.

To compare the activity of a test ligand to the reference ligand, we used a method based on the operational model of partial agonism. First described by Black and Leff in the 1980's, this model uses dose response data from both the test agonist and the reference agonist to calculate a measurement of intrinsic relative activity (RAi).[69] This metric takes into account both the potency and maximal efficacy of the test agonist, and is presented here as the LogRAi. While this metric can be calculated from fitting dose-response data directly to the operational model, when the Hill slope is equal to 1 it can be estimated using the E_{max} and EC_{50} values of the dose-response curve. For compounds that had very low intrinsic activity in a given assay, and therefore could not be fit to a traditional sigmoidal dose-response curve, we used a modified

version of the operational model (described by Stahl at al. 2015)[71] to directly calculate the LogRAi value from dose-response data. LogRAi values were calculated for each compound for both G-protein and arrestin assays, and compared to quantify ligand bias between the two signaling pathways (ΔLogRAi).

We could then use this composite ΔLogRAi metric, as well as metrics from both the in vitro assays alone, to investigate relationships between agonist activity in vitro and in vivo. Because of the use of heterologous cell lines and the context-dependent nature of many of these signaling pathways, it is difficult to use in vitro activity to predict in vivo behaviors. This is critical, however, for drug discovery efforts. The Bohn lab recently demonstrated that a calculated composite "bias factor" for MOR agonists tested in vitro correlated with the therapeutic window between antinociceptive effects and respiratory depression in mice.[46] Similarly, the Van Rijn lab demonstrated that efficacy measured in an arrestin assay correlated with increased alcohol intake caused by DOR activation in mice.[91] Both of these studies demonstrate how these in vitro-in vivo relationships could help to improve drug discovery efforts for safer and more effective opioid receptor agonists. In these studies, we looked at the relationship between KOR agonist activity in vitro and sedation in mice, measured by the rotarod assay.

3.2.1 Quantifying ligand activity bias with intrinsic relative activity metric

To compare each compound to U69,593, we calculated the $LogRAi_G$ and $LogRAi_{Arr}$, which give a quantitative comparison of the activity of each compound to the reference agonist U69,593 in the given assay (Figures 3.2 and 3.3). By definition the reference agonist U69,593 has a LogRAi of 0. A value larger than 0 indicates a compound that has higher relative intrinsic

activity in that assay, and any value below 0 indicates a compound that has less activity relative compared to the reference agonist in that assay, as seen in Figures 3.2 and 3.3. In certain cases where the maximal efficacy was very low in the β-arrestin-2 recruitment assay, a dose-response curve could not be fit to the data and no E_{max} and EC_{50} value was available for LogRAi estimation. This was the case for several morphinan compounds, as well as the diphenethylamines HS666 and BPHA (Figure 3.3). In these cases, additional dose-response curves of the compounds were tested in the presence of a steady concentration of U69,593 to determine the antagonist properties of the compounds. These antagonist curves were then fit to a modified version of the operational model of partial agonism and the LogRAi values were calculated from these parameters.[71]

In order to compare the bias of a compound between the two signaling pathway assays, the $\Delta LogRAi_{G\text{-}Arr}$ was calculated as ($\Delta LogRAi_{G\text{-}Arr} = LogRAi_{G} - LogRAi_{Arr}$) (Figure 3.6). Almost all the compounds tested were G-protein biased in this system compared to the reference agonist U69,593. Salvinorin A and its derivative mesyl salvinorin B were the most "balanced" compounds tested, and most of the other arylacetamide compounds were also relatively unbiased (Figure 3.6). The majority of the morphinan compounds, on the other hand, exhibited very robust G-protein bias. The exception in this structural class was nalfurafine, which was the only compound we tested that was biased for β-arrestin-2 recruitment over G-protein signaling (with a negative ($\Delta LogRAi_{G\text{-}Arr}$ value) (Figure 3.6). Both groups of recently-described KOR agonists, the quinoxalines and the diphenethylamines, were G-protein biased with varying degrees of bias.

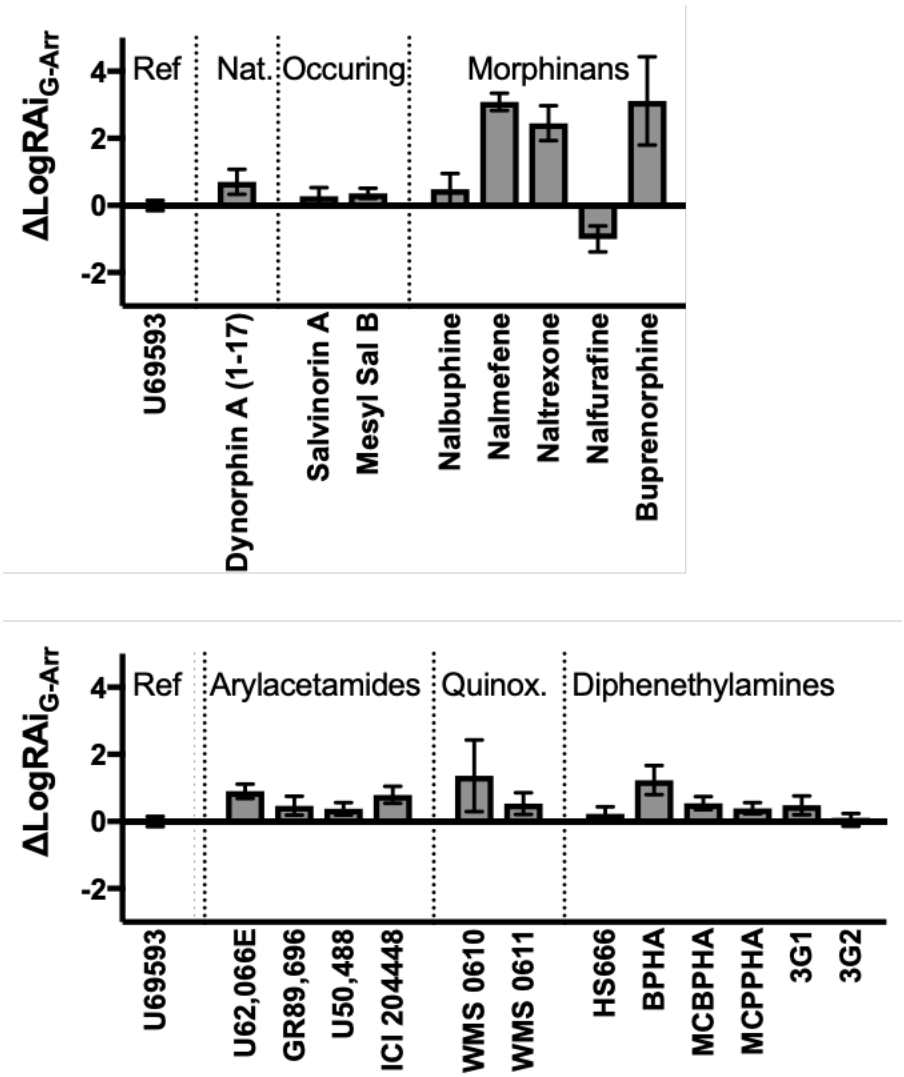

Figure 3.6. ΔLogRAi measurements of bias for KOR ligands

The $\Delta LogRAi_{G\text{-}Arr}$ values were calculated ($LogRAi_{G}$ - $LogRAi_{Arr}$) to quantify ligand bias for each compound compared to the reference agonist U69,593. Positive $\Delta LogRAi_{G\text{-}Arr}$ values indicate bias for G-protein signaling over β-arrestin-2 signaling, while negative $\Delta LogRAi_{G\text{-}Arr}$ values indicate bias for β-arrestin-2 signaling over G-protein signaling, relative to the reference agonist U69,593. $\Delta LogRAi_{G\text{-}Arr}$ values were calculated using the average EC_{50} and E_{max} as described in the methods from three separate experiments, and are shown here plus/minus combined standard deviations.

3.2.2 Correlation between ligand activity in vitro and in vivo sedation behavior

The goal of quantifying ligand activity in vitro was to develop a method to determine which compounds have the desired therapeutic properties. In order to better understand which in vitro measurements of ligand activity best modeled in vivo responses, we compared different in vitro metrics for both the G-protein and β-arrestin-2 signaling assays to an in vivo measurement of sedation / motor incoordination.

To assess the undesirable effects of sedation / motor incoordination, we used the rotarod assay. In this assay, C57BLJ6 mice were trained to run on an accelerating rod and their baseline ability to stay on the rod as it accelerates was recorded. Mice were then injected intraperitoneally with drug and tested for rotarod performance. Ligands that caused sedation or motor incoordination led to decreased rotarod performance compared to baseline (mice fell off of the rod earlier than they had in their baseline run). We tested high doses of these compounds in this assay, both to assess the maximum possible rotarod effect and to minimize the effect of differing pharmacokinetic properties between compounds.

The maximum effect of most compounds tested occurred at 30 minutes post-injection. Results are presented as the percentage of baseline rotarod performance (e.g. 100% of baseline performance is no impairment) at this 30 minute timepoint. Consistent with previous studies, we found that the arylacetamide compound U50,488 was very sedative at the high dose of 30mg/kg (Figure 3.7). The morphinan compound nalfurafine was also very sedative, and more potent than U50,488, with a similar effect at only 3mg/kg. Most of the diphenethylamine compounds tested (MCBPHA, MCPPHA, 3G1 and 3G2) had a partial effect in this assay, with rotarod performance between 54% and 70% of baseline performance (Figure 3.7). The diphenethylamine BPHA, on the other hand, did not cause any measurable rotorod impairment (Figure 3.7). The morphinan

compounds nalmefene and nalbuphine similarly did not cause any measurable rotarod impairment, with rotarod performance close to 100% that of baseline testing (Figure 3.7).

This maximum effect on the rotarod test was then compared to several different in vitro measurements of ligand activity using Pearson r correlation (Figure 3.8). There was a significant correlation ($r = -0.97$, $p<0.001$) between the E_{max} measured in the β-arrestin-2 recruitment assay and the maximum effect on the rotarod test (Figure 3.8 A). However, there was no significant correlation between the E_{max} measured in the [^{35}S]GTPγS assay and the rotarod performance (Figure 3.8 C). Likewise, there was no correlation between the EC_{50} in the [^{35}S]GTPγS assay or the $LogRAi_G$ measurement of relative activity (Figure 3.8 D). Because so many of the compounds tested in the β-arrestin-2 recruitment assay had very little intrinsic activity, the correlation for the arrestin EC_{50} data is not shown. From the limited data available, there was no significant correlation between arrestin EC_{50} and rotarod sedation. However, there was a significant correlation ($r = -0.96$, $p < 0.0001$) between the $LogRAi_{Arr}$ and rotarod performance (Figure 3.8 B). Finally, there was a weaker, but significant, correlation ($r = -0.76$, $p<0.05$) between the $\Delta LogRAi_{G\text{-}Arr}$ measurement of ligand bias and rotarod performance (Figure 3.8 F).

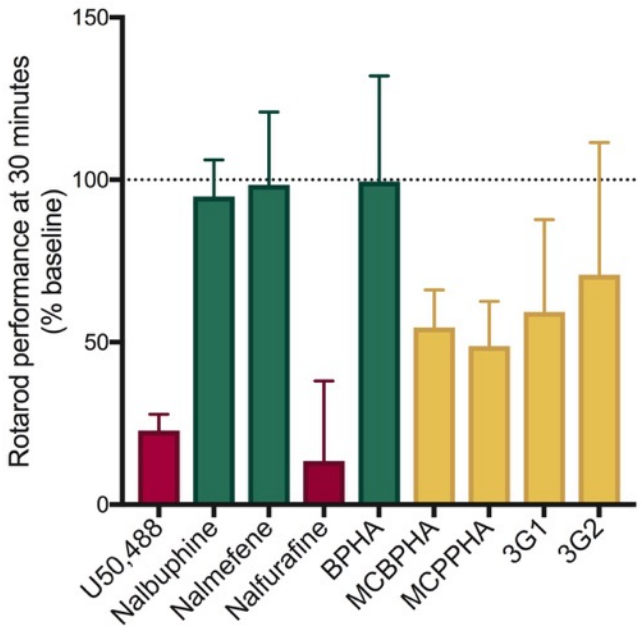

Figure 3.7. Rotarod sedation by select KOR ligands

Rotarod performance is reported here as the percentage of baseline performance 30 minutes after intraperitoneal injection of 30mg/kg compound (except nalfurafine, at 3mg/kg). N = 7-8 animals per group.

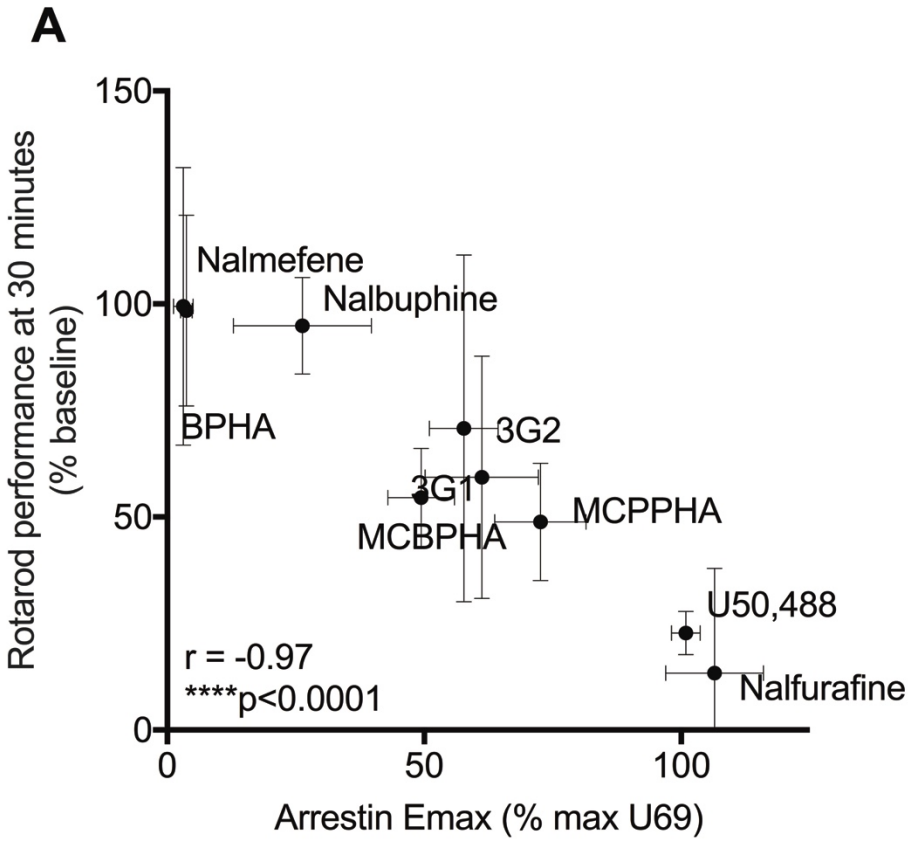
A
150
100
50
0
Rotarod performance at 30 minutes (% baseline)
Nalmefene
Nalbuphine
BPHA
3G2
3G1
MCPPHA
MCBPHA
U50,488
Nalfurafine
r = -0.97
****p<0.0001
0
50
100
Arrestin Emax (% max U69)

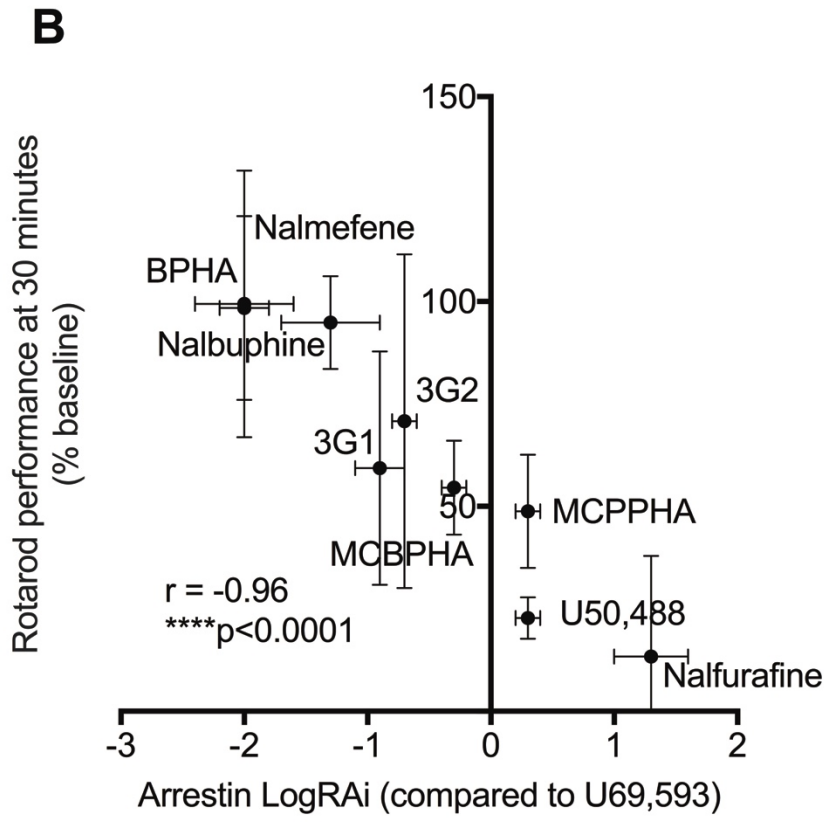
B
150
100
50
Rotarod performance at 30 minutes (% baseline)
Nalmefene
BPHA
Nalbuphine
3G2
3G1
MCPPHA
MCBPHA
U50,488
Nalfurafine
r = -0.96
****p<0.0001
-3
-2
-1
0
1
2
Arrestin LogRAi (compared to U69,593)

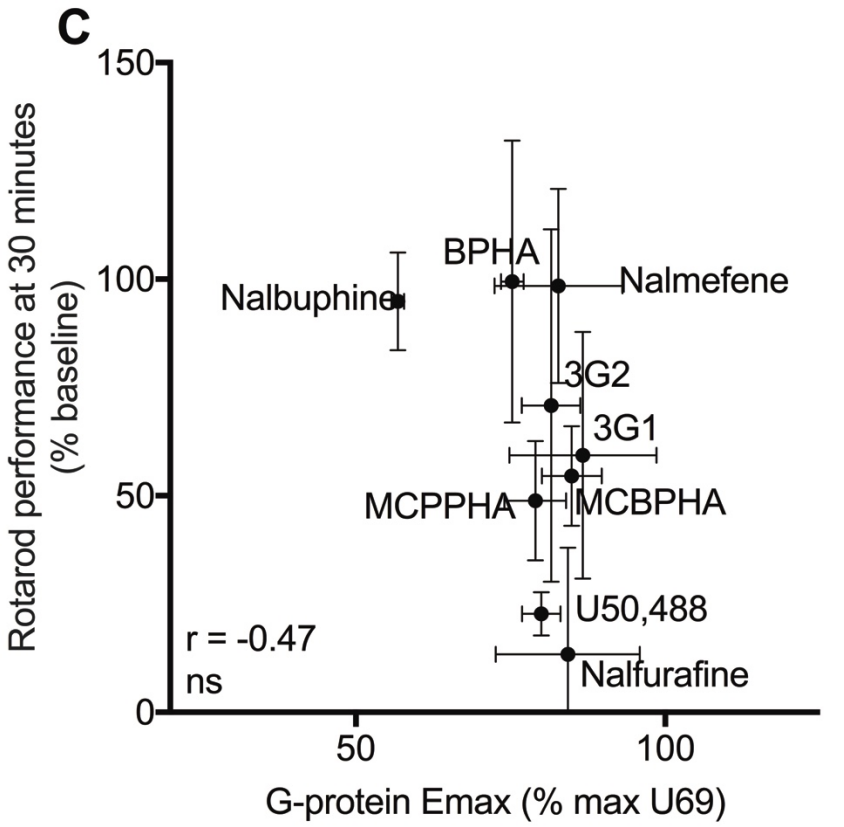
C
150
100
50
0
Rotarod performance at 30 minutes
(% baseline)
BPHA
Nalmefene
Nalbuphine
3G2
3G1
MCPPHA
MCBPHA
U50,488
r = -0.47
ns
Nalfurafine
50
100
G-protein Emax (% max U69)

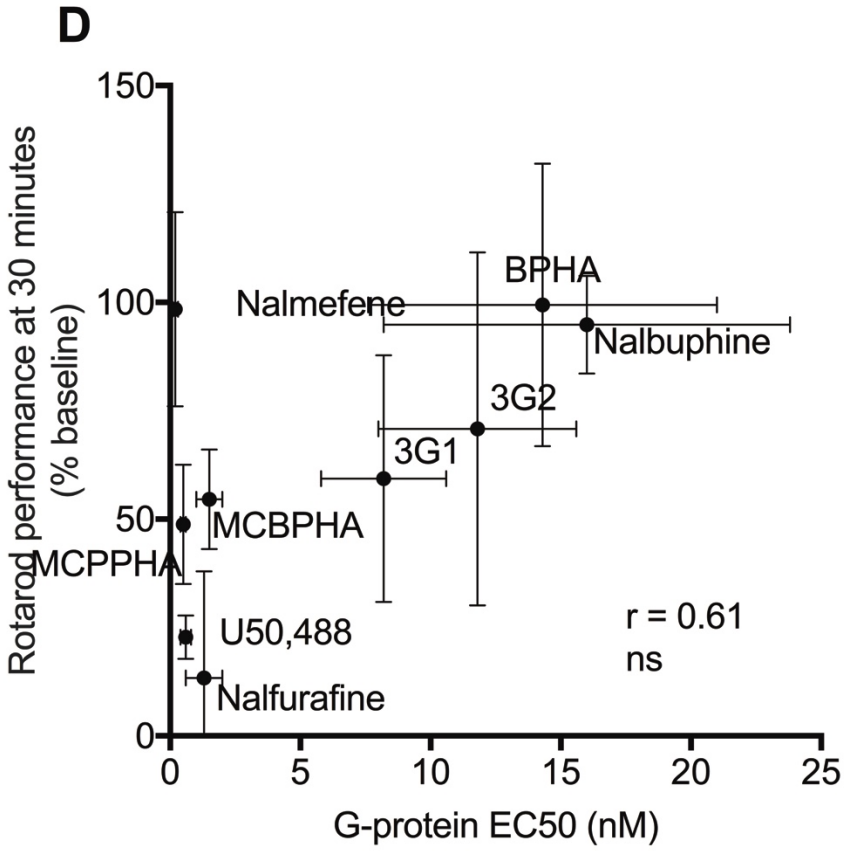
D
150
100
50
0
Rotarod performance at 30 minutes
(% baseline)
BPHA
Nalmefene
Nalbuphine
3G2
3G1
MCBPHA
MCPPHA
U50,488
r = 0.61
ns
Nalfurafine
0
5
10
15
20
25
G-protein EC50 (nM)

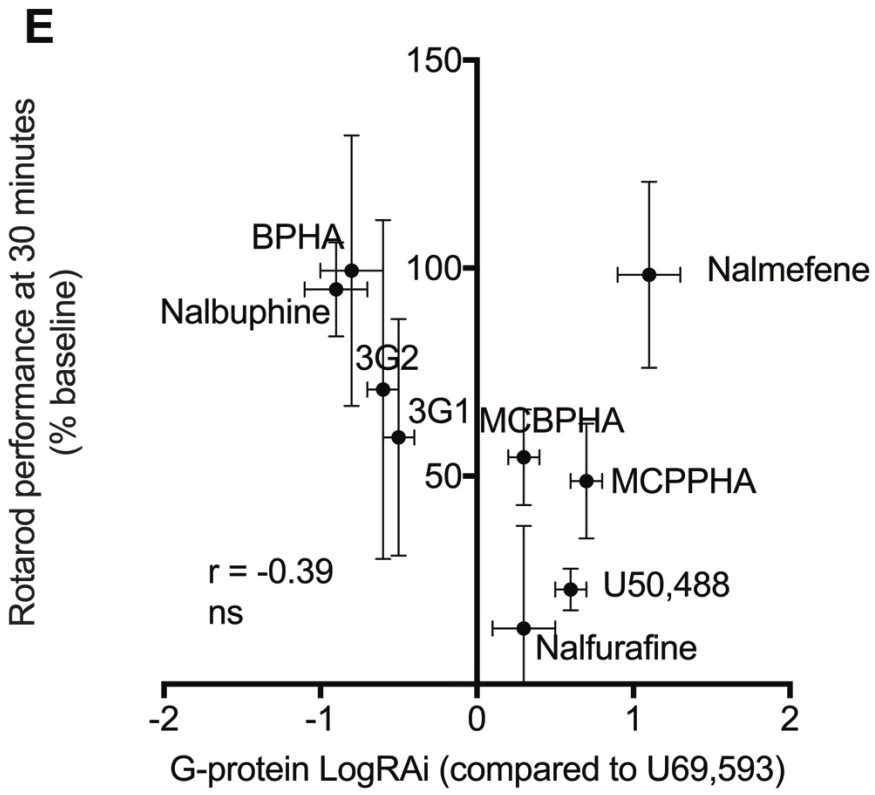
E
150
100
50
Rotarod performance at 30 minutes
(% baseline)
BPHA
Nalbuphine
3G2
3G1
MCBPHA
MCPPHA
Nalmefene
U50,488
Nalfurafine
r = -0.39
ns
-2
-1
0
1
2
G-protein LogRAi (compared to U69,593)

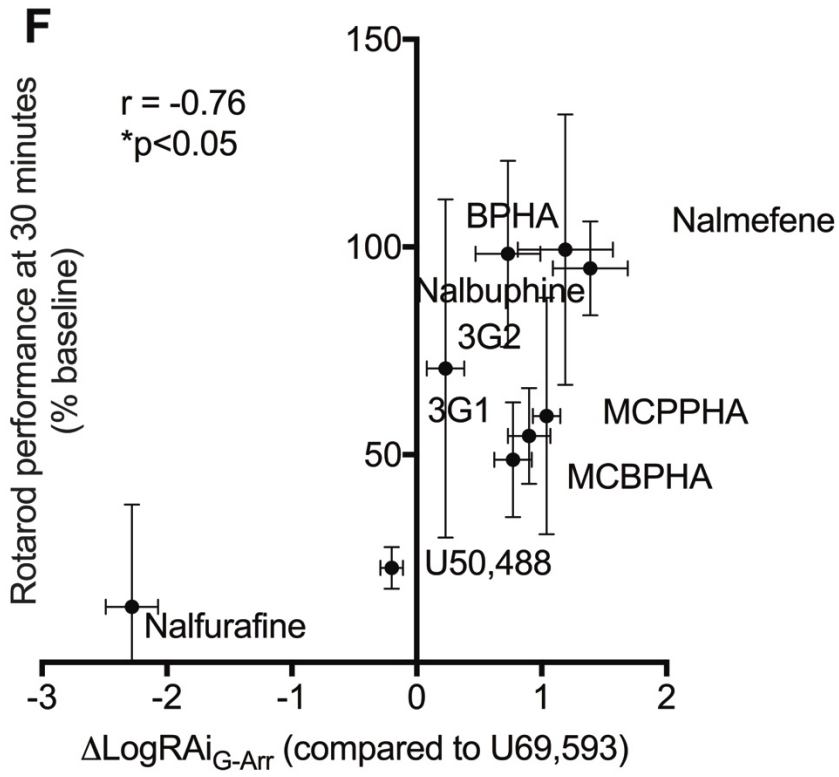
F
150
100
50
Rotarod performance at 30 minutes
(% baseline)
r = -0.76
*p<0.05
BPHA
Nalmefene
Nalbuphine
3G2
3G1
MCPPHA
MCBPHA
U50,488
Nalfurafine
-3
-2
-1
0
1
2
ΔLogRAi$_{G\text{-}Arr}$ (compared to U69,593)

Figure 3.8. Correlation of in vitro metrics with rotarod sedation

Pearson r correlations comparing in vitro measurements (X axis) with rotarod performance were calculated for (A) β-arrestin-2 E_{max}, (B) β-arrestin-2 LogRAi, (C) G-protein E_{max}, (C) G-protein EC_{50}, (E) G-protein E_{max}, and (F) the $\Delta LogRAi_{G\text{-}Arr}$ measurement of ligand bias. Both measurements of β-arrestin-2 activity (A and B) as well as the measurement of ligand bias (F) correlated significantly with rotarod activity.

3.2.3 Discussion

Using the U2OS DiscoverX PathHunter cell line for both the [^{35}S]GTPγS and β-arrestin signaling pathway assays and U69,593 as the reference agonist, we found the vast majority of the compounds we tested to be G-protein biased agonists (Figure 3.6). Even compounds that had previously been reported to be relatively unbiased compared to U69,593, such as salvinorin A, were slightly G-protein biased in this system, as well as the other arylacetamide compounds that are structurally very similar to U69,593. This indicates that U69,593 was uniquely effective at recruiting β-arrestin in this system compared to the other agonists, however it also suggests that our system was particularly sensitive to G-protein coupling over arrestin recruitment.

We found the majority of the morphinan compounds, namely nalbuphine, nalmefene, naltrexone and buprenorphine, to be very G-protein biased (Figure 3.6). This is consistent with previous reports of their ligand bias in these signaling pathways, even using other cell lines and other endpoints.[32,81] A study of ligand bias for MOR agonists demonstrated that measurements of ligand bias are most resilient to differing context in the cases of "extreme" bias, when there is little measurable activity at one of the signaling pathways.[46] Nalfurafine, on the other hand, was found to be arrestin-biased by our calculations (Figure 3.6), while it has been described as both unbiased and G-protein biased using other cell lines and other end-points for G-protein and arrestin signaling. In our hands nalfurafine had similar potency for G-protein signaling to the

reference agonist U69,593. In the β-arrestin-2 recruitment assay, however, nalfurafine was ~20-fold more potent than the reference agonist. This high potency in the β-arrestin-2 recruitment assay then translated to a negative $\Delta LogRAi_{G\text{-}Arr}$ value, which indicated arrestin-bias in our system. Further investigation into the signaling properties of nalfurafine could help to explain its unique behavioral profile compared to other KOR agonists.

The diphenethylamine series of compounds had varied bias profiles, with the compound BPHA having a larger $\Delta LogRAi_{G\text{-}Arr}$ value (indicating G-protein bias) while the remaining compounds had $\Delta LogRAi_{G\text{-}Arr}$ values closer to zero (Figure 3.6). Interestingly, BPHA was the only diphenethylamine compound tested that had a non-cyclic side chain off of the central amine, suggesting an important role for this part of the molecule in determining arrestin recruitment (Figure 3.1 E). WMS 0610 and WMS 0611 differ only in one phenyl ring (Figure 3.1 D), however WMS 0610 was significantly more G-protein biased than WMS 0611 (Figure 3.6). Data like these can be used in the future to help drive structure-activity relationship studies of KOR ligands, to improve drug discovery efforts.

Finally, we investigated the relationships between the in vitro measurements and quantifications of the activity of these ligands and their actual effect in an in vivo assay of sedation / motor incoordination in mice. We found that measurements of arrestin recruitment activity, including the maximum efficacy (E_{max}) and the LogRAi (which takes into account both E_{max} and EC_{50}) were significantly correlated with the maximum effect in the rotarod assay (Figure 3.8 A, B). None of the measurements of G-protein activity, on the other hand, correlated with this rotarod effect (Figure 3.8 C, D, E). This supports the hypothesis generated by previous studies of single structural classes of biased KOR ligands that β-arrestin-2 recruitment is involved in KOR-mediated sedation as measured by the rotarod assay.[51,52,86] While the

quantification of overall G-protein vs arrestin bias ($\Delta LogRAi_{G\text{-}Arr}$) did have a significant correlation (Figure 3.8 F), it was weaker than the arrestin correlations alone. Together, these data suggest that a G-protein biased agonist at the KOR could be more likely to have an acceptable therapeutic "window", due to a lack of sedative side effects even at high doses.

CHAPTER 4. OTHER SIGNALING PATHWAYS DOWNSTREAM OF THE KOR

4.1 ERK1/2 and mTOR signaling pathway activation by KOR ligands

In addition to profiling the G-protein and β-arrestin-2 recruitment of the ligands that target the KOR, there are several other signaling pathways that have been shown to be important for KOR activity and specifically addiction-related behaviors. Various mitogen-activated-protein kinases (MAPK), for example, have been shown to be phosphorylated by KOR agonist activity, including extracellular-related kinases 1 and 2 (ERK1/2).[92] ERK1/2 has also been shown to be important for the incubation of cocaine craving, and other drug-related behaviors.[93] There have been varying results in the literature linking ERK1/2 phosphorylation at different time points to either G-protein or arrestin signaling, however it is difficult to draw larger generalizations across these studies because of the diverse array of cell lines, time points and KOR agonists used. Importantly, a study of a series of novel triazole KOR agonists demonstrated that ERK1/2 phosphorylation can be modulated independently of G-protein vs arrestin bias.[62] This was one of the first studies to suggest that downstream signaling pathways like ERK1/2 should be tested independently of G-protein and arrestin pathways, and that the pharmacological profile of KOR agonists had the potential for much more diversity than was previously believed.

The mTOR signaling pathway is now known to be important for integrating cellular signaling in the central nervous system.[94] More recently, the mTOR pathway has been shown to be important for KOR-mediated behavior, specifically aversion.[36,39] It is unclear, however, if and how mTOR activation is related to G-protein or arrestin signaling pathways. In this study we tested the same set of diverse KOR agonists (Figure 3.1) for ERK1/2 phosphorylation and mTOR pathway activation and compared their activity in these pathways to their activity in the

early signaling pathways (G-protein and arrestin) tested in Chapter 1. This ERK1/2 and mTOR signaling pathway data was also included in the 2019 publication with G-protein and arrestin signaling data for these compounds.[34]

4.1.1 ERK1/2 phosphorylation by KOR ligands in HEK cells

Diverse KOR agonists were tested for ERK1/2 phosphorylation in HEK cells using in-cell western blotting. Figure 4.1 shows representative dose-response curves, with potency and maximal efficacy values as averages of 3 replicates per experiment, as well as the $LogRAi_{ERK}$ value comparing the activity of each ligand to the reference ligand U69,593. In the case of very low intrinsic activity, compounds were tested as antagonists against a steady concentration of the reference agonist (300nM U69,593) and that data was used to calculate the $LogRAi_{ERK}$ value (Figure 4.2).

Within the class of naturally-occurring compounds and their derivatives, both Salvinorin A and mesyl salvinorin B had increased potency and maximum efficacy for ERK1/2 phosphorylation compared to the reference agonist U69,593, shown in black on every graph. U69,593 had an EC_{50} of 113.9nM in this assay, and salvinorin A and mesyl salvinorin B had EC_{50}s of 20.3 and 37.3nM, respectively (Figure 4.1 A). Dynorphin A(1-17), however, had decreased activity with respect to the reference agonist with a potency of 710nM.

Generally, the morphinan compounds had very little activity for ERK1/2 phosphorylation, and buprenorphine was able to block U69,593-induced ERK1/2 phosphorylation (Figure 4.1 B, Figure 4.2). The exception in this structural class was again nalfurafine, which had comparable activity to the reference agonist U69,593. The arylacetamide compounds, which are structurally similar to the reference agonist (Figure 3.1), had comparable

activity as well. The exception in this structural class was the compound GR89,696, which had increased potency and maximal efficacy compared to U69,593 with the lowest EC_{50} tested in this assay of 8.7nM (Figure 4.1 C).

The quinoxaline WMS 0611 had more activity than the structurally-similar WMS 0610 in this assay (Figure 4.1 D). Similarly, the diphenethylamine compounds had divergent activities (Figure 4.1 E). Both the quinoxaline and diphenethylamine classes of compounds had less activity overall than the reference agonist U69,593, and several of the diphenethylamine compounds were able to antagonist U69,593-induced ERK1/2 phosphorylation (Figure 4.2).

These data were collected from in-cell western blots in 96-well plates (Figure 4.3 A), and while we were unable to use U2OS cells for these full dose-response curves, single-concentration data from regular western blots suggested that levels of ERK1/2 phosphorylation were similar for U2OS and HEK cells (Figure 4.3 B).

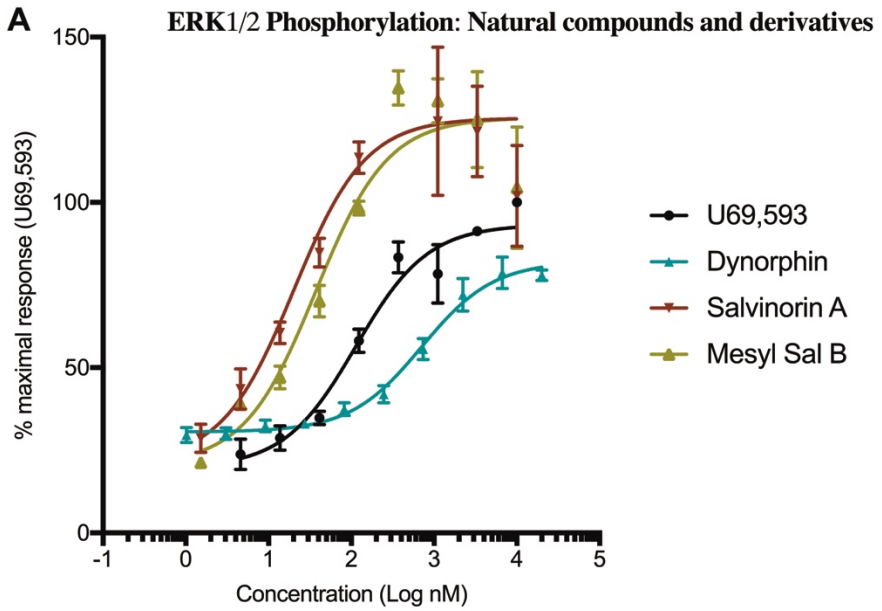

	EC50 (nM)	Emax (%max)	LogRAi$_{ERK}$
U69,593	113.9 (±40.1)	93.3 (±4.9)	0.0 (±0.03)
Dynorphin A (1-17)	710.5 (±149.7)	82.1 (±2.3)	-0.9 (±0.01)
Salvinorin A	20.3 (±10.5)	125.5 (±6.2)	0.9 (±0.1)
Mesyl Sal B	37.3 (±14.1)	125.6 (±5.3)	0.6 (±0.1)

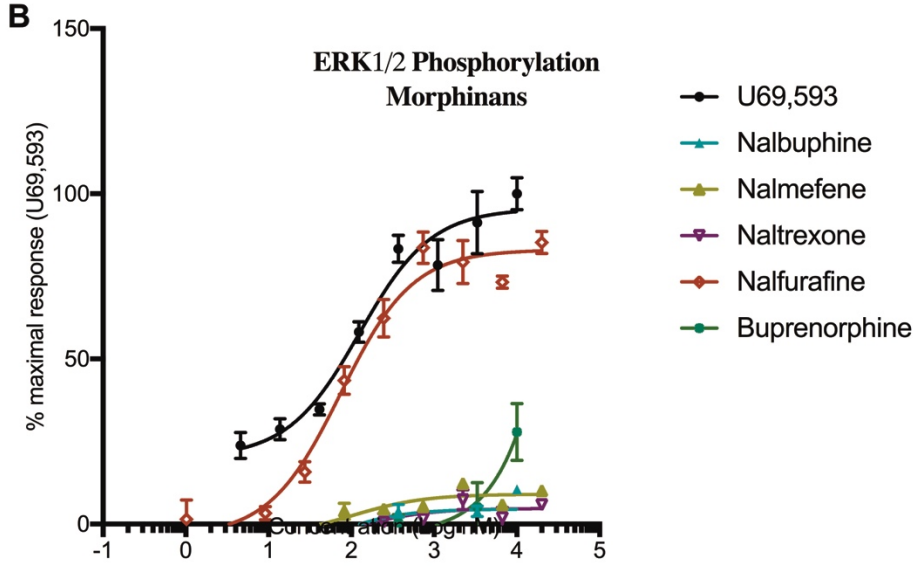

	EC50 (nM)	Emax (%max)	LogRAi$_{ERK}$
Nalbuphine	42.3 (±25.6)	4.6 (±1.3)	-0.9 (±0.3)
Nalmefene	105.1 (±52.6)	9.1 (±0.9)	-1.0 (±0.1)
Naltrexone	112.5 (±61.1)	4.8 (±0.9)	-1.3 (±0.1)
Nalfurafine	74.7 (±10.0)	83.1 (±1.7)	0.1 (±0.01)
Buprenorphine		27.9% at 20μM	-0.8 (±0.1)*

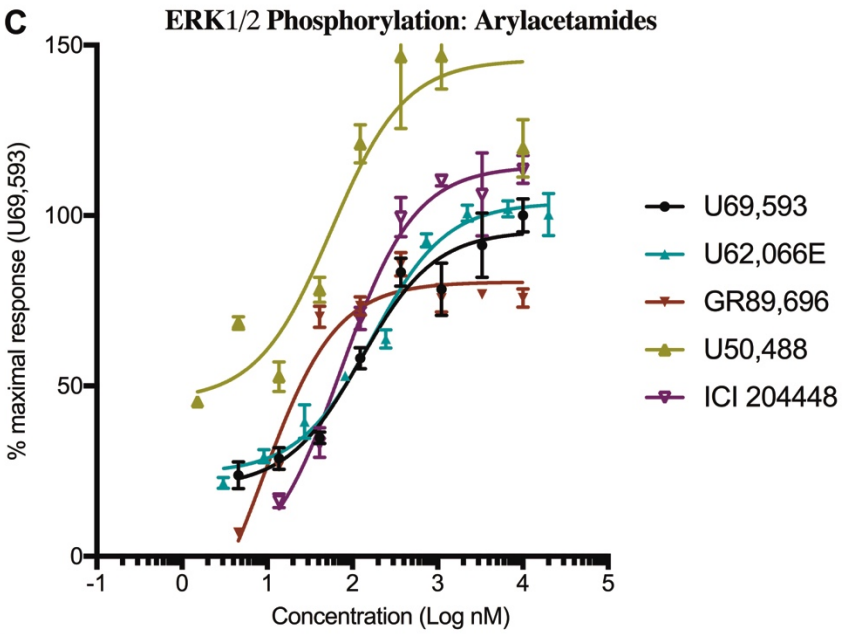

	EC50 (nM)	Emax (%max)	LogRAi$_{ERK}$
U62,066E	170.9 (±30.5)	103.7 (±2.2)	-0.1 (±0.01)
GR89,696	8.7 (±2.9)	80.5 (±2.0)	1.1 (±0.1)
U50,488	56.4 (±25.0)	145.7 (±6.4)	0.5 (±0.1)
ICI 204448	73.8 (±12.1)	114.5 (±2.1)	0.3 (±0.03)

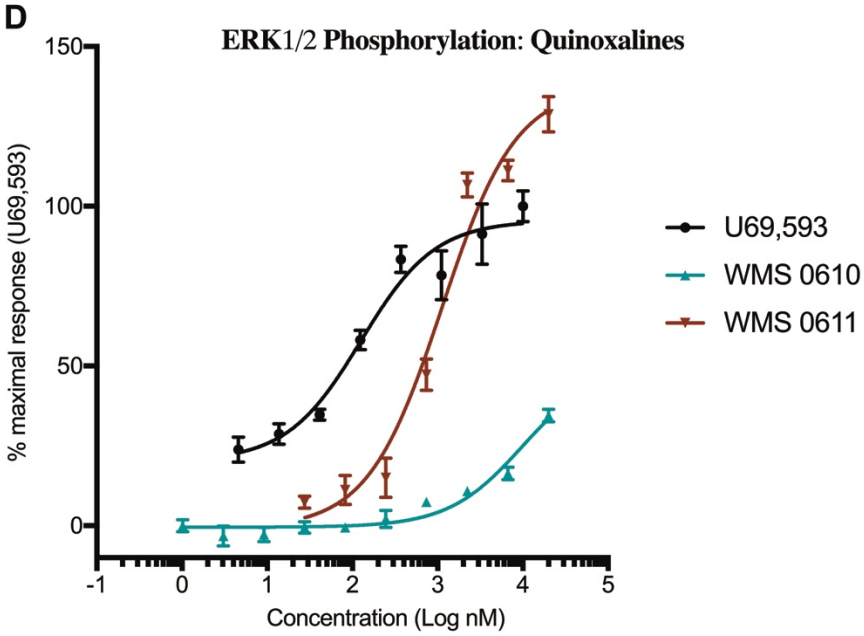

	EC50 (nM)	Emax (%max)	LogRAi$_{ERK}$
WMS 0610	9868 (±3740.0)	50.2 (±8.3)	-2.2 (±0.01)
WMS 0611	1125 (±236.6)	137.4 (±6.0)	-0.8 (±0.02)

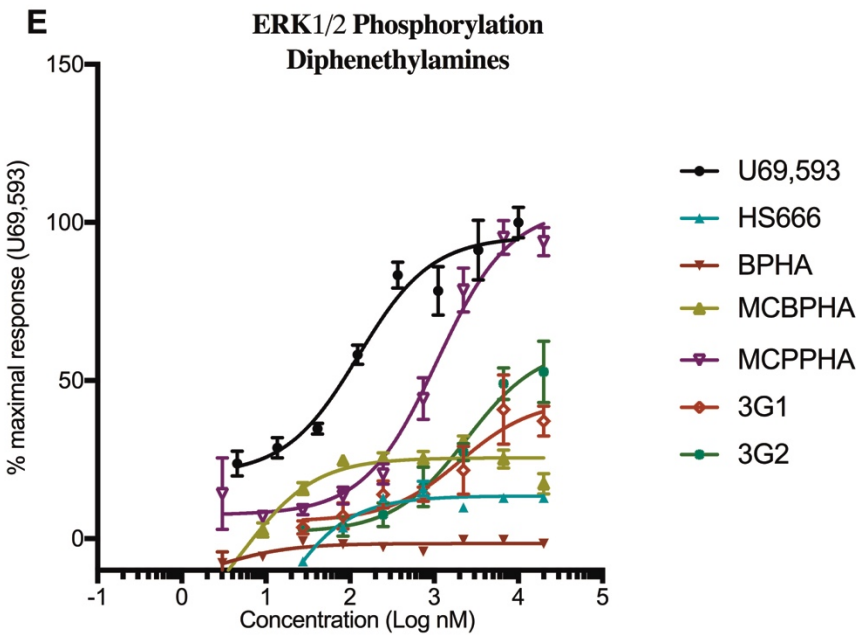

	EC50 (nM)	Emax (%max)	LogRAi$_{ERK}$
HS666	No Fit	13.5% at 20μM	-1.1 (±0.002)*
BPHA	No Fit	0% at 20μM	-1.1 (±0.04)*
MCBPHA	No Fit	25.6% at 20μM	-0.2 (±0.003)*
MCPPHA	1079 (±163.2)	104.5 (±3.3)	-0.9 (±0.01)
3G1	2057 (±928.1)	43.8 (±4.3)	-1.6 (±0.02)
3G2	2419 (±573.4)	61.0 (±3.6)	-1.5 (±0.01)

Figure 4.1. ERK1/2 phosphorylation by KOR ligands. Figures are arranged by structural class: (A) the endogenous ligand dynorphin A (1-17), the natural product salvinorin A and derivative mesyl salvinorin B, (B) morphinan compounds, (C) arylacetamide compounds, (D) quinoxaline compounds and (E) diphenethylamine compounds. All dose-response curves were normalized to the maximal U69,593 response from a concurrent sample of 10μM U69,593. Average EC_{50} and E_{max} values are represented as averages of 4 replicates per experiment (±SD). LogRAi values were estimated from these average EC_{50} and E_{max} values. For compounds with low intrinsic activity data from the antagonist curves were fit to the operational model of partial agonism to calculate LogRAi values (*). Dose-response curves are shown with a representative U69,593 dose-response curve, in black on each graph. U69,593 stimulation was between 160 and 250% above normalized baseline, and all cells were incubated with compound for 20 minutes.

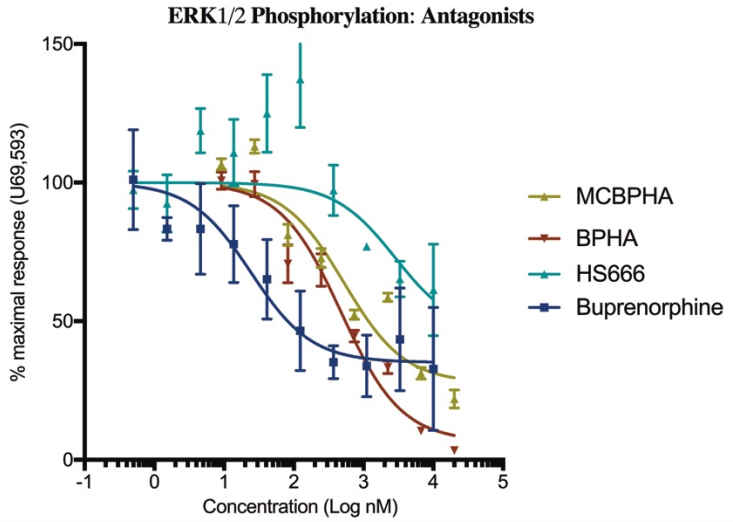

	IC50 (nM)	Max Inhibition (% 300nM U69)	LogRAi$_{ERK}$
HS666	2840 (±3971)	45.8 (±28.9)	-1.1 (±0.002)*
Buprenorphine	24.3 (±8.9)	35.1 (±5.5)	-0.8 (±0.1)*
BPHA	475.3 (±88.3)	6.6 (±3.9)	-1.1 (±0.04)*
MCBPHA	524.1 (±143.0)	27.8 (±4.5)	-0.2 (±0.003)*

Figure 4.2. Blockade of U69,593-induced ERK1/2 phosphorylation by KOR ligands

Compounds with low E_{max} values were tested as antagonists to block ERK1/2 phosphorylation by 300nM U69,593. Maximum inhibition values were calculated as the percentage of 300nM U69,593 response. IC50 and Max inhibition values are represented as averages of 4 replicates per experiment (±SD).

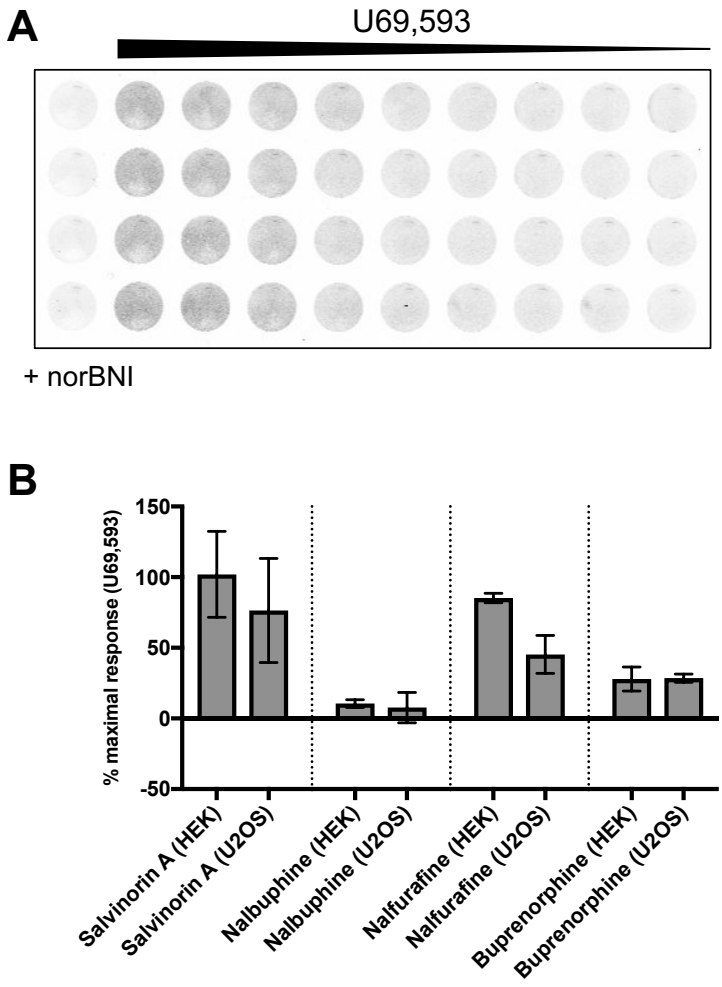

Figure 4.3. ERK1/2 phosphorylation in different cell lines and representative in-cell western. (A) A representative in-cell western blot in HEK293 cells, shown here in black and white. (B) Either HEK293 or DiscoverX U2OS cells were treated with 20μM ligand and levels of phosphorylated ERK1/2 were normalized to GAPDH expression and expressed as a percent of concurrent 10μM U69,593 activation. U69,593 stimulation was 160-250% of normalized baseline. U2OS data is from in-cell western blots with n = 4 replicates per experiment, and HEK293 data is from western blots with n=3 replicates per compound per experiment.

4.1.2 Quantifying the relationship between ERK1/2 activation and other signaling pathways with intrinsic relative activity metric

In order to quantify each compound's activity relative to the reference agonist U69,593 in this assay, we calculated the $LogRAi_{ERK}$ value, as described in Section 1.1.2. These $LogRAi_{ERK}$ values were then compared to the $LogRAi_{G}$ value and $LogRAi_{Arr}$ values for each compound, giving measurements of "bias" between these pathways: $\Delta LogRAi_{G\text{-}ERK} = LogRAi_{G} - LogRAi_{ERK}$ (Figure 4.4) and $\Delta LogRAi_{Arr\text{-}ERK} = LogRAi_{Arr} - LogRAi_{ERK}$ (Figure 4.5).

Overall, the $\Delta LogRAi_{G\text{-}ERK}$ were positive, indicating more G-protein signaling than ERK1/2 signaling compared to the reference agonist U69,593. Exceptions to this were the salvinorin-based compounds, as well as nalfurafine, U50,488 and several diphenethylamine compounds that had $\Delta LogRAi_{G\text{-}ERK}$ values close to 0 (Figure 4.4).

$\Delta LogRAi_{Arr\text{-}ERK}$ values, on the other hand, were mixed. Some compounds, such as the endogenous peptide agonist dynorphin A(1-17) had more arrestin signaling than ERK signaling compared to the reference agonist, indicated by its positive $\Delta LogRAi_{Arr\text{-}ERK}$ value (Figure 4.5). Other compounds, like the majority of the morphinans, had negative $\Delta LogRAi_{Arr\text{-}ERK}$ values, indicating more ERK signaling than arrestin signaling compared to the reference agonist in this system (Figure 4.5).

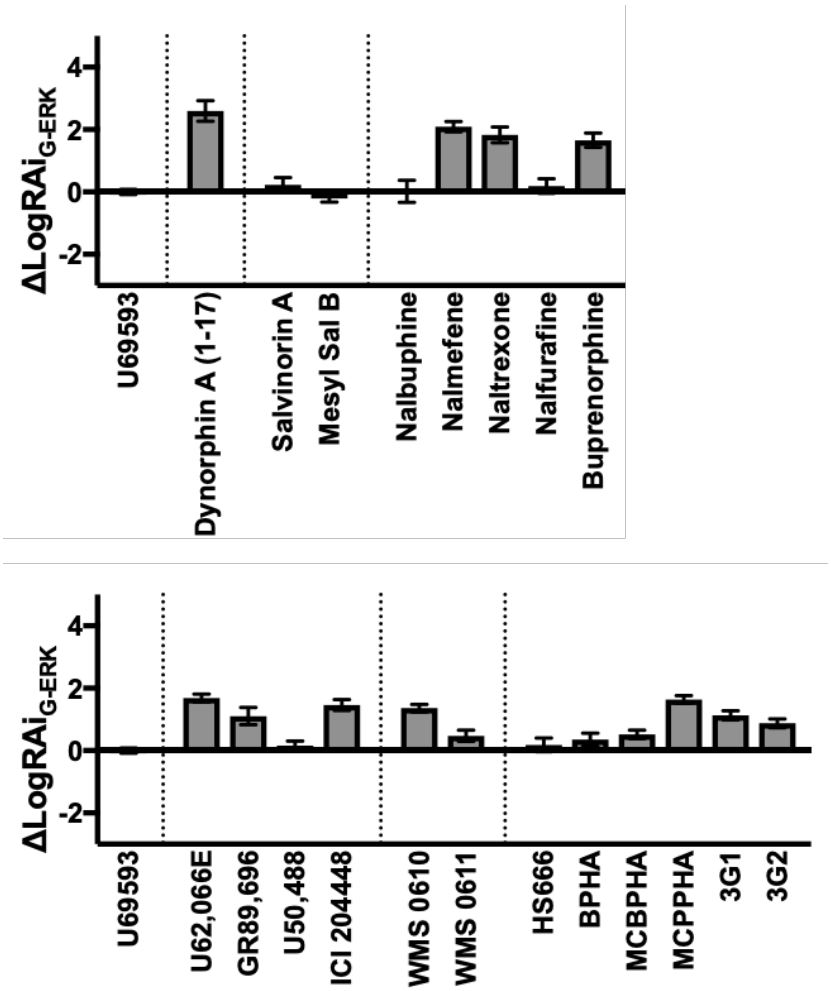

Figure 4.4. ΔLogRAi measurements between G-protein binding and ERK1/2 phosphorylation for KOR ligands

The $\Delta LogRAi_{G\text{-}ERK}$ ($LogRAi_G - LogRAi_{ERK}$) values were calculated to quantify discrepancies between G-protein activation and ERK phosphorylation for each compound compared to the reference agonist U69,593. Positive ΔLogRAi values indicate more G-protein signaling proportional to ERK1/2 phosphorylation, while negative $\Delta LogRAi_{G\text{-}ERK}$ values indicate more ERK1/2 phosphorylation compared to G-protein signaling, relative to the reference agonist U69,593. ΔLogRAi values are represented as the average of N=3 experiments, ±SD. $\Delta LogRAi_{G\text{-}ERK}$ values were calculated using the average EC_{50} and E_{max} as described in the methods from three separate experiments, and are shown here plus/minus combined standard deviations.

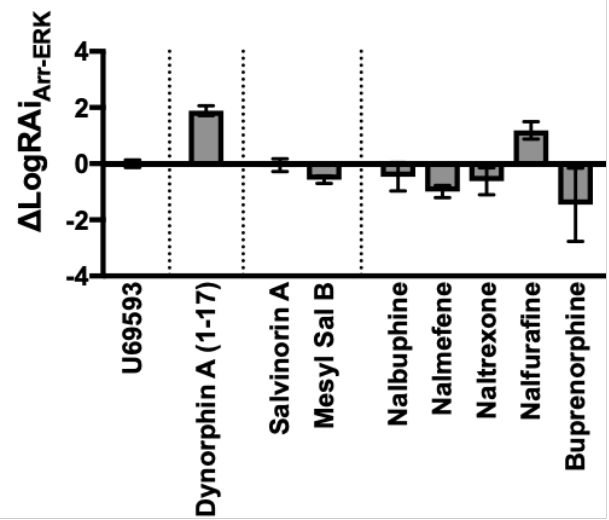

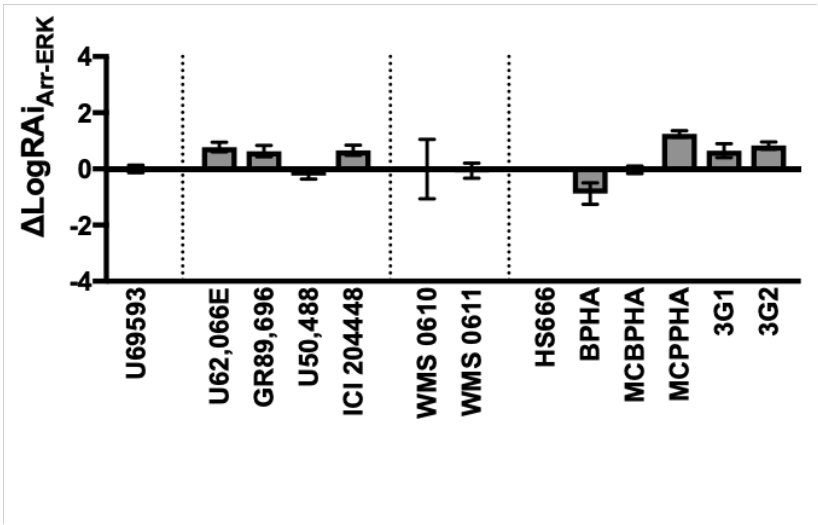

Figure 4.5. ΔLogRAi measurements between β-arrestin-2 and ERK1/2 phosphorylation for KOR ligands

The $\Delta LogRAi_{Arr\text{-}ERK}$ ($LogRAi_{Arr} - LogRAi_{ERK}$) values were calculated to quantify discrepancies between β-arrestin-2 recruitment and ERK phosphorylation for each compound compared to the reference agonist U69,593. Positive ΔLogRAi values indicate more β-arrestin-2 signaling proportional to ERK1/2 phosphorylation, while negative $\Delta LogRAi_{Arr\text{-}ERK}$ values indicate more ERK1/2 phosphorylation compared to β-arrestin-2 signaling, relative to the reference agonist U69,593. ΔLogRAi values are represented as the average of N=3 experiments, ±SD. $\Delta LogRAi_{Arr\text{-}ERK}$ values were calculated using the average EC_{50} and E_{max} as described in the methods from three separate experiments, and are shown here plus/minus combined standard deviations.

4.1.3 mTOR signaling pathway differentially regulated by KOR agonists

We also investigated the ability of these KOR agonists to activate the mTOR signaling pathway at a single high concentration (10-20 μM) by western blotting for phosphorylation of the selective downstream target Rps6 (ribosomal protein S6, Ser240/244) in DiscoverX U2OS cells (Figure 4.6). All data is shown as the mean intensity of Rps6 staining, normalized to GAPDH and compared to the reference agonist U69,593, with 3 replicates per experiment. A representative western blot is shown in Figure 4.6 as well. The reference agonist U69,593 showed robust phosphorylation of Rps6, similar to the serum positive control for mTOR activation. KOR-selectivity was tested by blocking Rps6 phosphorylation with norBNI co-treatment, and mTOR-selectivity was tested by inhibiting Rps6 phosphorylation with Torin1. LY2444296 and norBNI, both antagonists at the KOR, were used as negative controls and showed very low levels of Rps6 phosphorylation on their own (Figure 4.6). Almost all agonists tested showed at least 50% of maximum U69,593 Rps6 phosphorylation. Even lower-efficacy agonists in other assays, such as the morphinans naltrexone and buprenorphine, showed robust Rps6 phosphorylation in these western blots (Figure 4.6).

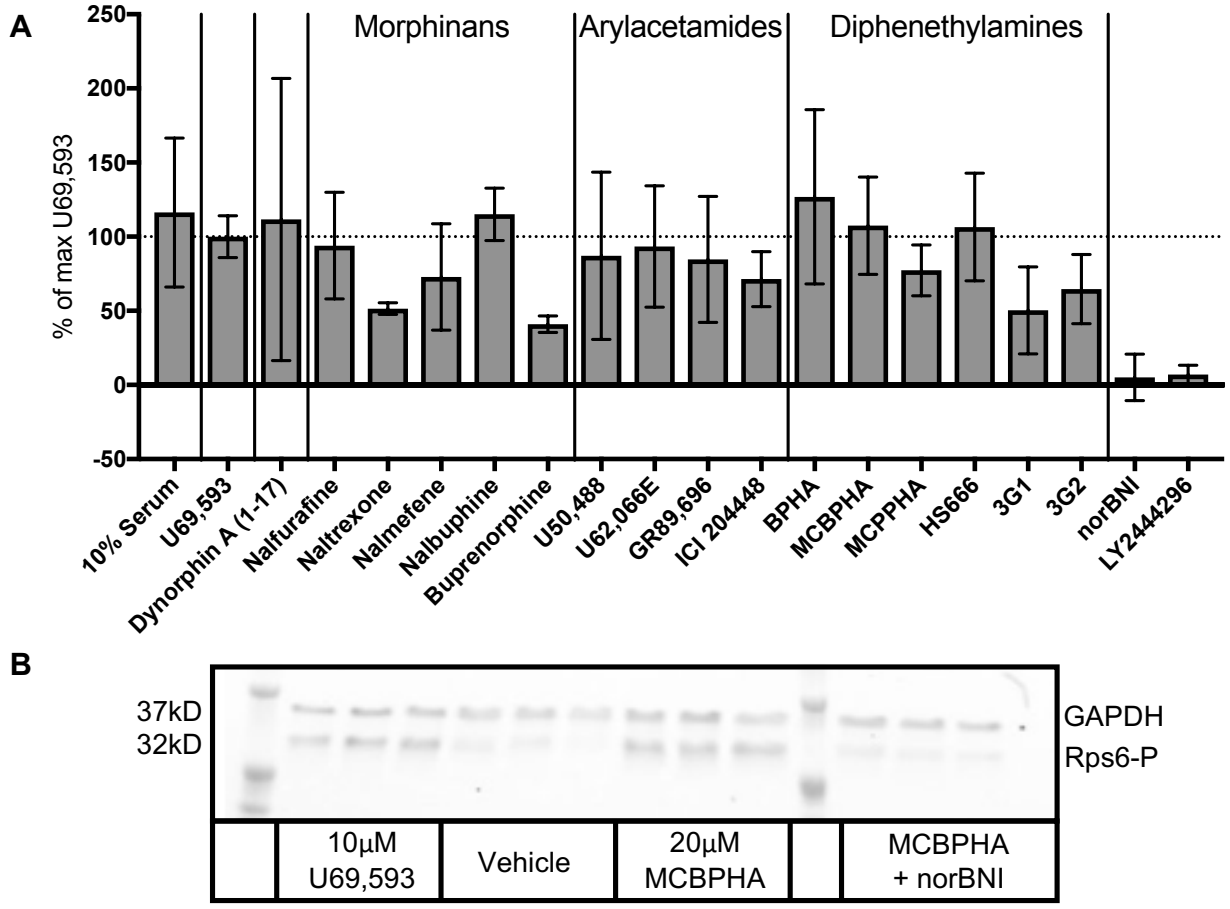

Figure 4.6. Rps6 phosphorylation by KOR ligands

Rps6 phosphorylation (Ser240/244) was quantified at a high concentration (10-20uM) of each compound (A) and normalized to the maximum Rps6 phosphorylation by U69,593. All signal was normalized to GAPDH expression. Data are presented as averages of 3 replicates per experiment, with standard deviation error bars. U69,593 stimulation was between 100-200% of normalized baseline. (B) Representative western blot, with 3 replicates per condition, probed for GAPDH (37 kD) and phosphorylated Rps6 (ribosomal protein S6, Ser240/244 – 32 kD).

4.1.4 Discussion

Here, we have systematically tested a diverse set of ligands for their ERK1/2 and mTOR activation and compared their activity in these pathways to their activity in the early GPCR signaling pathways (G-protein and β-arrestin). The differential activation of all of these signaling

pathways is known to be dependent on what components are available in the cell, and therefore cell line or tissue tested. While the G-protein, β-arrestin and mTOR assays were all done in the DiscoverX U2OS cell lines (expressing human KOR) for comparison, these cells did not adhere to the plates used for the ERK1/2 phosphorylation assay. Instead, HEK cells, expressing a FLAG-tagged mouse KOR were used for this assay, and therefore these studies are limited by the fact that these assays were done in different cell lines that express KORs of different species. Both HEK and U2OS cell lines showed a single peak of ERK1/2 phosphorylation in the first 20 minutes of treatment, however, and this early-phase peak phosphorylation was used for all studies. Phosphorylated ERK1/2 was comparable for compounds that were tested at single concentrations in both cell lines (Figure 4.3).

Dynorphin A (1-17) showed significantly less ERK1/2 phosphorylation compared to the reference agonist U69,593 (Figure 4.1 A). In addition to its G-protein over arrestin bias, this suggests that dynorphin A(1-17) may activate the KOR differently than many of the synthetic agonists tested. A recent study has shown that there can be dramatic differences in the physiological response of the MOR between peptide and synthetic agonists,[63] and our data suggest that the peptide dynorphin A(1-17) might also lead to differential signaling outcomes compared to synthetic KOR agonists. This is an important consideration for therapeutic development, which may rely on data from endogenous activation to establish the desired therapeutic effect. Salvinorin A and mesyl salvinorin B, on the other hand, showed uniquely robust ERK1/2 phosphorylation (Figure 4.1 A), that could potentially contribute to their unique downstream behavioral profiles.[95]

When the activity of these compounds in the ERK1/2 phosphorylation assay was compared to their activity in the G-protein and β-arrestin-2 assays, the many non-zero

$\Delta LogRAi_{G\text{-}ERK}$ and $\Delta LogRAi_{Arr\text{-}ERK}$ values overall (Figure 4.4 and Figure 4.5) indicated that ERK1/2 phosphorylation is not directly or uniquely downstream of just one of these other pathways. Overall positive $\Delta LogRAi_{G\text{-}ERK}$ values (Figure 4.4) indicated again that U69,593 may uniquely activate ERK1/2 phosphorylation compared to G-protein activation, and demonstrated further that our system is very sensitive to G-protein activation by other compounds. The smaller $\Delta LogRAi_{G\text{-}ERK}$ values for salvinorin A and mesyl sal B (Figure 4.4) indicated that G-protein signaling may be related to ERK1/2 phosphorylation for this structural class of compounds at this timepoint, consistent with previous work demonstrating that early-phase ERK1/2 phosphorylation by the KOR is G-protein mediated.[96] This is also consistent with a study showing that both ERK1/2 phosphorylation and $G\alpha_i$ activation are necessary for salvinorin A and mesyl salvinorin B action on dopamine transporter activity.[79] However, it is clear that other factors contribute to ERK1/2 phosphorylation downstream of the KOR as this is not consistent across structural classes.

The original study of triazole compounds demonstrated that agonist structure can impact ERK1/2 phosphorylation downstream of the KOR independently from G-protein / arrestin bias.[62] Additionally, studies have shown that many of the downstream signaling dynamics of both G-protein and arrestin pathways are complex and interacting.[97] These data support the idea that one or both early signaling pathways likely contribute to KOR-induced ERK1/2 phosphorylation, and that ERK1/2 phosphorylation could be mediated differently across structurally diverse agonists at this timepoint. It is not ideal to compare between cell lines because many signaling events are context-dependent, however, and future studies of many agonists in a single cellular context are needed. These data support that ERK1/2 phosphorylation should be considered independently in studies of KOR signaling.

Unlike ERK1/2 phosphorylation, mTOR pathway activation has only recently been implicated in KOR signaling. Recent studies have demonstrated that the mTOR signaling pathway may be involved in mediating aversion caused by KOR agonists.[36,39] These studies characterized several KOR agonists, including U50,488 and MCBPHA (HS665 in Liu, et al. 2018), as activators of the mTOR pathway in the mouse striatum and cortex. They found that other KOR agonists, such as HS666 and nalfurafine, did not activate the mTOR pathway in these regions at the doses tested. They also found that mTOR activation tracked with KOR-mediated aversion caused by these compounds – U50,488 and MCBPHA caused aversion at the doses that also caused mTOR activation, while nalfurafine and HS666 were not aversive and did not cause mTOR activation at the doses tested. Further, they found that blocking mTOR activation was able to block U50,488-mediated conditioned-place aversion.

In our experiments, robust Rps6 phosphorylation (at least 50% of maximum U69,593 stimulation) was caused by the vast majority of agonists tested (Figure 4.6). Compounds such as nalfurafine, which did not show mTOR activation in previous studies at lower concentrations, were still robust activators of the pathway in this experiment. The differences between this study, in which all KOR agonists tested activated the mTOR pathway, and the previous study in which only a subset of KOR agonists activated the pathway, are likely due in part to differences in both tissue tested and concentrations used.

Similarly to ERK1/2 phosphorylation, there are discrepancies between the early signaling pathways (G-protein and arrestin) and Rps6 phosphorylation in this system. Agonists that had very little β-arrestin-2 recruitment, such as nalmefene and naltrexone (Figure 3.2 B), still showed robust Rps6 phosphorylation (Figure 4.6), suggesting that G-protein activation may be more involved than arrestin signaling in activating the mTOR pathway. The dynamics appear more

complex than this, however, as agonists such as 3G1 and 3G2 showed 100% maximum effect for G-protein signaling but only partial Rps6 phosphorylation (Figure 3.4 E and Figure 4.6). Full quantitative dose-response and functional studies are needed to further elucidate the relationships between the early signaling pathways and complex downstream mTOR activation. Overall, these data demonstrate that diverse KOR agonists can differentially regulate both ERK1/2 phosphorylation and mTOR activation (through Rps6 phosphorylation). This indicates that individual signaling modalities should be studied independently, and these complex downstream pathways should not be used as proxies for initial signaling events, as has been done in some studies of G-protein and arrestin bias.[35] These downstream signaling pathways are likely the consequence of complex crosstalk between pathways, including G-protein, β-arrestin-2, and potentially additional signaling pathways.

4.2 Identification of novel KOR-signaling pathways

Data from other studies, as well as our ERK1/2 and mTOR studies in Chapter 2.1, have indicated that there are signaling pathways that can be differentially regulated by agonists at the KOR in addition to the well-characterized G-protein and arrestin pathways.[36,62] While it is possible that these pathways are affected by events further downstream of the receptor, it is also possible that there are additional receptor-proximal signaling partners that are differentially regulated directly by changes in receptor conformation caused by specific agonists (Figure 4.7). In this case, these other signaling partners could be involved in KOR-mediated behaviors and used to further refine a desired ligand "bias" profile for therapeutically-beneficial downstream effects.

Here, we aimed to identify novel protein binding partners of the KOR. First, we optimized an immunoprecipitation protocol for a FLAG-tagged KOR. Then, we compared protein-binding partners of the KOR under different signaling conditions to identify differentially-regulated proteins.

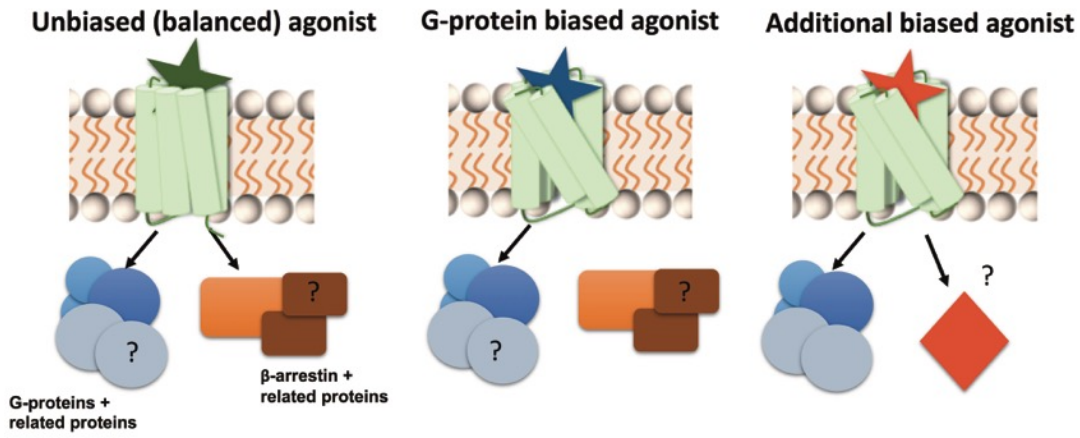

Figure 4.7. Effect of biased agonists on receptor-protein interactions

4.2.1 Validation of KOR immunoprecipitation

First, KOR-FLAG proteins and interacting protein binding partners were immunoprecipitated from HEK cells to optimize the immunoprecipitation protocol using M2-agarose beads. The sample eluted from the beads was prepared via trypsin digestion and proteins were identified using LC-MS/MS and FLAG-KOR proteins were additionally identified by western blot. We found that KOR-FLAG proteins were enriched in the immunoprecipitated sample relative to total protein, shown both through western blotting (Figure 4.8) and later LC-MS/MS analysis. While only 2 KOR peptides were reliably identified in the immunoprecipitated samples, this is consistent with previous reports of KOR immunoprecipitations, likely due to poor solubility and interference from membrane components. Overall, these data indicate that the KOR was successfully immunoprecipitated.

To identify which proteins were interacting with the KOR, protein hits from the LC-MS/MS were analyzed by MaxQuant software and subsequently filtered, as described below. Over 1000 proteins were identified in the experiment. First, these were filtered for their posterior error probability (PEP) score, which is the probability that the identification of any given peptide is incorrect.[73] All proteins with peptide PEP scores of greater than 10^{-4} were eliminated, as well as proteins that only had 1 identified peptide. In the optimized immunoprecipitation, this left 947 identified proteins. A significant number of these proteins were related to protein trafficking, including ER and Golgi-bound proteins. This indicated that much of the KOR-FLAG may not have been at the membrane surface, and that the proteins identified may have been unrelated to KOR signaling at the membrane. This is not unusual for membrane-bound proteins. However, a large number of signaling and receptor-related proteins were also identified (Table 4.1). Proteins that were expected to interact with the KOR, such as G-proteins and ubiquitin-related proteins, were identified, as well as proteins that have previously been shown to interact with other opioid receptors in previous yeast-2-hybrid experiments.[98]

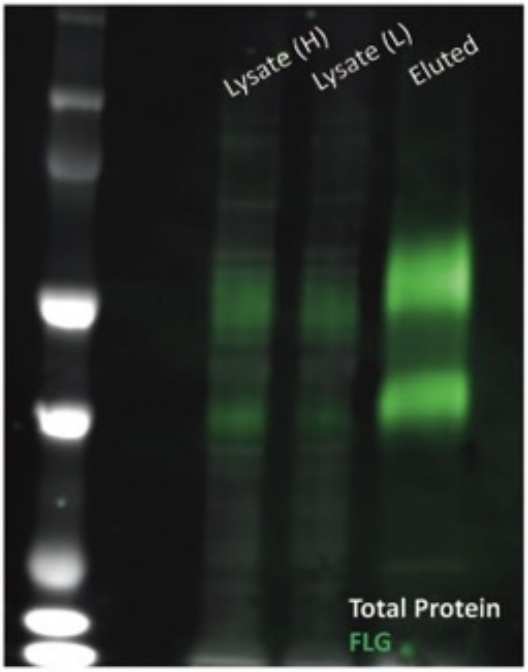

Figure 4.8. FLAG-KOR proteins enriched in immunoprecipitation
FLAG-KOR proteins were immunoprecipitated and run on SDS-PAGE gel from both two different cell lysates (H and L). Lysate and eluted samples were stained for total protein using REVERT total protein stain and (grey) and FLAG (green) expression, showing enrichment of the FLAG-KOR protein in the eluted fraction.

Protein Identity	LogPEP	Total peptides
OPRK1, opioid receptor, kappa 1	-12.7	4
G-proteins (shown to be involved in KOR signaling)		
GNAI3, guanine nucleotide binding protein (G protein), alpha inhibiting activity polypeptide 3	-52.4	8
GNAI2, G protein subunit alpha i2	-42.7	2
GNB1, guanine nucleotide binding protein (G protein), beta polypeptide 1	-77.5	12
GNB2, guanine nucleotide binding protein (G protein), beta polypeptide 2	-65.3	3
GNB2L1, guanine nucleotide binding protein (G protein), beta polypeptide 2-like 1	-22.7	5
MAPK-related proteins (shown to be involved in KOR signaling)		
TAB1, TGF-beta activated kinase 1/MAP3K7 binding protein 1	-275.7	61
MAP3K7, mitogen-activated protein kinase kinase kinase 7	-195.8	39
TAB3, TGF-beta activated kinase 1/MAP3K7 binding protein 3	-63.3	9
Ubiquitin-related (shown to interact with KOR)		
UBAP2L, ubiquitin associated protein 2 like	-163.9	23
RNF20, ring finger protein 20, E3 ubiquitin protein ligase	-15	2
USP10, ubiquitin specific peptidase 10	-9.1	2
Ribophorin1 (shown to interact with KOR) and Ribophorin2		
RPN1, ribophorin I	-205.5	34
RPN2, ribophorin II	-67.5	12
Calmodulin (shown to interact with MOR and DOR)		
CALM2, calmodulin 2	-99	20
Calnexin (shown to interact with DOR)		
CANX, calnexin	-92.4	5
Filamin A (shown to interact with MOR) and Filamin B		
FLNA, filamin A	-2077.7	459
FLNB, filamin B	-1201.8	148
Synaptophysin (shown to interact with MOR)		
SYPL1, synaptophysin-like 1	-14.1	2

Table 4.1. Signaling and receptor-related proteins identified in co-immunoprecipitation with FLAG-KOR. Proteins that co-immunoprecipitated with FLAG-KOR were identified by LC-MS/MS and data analyzed using MaxQuant software. Proteins with previously demonstrated interactions with opioid receptors were based on previous experiments reviewed in Georgoussi et. al. 2012.[98]

4.2.2 SILAC preparation of cells for investigation of activation-specific interactions

After optimizing the immunoprecipitation protocol, we used a SILAC (stable isotope-labeled amino acids in cell culture) approach to compare protein-binding partners under different signaling conditions (Figure 4.9). Cells were grown with heavy (15N lysine and arginine) amino acid media and treated with vehicle, alongside cells grown with regular (light) amino acid media that were treated with 10-20μM of a KOR agonist. Cells were then lysed, membranes isolated and solubilized and equal amounts of protein lysate from the vehicle (heavy) and agonist-treated (light) samples were mixed for immunoprecipitations. Protein-receptor interactions were then

identified using LC-MS/MS, and filtered for quality by PEP score and number of peptide. Additionally, protein identities were matched against a database of commonly-identified proteins in similar protocols, to eliminate proteins that are incredibly abundant in the cell and likely to immunoprecipitate with many different bait proteins.[99]

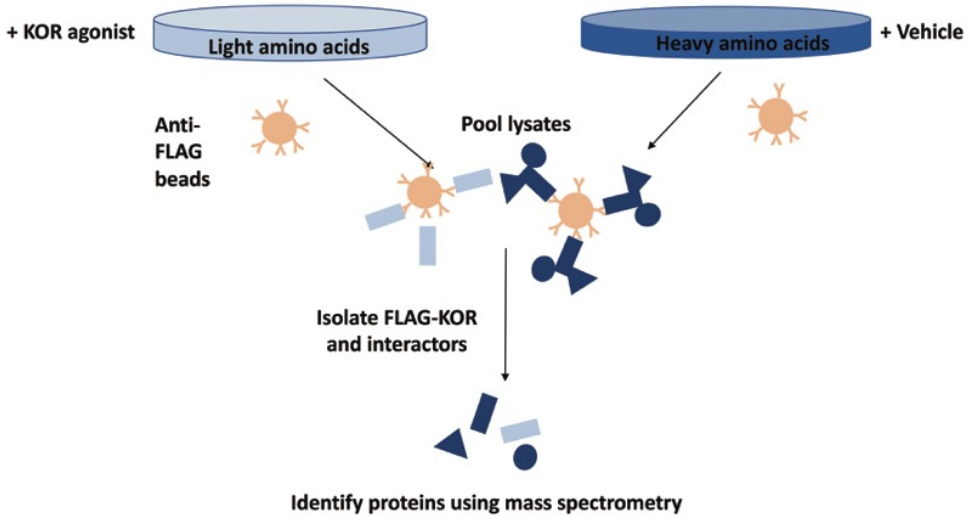

Figure 4.9. SILAC approach for identifying differences in receptor-protein interactions with KOR agonist treatment

For each protein, an intensity ratio was calculated, comparing the amount of that protein in the light sample (treated with agonist) to the amount of that protein in the heavy sample (treated with vehicle). An intensity ratio of 0.5 indicated no change in intensity between the vehicle and treated cells. An intensity ratio of >0.5 indicated increased intensity of that protein in the agonist-treated cells, and an intensity ratio of <0.5 indicates decreased intensity of that protein in the agonist-treated cells. The range of intensity ratios was not very large for the proteins identified (0.6-0.4), suggesting that there were not large fluctuations in receptor-protein interactions with

agonist treatment overall. The intensity ratios were consistent across two replicates, however (Figure 4.10), suggesting that these small fluctuations in intensity ratio may be biologically relevant.

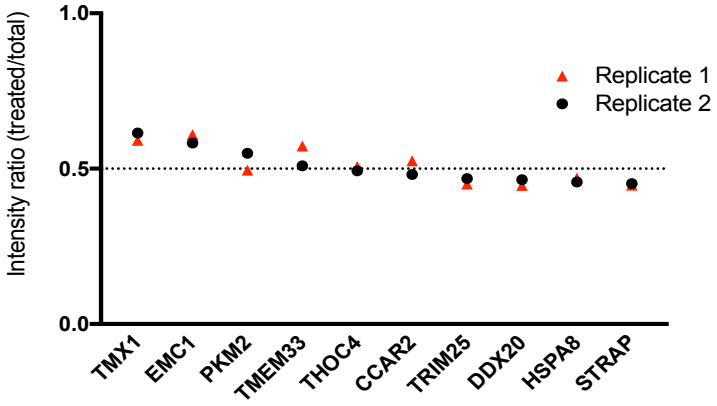

Figure 4.10. Intensity ratios consistent across SILAC replicates

Intensity ratios were calculated as the [Intensity in Light Sample / (Intensity in Light Sample + Intensity in Heavy Sample)]. An intensity ratio of 0.5 indicates equal intensity in both the vehicle-treated (Heavy) and KOR agonist-treated (Light) sample. Replicate data are shown for 10 proteins that were reliably identified across several different experiments, with filtering as described in the text and methods. In this case, both replicates compared 10μM U69,593 and vehicle treatments.

4.2.3 Ligand identity affects activation-specific interactions

Intensity ratios for many proteins were then compared for different agonist treatments including the reference agonist U69,593, the G-protein biased diphenethylamine agonist MCBPHA or the extremely G-protein biased diphenethylamine agonist BPHA (Figure 4.11). In each graph, a dot represents a single protein that was identified in all experiments. The intensity ratios from the different agonist treatments for each protein were then plotted against each other.

Intensity ratios for the proteins in the sample treated with U69,593 did not correlate with the intensity ratios for the same proteins in samples treated with either MCBPHA or BPHA (Figure 4.11 A, B). Intensity ratios for proteins in the sample treated with MCBPHA did show a significant correlation with the intensity ratios for the same proteins in the sample treated with BPHA (Figure 4.11 C).

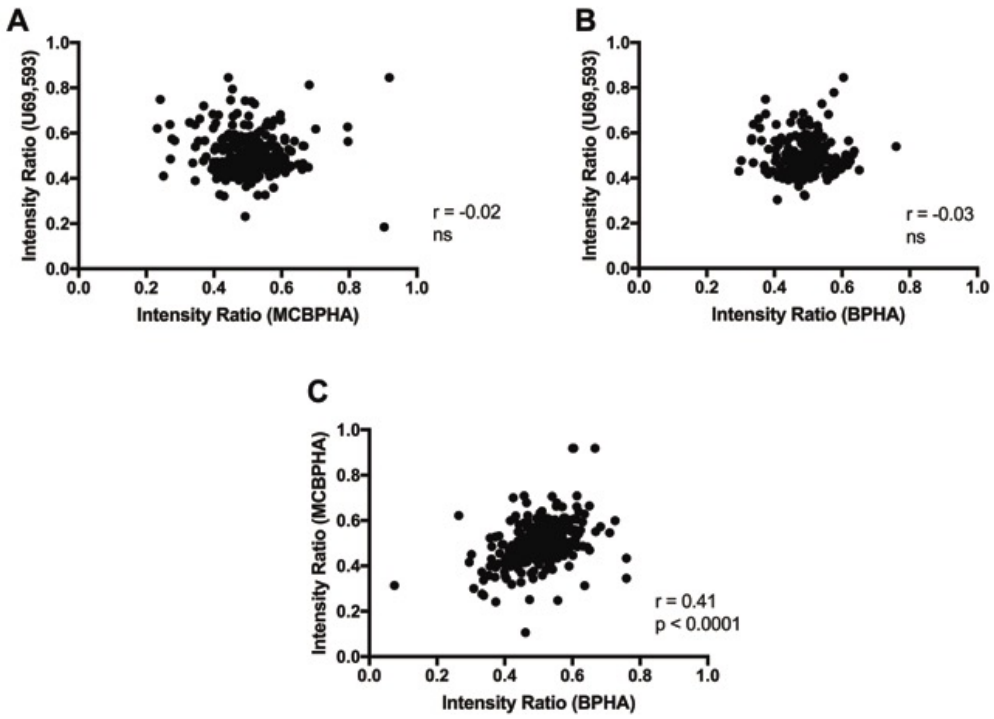

Figure 4.11. Intensity ratios for proteins identified in co-immunoprecipitations after different treatment conditions

Intensity ratios were calculated for protein-receptor interactions when vehicle-treated cell were compared with U69,593-treated cells, BPHA-treated cells and MCBPHA-treated cells and intensity ratios compared here. Each dot represents an individual protein that interacted with the KOR under all conditions tested. There was no significant correlation between the U69,593-treated intensity ratios and either (A) MCBPHA or (B) BPHA-treated intensity ratios. (C) There was a significant correlation (Pearson $r = 0.41$, $p<0.001$) between the MCBPHA and BPHA-treated intensity ratios.

Table 4.2 shows the intensity ratios for 10 of the top proteins in all 3 treatment conditions. Four of the proteins are involved in protein folding and trafficking, suggesting that many of the candidate proteins identified may be background noise. Interestingly, 2 of these top 10 proteins are involved in 14-3-3 signaling (TRIM25 and STRAP).

		U69,593 ratio	MCBPHA ratio	BPHA ratio
TMX1*	Transmembrane thioredoxin-related protein, chaperone	0.59	0.46	0.48
EMC1*	ER membrane protein complex subunit 1	0.61	0.44	0.49
TMEM33*	Transmembrane protein 33, ER stress-inducible transmembrane protein	0.57	0.40	0.40
PKM2	Pyruvate kinase M2, metabolic kinase that may have protein kinase function	0.50	0.49	0.53
CCAR2	Cell cycle and apoptosis regulator protein 2, inhibits transcription	0.53	0.52	0.55
THOC4	ALYREF, nuclear chaperone that leads to transcriptional changes	0.51	0.55	0.50
HSPA8*	Heat shock protein, chaperone	0.47	0.43	0.47
TRIM25	E3 ubiquitin ligase, promotes ISGlyation of 14-3-3	0.45	0.48	0.49
DDX20	Gemin3, RNA helicase, regulates gene expression	0.45	0.50	0.57
STRAP	Serine-threonine kinase receptor-associated protein, involved in 14-3-3 signal transduction	0.45	0.47	0.65

Table 4.2. Intensity ratios for top 10 proteins identified in all co-immunoprecipitations
Descriptions of the top 10 protein-receptor interactions in all treatment conditions (based on filtering criteria described in text and methods) and intensity ratios for different treatment conditions. Proteins marked with an asterisk(*) were involved in membrane-protein trafficking and processing.

4.2.4 14-3-3 localization affected by KOR activation

14-3-3 proteins are ubiquitously expressed signaling scaffolds, that have been shown to play an important role in GPCR signaling, and to interact with the KOR under different conditions.[100,101] To assess the effect of KOR activation on 14-3-3 signaling, we looked at 14-3-3 localization in HEK cells expressing a GFP-tagged KOR following treatment with U69,593

(Figure 4.12). When cells were treated with vehicle, in this case serum-free DMEM media, 14-3-3 was localized to the cytoplasm of the cell. After 1 hour treatment with 10uM of the full, unbiased KOR agonist U69,593, however, a portion of the 14-3-3 protein was localized to the nucleus of the cell (Figure 4.12 B).

To investigate this further, high-throughput imaging of 200-300 nuclei per sample indicated a dose-dependent increase in 14-3-3 nuclear localization with increasing concentrations of U69,593 (Figure 4.13). This effect was partially blocked by co-treatment of the cells with the KOR-selective antagonist norBNI, suggesting that this effect is mediated by KOR (Figure 4.13). While one-way ANOVA revealed a significant effect of treatment ($F(4,2098) = 28.47$), the overall effect size was small, with only 5% of the variation coming from different treatment conditions ($\eta 2 = 0.05$).

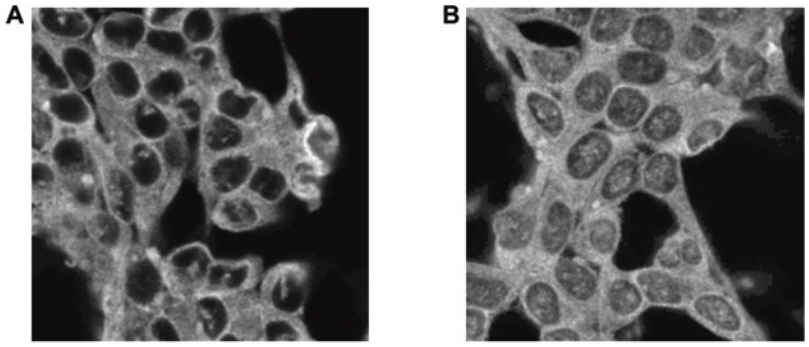

Figure 4.12. 14-3-3 proteins localize to the nucleus after KOR activation
HEK cells expressing a GFP-tagged KOR were stained for pan-14-3-3 expression (grey) and imaged with confocal microscopy. Cells were treated with (A) vehicle and (B) 10μM U69,593.

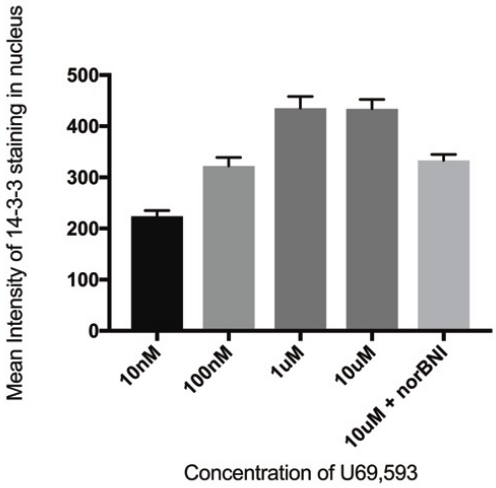

Figure 4.13. U69,593 treatment causes dose-dependent nuclear localization of 14-3-3
HEK cells expressing GFP-tagged KOR were plated in 96-well plates, treated with varying doses of the agonist U69,593 and stained with DAPI and for pan-14-3-3 localization using wide-field microscopy. Intensity of 14-3-3 staining in the nucleus was quantified by co-localization with DAPI staining. Data are represented as the mean of 600-1200 nuclei from two samples (±SD).

4.2.5 Discussion

The identification of additional pathways directly involved in GPCR signaling has been historically difficult, due to the technical complexity of biochemical experiments with membrane-bound proteins. Previously, work has been done to identify phosphorylated proteins that were differentially regulated by structurally diverse GPCR agonists (including the KOR),[36,102] and as well as to identify proteins that differentially interact with arrestins after agonist activation.[103] More recently, innovative methods for labeling proteins in close proximity to opioid receptors after agonist activation have identified potential novel protein-receptor interactions as well.[104] Here, we attempted to directly identify novel protein-receptor interactions through immunoprecipitation and mass spectrometry, using an isotope-labeling approach (Figure 4.9).

First, we validated our immunoprecipitation by comparing the proteins that we identified in our sample to a list of proteins that had previously been identified as interactors with opioid

receptors (Table 4.1). Combined with the clear enrichment of FLAG-KOR protein in our eluted sample (Figure 4.8), these data suggested that our immunoprecipitation likely included proteins that interacted with the KOR at the membrane where it could be activated by agonists. To identify proteins specifically involved in signaling, we compared protein-receptor interactions when the cells were treated with vehicle to interactions when the cells were treated with a KOR agonist using stable-isotopes to label amino acids in the different cell populations (Figure 4.9).

With the intensity ratios calculated from these samples, we examined both the larger patterns of receptor-protein interaction as well as specific candidate proteins. When comparing the intensity ratios of all of the proteins identified, we found that the structurally similar diphenethylamine agonists had correlated intensity ratios, while U69,593 did not (Figure 4.11). This suggests that the intensity ratios for proteins, which is a measure of the change in binding interaction upon KOR activation, was related to the ligand identity, and many proteins could be differentially regulated by agonist identity. Additional studies with diverse agonists could help to identify relationships between intensity ratios overall and any specific feature of agonists - such as G-protein or arrestin signaling, a certain structural feature, or even a downstream behavior.

We then examined specific proteins that interacted with the KOR for candidate signaling pathways that may be involved in KOR signaling. Of the 10 most abundant proteins that were identified in all samples (after filtering as described in the methods), two were involved in 14-3-3 signaling (Table 4.2). We found a weak, but significant, dose-dependent increase in 14-3-3 nuclear localization following treatment of cells with U69,593, and this was partially blocked by the KOR-selective antagonist norBNI (Figure 4.12, Figure 4.13). These experiments used a pan-14-3-3 antibody, however, so further investigation into the subtypes of 14-3-3 involved in KOR signaling are necessary. 14-3-3 proteins are ubiquitously and abundantly expressed, actually

comprising 1% of all protein in the brain.[105] For this reason, 14-3-3 proteins themselves often emerge as hits in high-throughput protein expression screens like the one here. Despite this, the imaging data, along with previous data describing 14-3-3 and KOR interactions, suggests that 14-3-3 may be involved in KOR signaling in a meaningful way that involves nuclear localization.

It has been shown recently that 14-3-3 signaling can be differentially regulated downstream of GPCRs, depending on agonist identity.[100] Further investigation into the regulation of 14-3-3 by diverse KOR agonists, particularly agonists that are known to be biased for other pathways, will be important for elucidating the role that 14-3-3 proteins play in regulating the signaling or trafficking of the KOR. Additionally, the majority of GPCR-14-3-3 research has focused on the role of 14-3-3 as a scaffolding protein. Further research into the role of 14-3-3 in the nucleus following GPCR activation is needed.

CHAPTER 5. IN VIVO EFFECTS OF DIFFERENT KOR AGONISTS

5.1 Effect of diverse KOR agonists on prolactin release in mice

In addition to mediating the effects of drugs of abuse, the dopaminergic effects downstream of opioid receptors regulate other processes in the brain and body. For example, the release of the hormone prolactin is under inhibitory control by dopamine, from neurons projecting from the hypothalamus to the pituitary. Prolactin is known for its involvement in pregnancy and lactation, however it also plays an important part in the stress response.[106] It has been shown that activation of the KOR by dynorphin peptides following stress,[107,108] or by exogenous KOR agonists, [109,110] leads to an increase in prolactin levels, mediated by dopamine in this tuberoinfundibular dopaminergic system.

Work from Butelman, et. al. has shown that levels of prolactin can be used as a quantitative biomarker of KOR activation,[111] and prolactin levels have been used in rodents,[86] non-human primates[112] and humans[32] to investigate KOR activity in vivo. In this study, we investigated the effects of several, structurally diverse KOR agonists on the release of prolactin in mice.

5.1.1 Prolactin release caused by diverse KOR agonists

For all experiments, mice were injected intraperitoneally with compound or vehicle and then sacrificed 30 minutes later (unless otherwise noted) and trunk blood was collected. Prolactin levels in the serum were measured by sandwich ELISA. We found an increase in serum prolactin after treatment with the full, unbiased arylacetamide agonist U50,488, and that this increase was blocked, at least in part, by a KOR-selective dose of the antagonist LY2444296 (Figure 5.1). The

diphenethylamine compounds BPHA, MCBPHA and MCPPHA all caused significant prolactin release at doses of 30mg/kg (Figure 5.1), and these effects were blocked by the antagonist LY2444296.

We also examined the morphinan compound nalfurafine, that had a unique signaling profile in vitro (Figure 3.2, Figure 3.3). A dose of 10μg/kg nalfurafine caused significant prolactin release after 30 minutes compared to saline treatment (Figure 5.2 A). This effect was blocked by the KOR-selective dose of LY2444296, indicating that this nalfurafine-induced prolactin release was mediated by the KOR (Figure 5.2 A). The lower dose of 3μg/kg nalfurafine caused significant prolactin release, however there was no effect of the doses lower than this (1 and 0.3μg/kg nalfurafine) (Figure 5.2 B). Levels of prolactin in the serum remained elevated for at least 60 minutes after intraperitoneal injection of 10μg/kg nalfurafine, but returned to normal by 120 minutes (Figure 5.2 C).

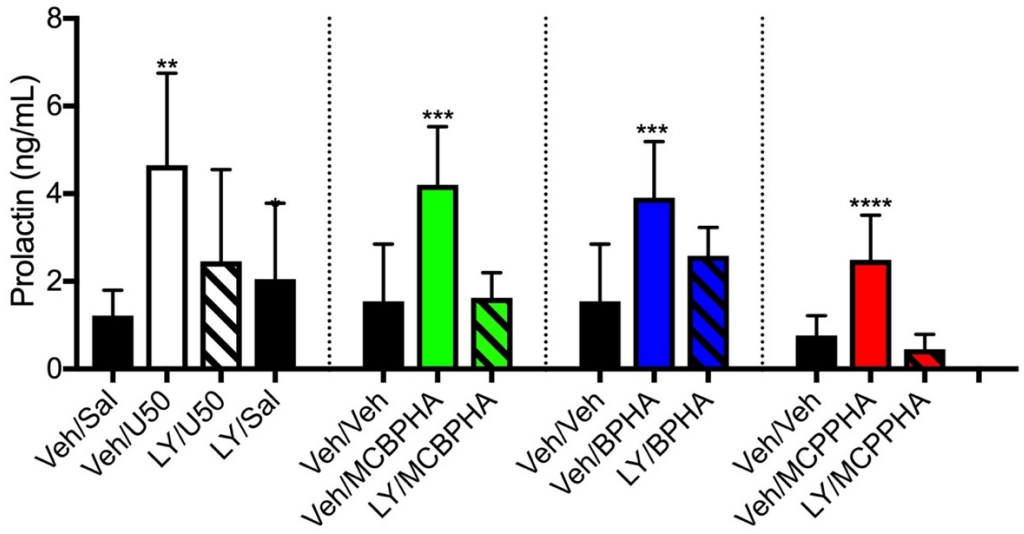

Figure 5.1. Prolactin release caused by U50,488, and diphenethylamine compounds. Mice were pretreated with either vehicle or 3mg/kg LY2444296 15 minutes before an injection of 30mg/kg U50,488, MCBPHA, BPHA or MCPPHA. Serum prolactin levels were measured in samples taken 30 minutes after the second injection. * = $p < 0.05$, *** = $p < 0.0005$, **** = $p < 0.0001$, by one-way ANOVA followed by followed by Dunnett's multiple comparison test compared vehicle-saline control group. Each experiment was tested independently for significance.

Figure 5.2. Prolactin release caused by the morphinan compound nalfurafine. A. Mice received an injection intraperitoneally of either LY2444296 or vehicle 15 minutes before an injection of 10μg/kg nalfurafine. Samples were collected 30 minutes after the second injection. Two-way ANOVA (LY244296 pretreatment x Nalfurafine treatment) revealed a significant effect of both LY2444296 pretreatment ($F(1,30) = 86.75$, $p < 0.0001$), Nalfurafine treatment ($F(1,30) = 115.3$, $p < 0.0001$) and their interaction ($F(1,30) = 96.36$, $p < 0.0001$). Newman-Keuls multiple comparison test revealed significant differences between Vehicle/Nalfurafine group and all other groups (****$p<0.0001$). B. Serum prolactin levels were measured in samples taken 30 minutes after intraperitoneal injection of varying doses of nalfurafine. One-way ANOVA revealed a significant effect of Treatment ($F(4,35) = 9.67$, $p < 0.0001$). Dunnett's multiple comparison test revealed significant differences between nalfurafine or U50,488 treated groups and saline-treated control group (*$p < 0.05$, ***$p < 0.0005$). C. Serum prolactin levels were measured in samples taken 15-120 minutes after intraperitoneal injection of 10μg/kg nalfurafine or saline. Two-way ANOVA (Treatment x Time) revealed a significant effect of Treatment ($F(1,56) = 62.56$, $p < 0.0001$), Time ($F(3,56) = 7.24$, $p < 0.0005$) and their interaction ($F(3,56) = 5.73$, $p < 0.005$). Newman-Keul's multiple comparison at each timepoint revealed significant differences between saline and nalfurafine-treated groups (**$p < 0.005$, ***$p < 0.0005$, ****$p < 0.0001$).

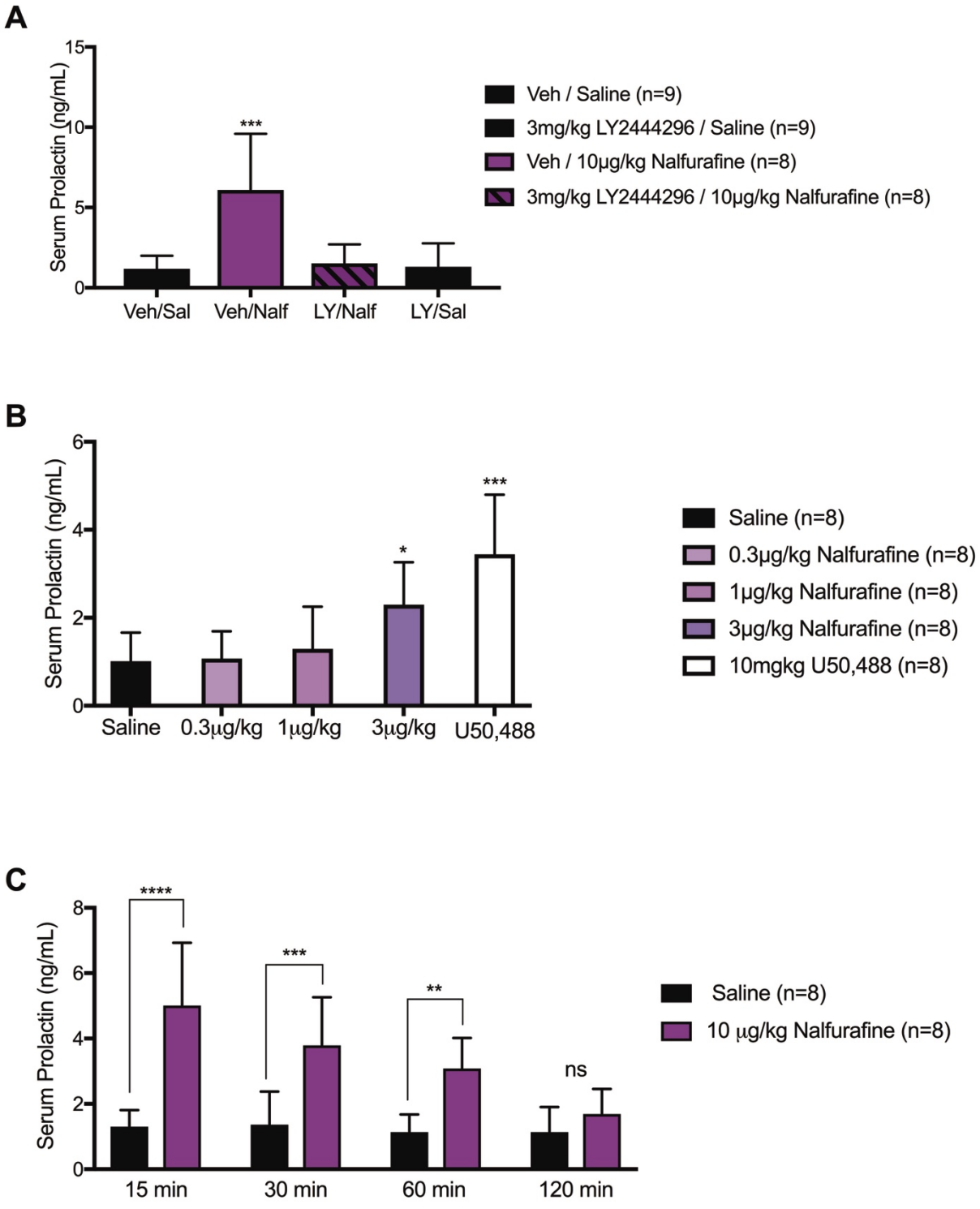
A
Serum Prolactin (ng/mL)
15
10
5
0
***
Veh/Sal
Veh/Nalf
LY/Nalf
LY/Sal
Veh / Saline (n=9)
3mg/kg LY2444296 / Saline (n=9)
Veh / 10µg/kg Nalfurafine (n=8)
3mg/kg LY2444296 / 10µg/kg Nalfurafine (n=8)
B
Serum Prolactin (ng/mL)
6
4
2
0
*
***
Saline
0.3µg/kg
1µg/kg
3µg/kg
U50,488
Saline (n=8)
0.3µg/kg Nalfurafine (n=8)
1µg/kg Nalfurafine (n=8)
3µg/kg Nalfurafine (n=8)
10mgkg U50,488 (n=8)
C
Serum Prolactin (ng/mL)
8
6
4
2
0
****
***
**
ns
15 min
30 min
60 min
120 min
Saline (n=8)
10 µg/kg Nalfurafine (n=8)

5.1.2 Discussion

All compounds tested were compared to a concurrently-run vehicle or saline-treated group, in order to control for the variation in prolactin levels caused by handling and stress across animal groups. All of the compounds tested caused an increase in serum prolactin, including the extremely G-protein biased agonist BPHA (Figure 5.1). This increase in prolactin was blocked by the KOR-selective dose of the antagonist LY2444296 (Figure 5.1). BPHA showed no measurable arrestin recruitment in the PathHunter DiscoverX assay, and was able to block arrestin recruitment caused by the full agonist U69,593 (Figure 3.2 E, Figure 3.3 B). This suggests that arrestin recruitment is not required for prolactin release, and potentially not required for the effects of KOR activation on dopamine levels, at least in the tuberoinfundibular dopamine system. Additional research into the mechanism of KOR modulation of dopamine tone in different dopaminergic systems will be important for understanding more about prolactin release as a biomarker for KOR activation, as well as for understanding more about KOR actions on dopamine levels in general.

5.2 Effects of KOR agonists on sedative and aversive side effects in mice

KOR agonists have also been shown to cause side effects such as sedation and aversion in human and animal models that have stalled the development of KOR agonists as therapeutics. To avoid these negative side effects, there has been a focus on the development of biased agonists at the KOR, particularly with more G-protein than arrestin activity.[50] Several studies of G-protein biased agonists, along with the work that is presented in Chapter 3, suggest that arrestin recruitment is required for KOR-mediated sedation.[34,51,52] It is unclear, however, if this

signaling pathway is related to the aversive or dysphoric side effects of KOR agonists. Several of the studies of G-protein biased agonists have shown that they cause antinociception or antipruritus without causing dysphoria or anhedonia,[51,52] and mechanistic studies have shown that arrestin-dependent p38 phosphorylation is needed for this KOR-mediated aversion.[59] However, recent studies have also suggested that the mTOR pathway is necessary for KOR-mediated aversion, but not sedation, suggesting that these negative side effects could be mediated by different signaling pathways.[36,39] Here, we examined the effect of BPHA, an extremely G-protein biased agonist with no measurable arrestin recruitment on conditioned-place aversion.

Data from previous human studies are also essential for establishing the translational potential of KOR agonists. Interestingly, there is only one selective KOR agonist that is currently in clinical use in humans. Nalfurafine was approved to treat pruritus in Japan in 2009, and post-marketing studies of over 3,000 patients have shown very few KOR-associated side effects.[37] In rodent studies, nalfurafine has been shown to cause antipruritic and antinociceptive effects at doses that do not cause sedation or aversion, while traditional KOR agonists like U50,488 and salvinorin A caused both the therapeutic and side effects at similar doses.[35,78,113] There are fewer studies, however, comparing the effective doses of KOR agonists in modulating drug-related behaviors compared to negative side effects. Here, we also examined the effects varying doses of nalfurafine on KOR-mediated sedation to compare to other in vivo effects such as prolactin release (Subsection 5.1) and the modulation of cocaine-induced behaviors (Subsection 5.3).

5.2.1 Sedation caused by KOR agonists measured by rotarod assay

Multiple doses of the arylacetamide compound U50488 and the morphinan compound nalfurafine were tested for rotarod sedation. As noted in Chapter 3.2, high doses of both of these compounds caused very robust sedation in the rotarod assay at 30 minutes post-injection (Figure 3.8). This maximally effective dose of 30mg/kg U50,488 was sedative almost immediately after injection, with rotarod performance beginning to recover at 60 minutes post-injection (Figure 5.3). 10mg/kg U50,488 was sedative compared to a saline control group only 30 minutes post-injection, while mice treated with 3mg/kg U50,488 were not impaired in the rotarod assay at any timepoint tested (Figure 5.3)

100μg/kg nalfurafine caused significant sedation, as measured by the rotarod assay, compared to a saline injected group (Figure 5.4 A). This effect was completely blocked by a KOR-selective dose of 3mg/kg LY2444296, indicating that this nalfurafine-induced sedation was mediated by the KOR (Figure 5.4 A). Higher doses of 300μg/kg and 3mg/kg nalfurafine caused significant sedation in this assay; mice performed at approximately 13% of their baseline performance after 30 minutes and the effect was still significant after 60 minutes (Figure 5.4 B). Mice had fully recovered after 24 hours, however. A dose of 30μg/kg nalfurafine had comparable sedation to a moderate dose of 10mg/kg U50,488 (Figure 5.4 C). At the doses of 3μg/kg and 10μg/kg however, there was no significant effect on rotarod sedation compared to saline injections at the same timepoint (Figure 5.4 C).

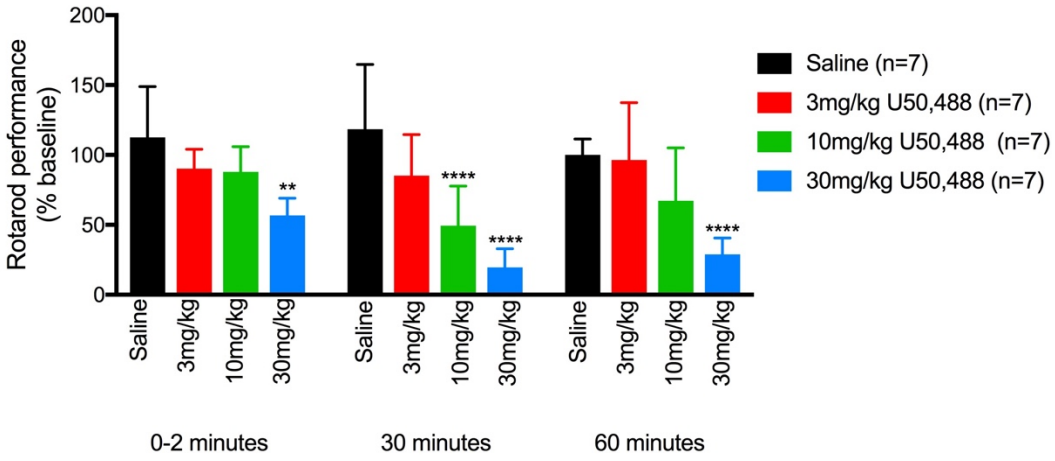

Figure 5.3 Rotarod sedation caused by U50,488. Mice were treated with varying doses of U50,488 or saline and rotarod performance was measured at selected timepoints after injection, and compared to baseline. Two-way ANOVA (Treatment x Time) revealed a significant effect of Treatment ($F(3,24) = 13.77$, $p < 0.0001$), Time ($F(2,48) = 7.05$, p , 0.005) and their interaction ($F(6,48) = 3.03$, $p < 0.05$). Dunnett's multiple comparison test at each timepoint revealed significant differences between U50,488 and Saline treated groups (**$p < 0.005$, ****$p < 0.0001$).

Figure 5.4. Rotarod sedation caused by nalfurafine. Rotarod performance was measured at select timepoints after IP injection of KOR nalfurafine, or saline, and compared to baseline rotarod performance in all experiments. A. Mice were pretreated for 15 minutes with 3mg/kgLY2444296 before injection with 100μg/kg nalfurafine. There was no effect of LY2444296 alone on rotarod sedation (see Dunn and Reed, 2018).[86] Two-way ANOVA (Treatment x Time) revealed a significant effect of Treatment ($F(2,21)=14.38$, $p < 0.0005$), Time ($F(2,24)=7.99$, $p < 0.005$) and their interaction ($F(4,42)=2.66$, $p<0.05$). Dunnett's multiple comparison test at each timepoint revealed significant differences between the Vehicle/Saline control group and Vehicle/Nalfurafine group only (**p<0.005, ***p<0.0005). B. Two-way ANOVA (Treatment x Time) revealed a significant effect of Treatment ($F(4,31) = 48.72$), $p < 0.0001$), Time ($F(2,62) = 26.64$, $p < 0.0001$) and their interaction ($F(8,62) = 4.0$, $p < 0.0005$). Dunnett's multiple comparison test at each timepoint revealed significant differences between nalfurafine treatment groups and Saline-treated control group (**p < 0.05, *** = p < 0.0005, **** = p < 0.0001). C. Two-way ANOVA (Treatment x Time) revealed a significant effect of Treatment ($F(4,30) = 3.38$), $p < 0.05$) and Time ($F(2,60) = 7.12$, $p < 0.005$) but no effect of their interaction ($F(8,60) = 1.19$). Dunnett's multiple comparison test at each timepoint revealed significant differences between nalfurafine and U50,488 treatment groups and Saline-treated control group (**p < 0.05).

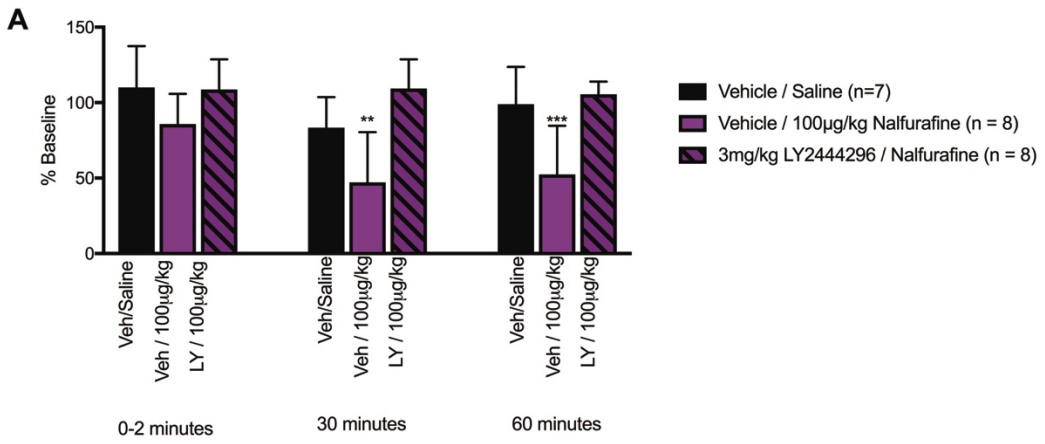
A
% Baseline
150
100
50
0
Veh/Saline
Veh / 100µg/kg
LY / 100µg/kg
0-2 minutes
30 minutes
60 minutes
**
***
Vehicle / Saline (n=7)
Vehicle / 100µg/kg Nalfurafine (n = 8)
3mg/kg LY2444296 / Nalfurafine (n = 8)

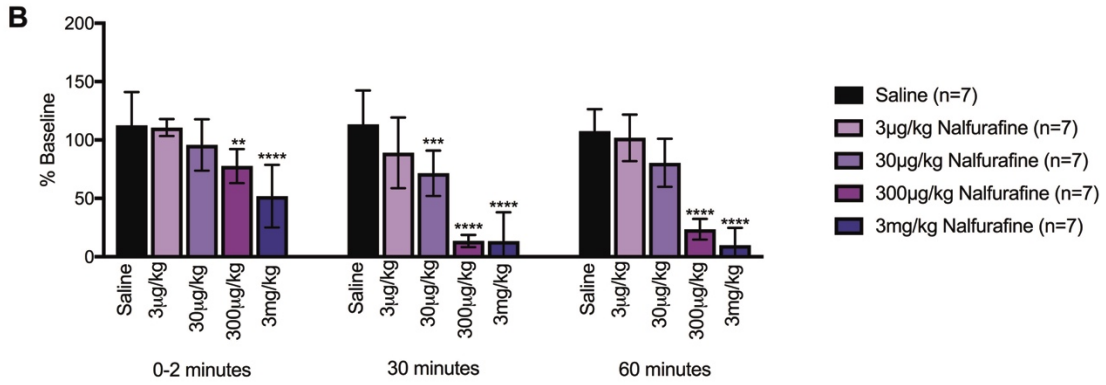
B
% Baseline
200
150
100
50
0
Saline
3µg/kg
30µg/kg
300µg/kg
3mg/kg
0-2 minutes
30 minutes
60 minutes
**
****
***
Saline (n=7)
3µg/kg Nalfurafine (n=7)
30µg/kg Nalfurafine (n=7)
300µg/kg Nalfurafine (n=7)
3mg/kg Nalfurafine (n=7)

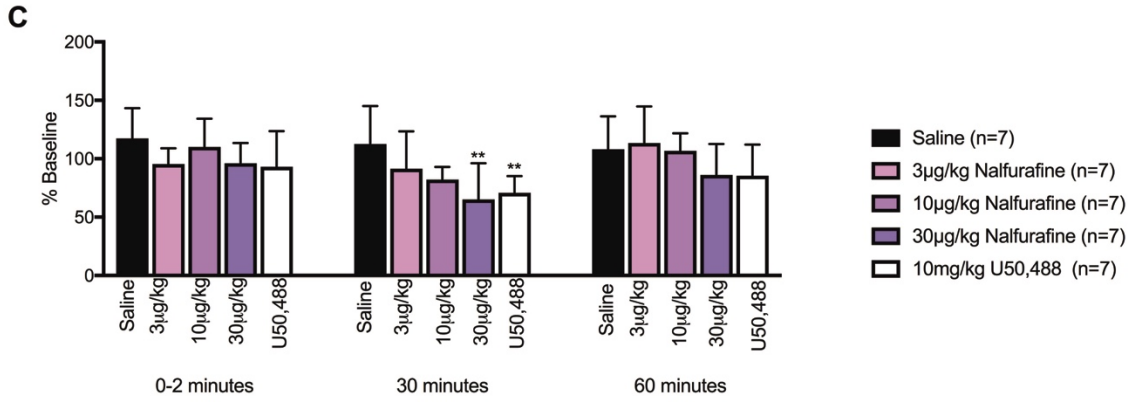
C
% Baseline
200
150
100
50
0
Saline
3µg/kg
10µg/kg
30µg/kg
U50,488
0-2 minutes
30 minutes
60 minutes
**
**
Saline (n=7)
3µg/kg Nalfurafine (n=7)
10µg/kg Nalfurafine (n=7)
30µg/kg Nalfurafine (n=7)
10mg/kg U50,488 (n=7)

5.2.2 Aversion caused by KOR agonists measured by place conditioning assay

For the conditioned-place aversion assay, mice were first allowed to freely explore the 3-chamber apparatus and the time spent in each chamber was recorded. During conditioning sessions, mice received an injection of vehicle or KOR agonist and were placed in the drug-paired chamber for 30 minutes. The same day, they received an injection of vehicle or KOR agonist (opposite of AM injection) and were immediately placed in the opposite chamber for 30 minutes. Chambers had different colored walls, as well as different textured floors. The day after all conditioning sessions were finished, mice were allowed to freely explore the 3-chamber set up again and the time spent in each chamber was recorded. If mice spent less time in the drug-paired chamber after the conditioning sessions than they did before the conditioning sessions, that suggested aversion to the drug-paired context, and by extension, the drug.

Several KOR agonists were tested at doses that were non-sedative. The non-sedative dose of 3mg/kg U50,488 did not cause any difference in time spent in the drug-paired chamber (Figure 5.5), suggesting that it was not aversive. Nalfurafine, at doses of both 3μg/kg and 10μg/kg, also did not cause any change in time spent in the drug paired chamber compared to saline (Figure 5.6 A and B). When mice were treated with 30mg/kg of the extremely G-protein biased diphenethylamine agonist BPHA before conditioning, however, they spent significantly less time in the drug-paired chamber compared to the vehicle-paired chamber (Figure 5.7).

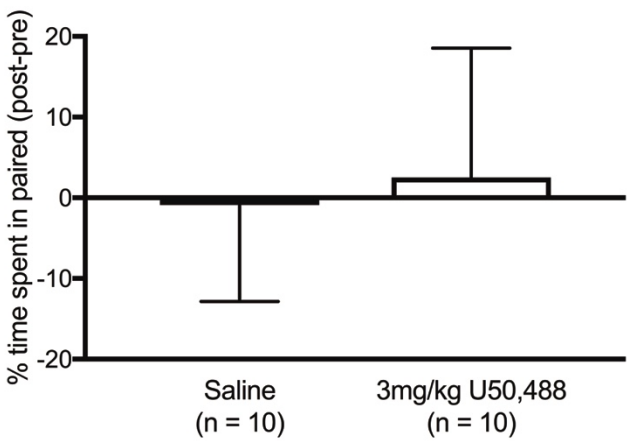

Figure 5.5. Conditioned-place aversion with a non-sedative dose of U50,488

Mice were injected IP with 3mg/kg U50,488, and then injected with saline and placed in drug-paired chambers 15 minutes later. Mice were conditioned for 2 session (30 minutes each) in the paired chamber, as well as 2 sessions (30 minutes each) in the opposite chamber following injections of saline in place of drug. Data is represented as the difference in the time spent in the paired chamber after the conditioning sessions, compared to before the conditioning sessions. There was no effect of treatment by unpaired T-test.

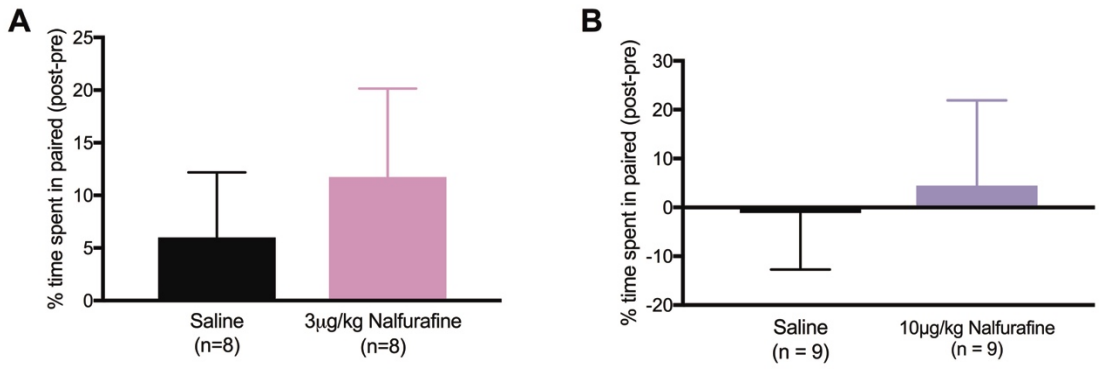

Figure 5.6 Conditioned-place aversion with non-sedative doses of nalfurafine

Mice were IP injected with 3µg/kg (A) or 10µg/kg (B) nalfurafine, and then injected with saline and placed in drug-paired chambers 15 minutes later. Mice were conditioned for 2 session (30 minutes each) in the paired chamber, as well as 2 sessions (30 minutes each) in the opposite chamber following injections of saline in place of drug. Data is represented as the difference in the time spent in the paired chamber after the conditioning sessions, compared to before the conditioning sessions. There was no effect of treatment by unpaired T-test in either experiment.

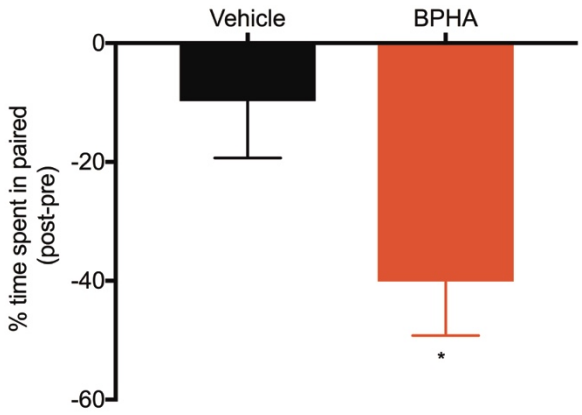

Figure 5.7 Conditioned-place aversion caused by BPHA

Mice were conditioned for 4 sessions (30 minutes each) in a paired chamber following IP injection of either vehicle or 30mg/kg BPHA as well as 4 sessions (30 minutes each) in the opposite chamber following injection of vehicle. Data is represented as the difference in the time spent in the paired chamber after the conditioning sessions, compared to before the conditioning sessions. T-test revealed significant effect of BPHA treatment compared to vehicle (*$p<0.05$).

5.2.3 Discussion

Here, we found that although high doses of the full agonists U50,488 and nalfurafine were extremely sedative, lower doses were not sedative or aversive in these assays. Low doses of nalfurafine, such as the 3μg/kg and 10μg/kg doses tested here, have been shown to cause antipruritic and antinociceptive effects, as well as prolactin release (Figure 5.2), suggesting that they are still able to activate the KOR. Higher doses of nalfurafine, have been shown to be sedative, [114,115] consistent with findings here (Figure 5.4). These data are also consistent with previous studies demonstrating that nalfurafine is more potent for therapeutic endpoints, in this case prolactin release, than side effects like sedation. Here, nalfurafine at 3μg/kg and 10μg/kg caused significant prolactin release (Figure 5.2) but not sedation (Figure 5.4).

While our CPA findings are consistent with other groups demonstrating that these doses of nalfurafine are not aversive, a recent study found that 10μg/kg nalfurafine could potentially increase thresholds in intracranial self-stimulation, suggesting that it could cause dysphoria, depending on the assay used.[116]

Interestingly, BPHA, which is an extremely G-protein biased agonist with no measurable arrestin activity (Figure 3.2), caused significant aversion compared to vehicle (Figure 5.3). This suggests that arrestin recruitment may not be necessary for the aversive side effects of KOR agonists, in the way that arrestin recruitment appears to be necessary for the sedative side effects of KOR agonists. Recent work has shown that the mTOR signaling pathway may be important for KOR-mediated aversion, but not sedation, and these data further support that these two negative side effects are mediated by different signaling pathways. Further research into the signaling mechanisms and circuits that lead to these behaviors is necessary to better understand how to develop drugs that can activate the KOR for therapeutic purposes, while avoiding aversive side effects.

5.3 Effect of KOR agonists on cocaine-related behaviors in mice

In addition to pain and pruritus, KOR agonists have been of particular interest in treating cocaine and psychostimulant addiction, as KOR activation inhibits the dopamine release caused by these drugs[17] and there are currently no available treatments for these diseases. KOR agonists have been shown to block the rewarding effects of drugs of abuse, including cocaine. Because of its positive clinical and post-marketing data in treating pruritus, nalfurafine is of particular interest for future clinical studies in this area. However, there are few studies that have examined effects of nalfurafine on cocaine-related behavior or comparing nalfurafine and other KOR

agonists head-to-head for this therapeutic effect.[114,117] Here, we investigated the effects both nalfurafine and the full KOR agonist U50,488 in two mouse models of cocaine-induced reward at doses that did not cause sedative side effects (Figure 5.3 and Figure 5.4).

5.3.1 Effect of KOR agonists on cocaine-conditioned place preference

In a 3-chamber conditioned place preference paradigm, similar to the CPA assay in Subsection 5.2.1, mice that were conditioned with an injection of 15mg/kg cocaine spent more time in the drug-paired chamber after conditioning, indicating cocaine preference or reward, as expected. When mice were pretreated for 15 minutes with a relatively low dose of 3mg/kg U50,488 before receiving cocaine, however, this preference was attenuated (Figure 5.8). When mice were pretreated for 15 minutes with 10μg/kg nalfurafine (Figure 5.9 A) or 3μg/kg nalfurafine (Figure 5.9 B), conditioned-place preference for the cocaine-paired chamber was also attenuated. These same doses of U50,488 and nalfurafine were not aversive on their own (Figure 5.5 and 5.6).

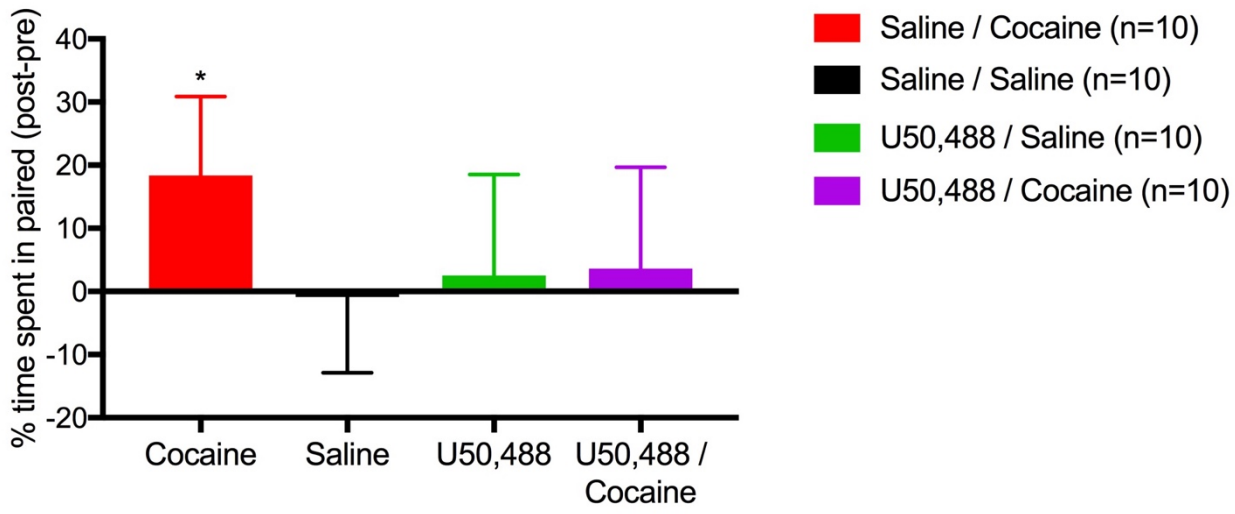

Figure 5.8. U50,488-induced blockade of cocaine-conditioned place preference. Mice were treated with 3mg/kg U50,488 or saline, and then 15 minutes later treated with 15mg/kg cocaine or saline before immediately being placed in appropriate conditioning chambers for 30 minutes. 4 total conditioning sessions were done, 2 in each box, across 2 days. Two-way ANOVA (U50,488 Pretreatment x Cocaine Treatment) revealed a significant effect of Cocaine Treatment ($F(1,36) = 5.11$, $p < 0.05$) but no effect of U50,488 Pretreatment ($F(1,36) = 1.60$) or interaction ($F(1,36) = 4.07$). Newman-Keuls multiple comparison test revealed significant differences Cocaine group and all other groups (*$p<0.05$).

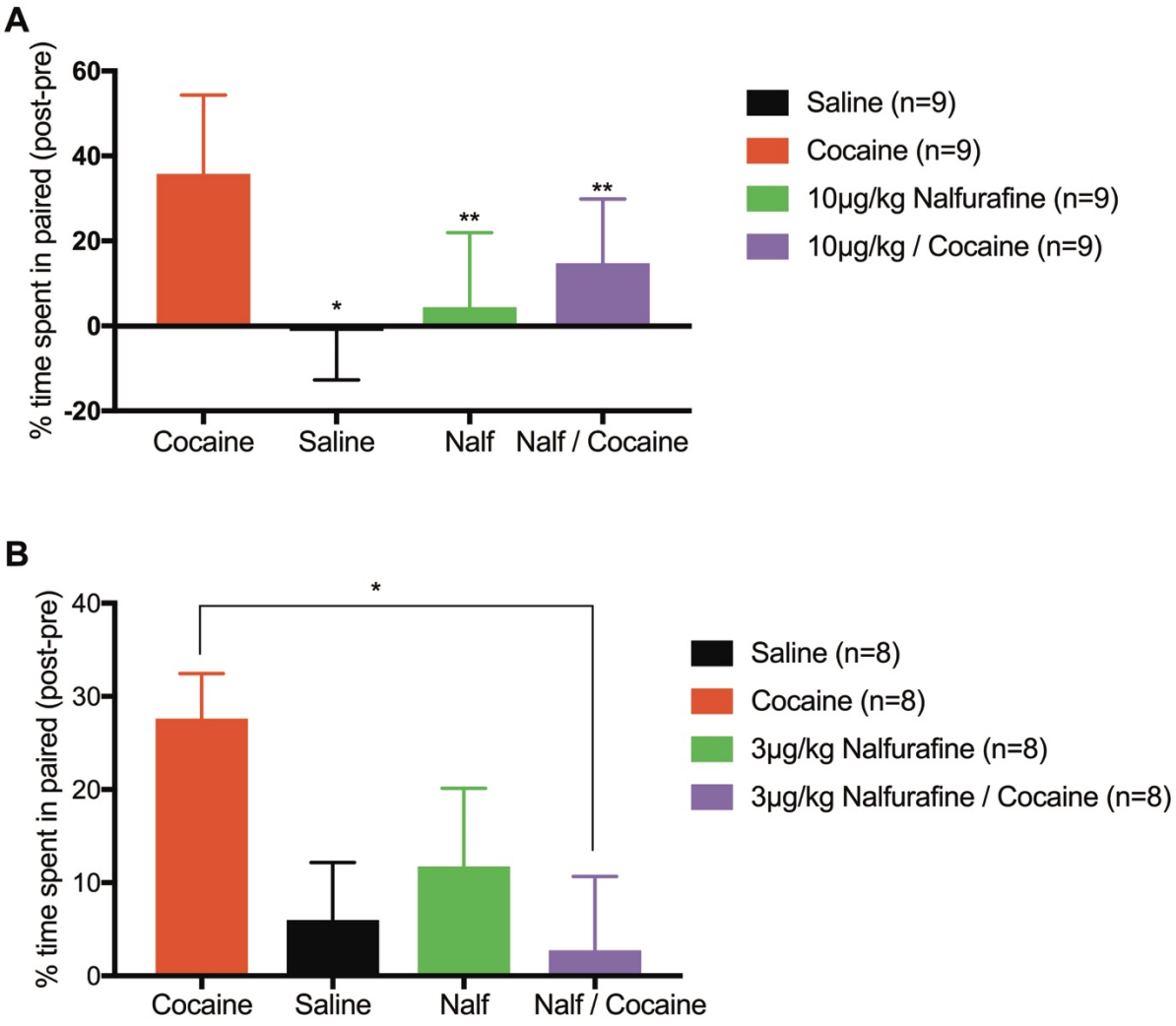

Figure 5.9. Nalfurafine blockade of cocaine-conditioned place preference. A. Mice were treated with 10µg/kg nalfurafine or saline, and then 15 minutes later treated with 15mg/kg cocaine or saline before immediately being placed in appropriate conditioning chambers for 30 minutes. 4 total conditioning sessions were done, 2 in each box, across 2 days. Two-way ANOVA (Nalfurafine Pretreatment x Cocaine Treatment) revealed significant effect of Cocaine Treatment ($F(1,32) = 22.59$, $p < 0.0001$) but not Nalfurafine Pretreatment ($F(1,32) = 1.68$), as well as a significant Cocaine x Nalfurafine interaction ($F(1,32) = 9.01$, $p < 0.01$). Post-hoc Newman-Keuls analysis revealed significant differences between Saline/Cocaine and

Nalfurafine/Cocaine (**p < 0.005), Nalfurafine/Saline (**p < 0.005) and Saline/Saline (***p < 0.0005) and no differences between other groups. B. Mice were treated with 3μg/kg nalfurafine or saline, and then with 15mg/kg cocaine or saline using identical methods. Two-way ANOVA (Nalfurafine Pretreatment x Cocaine Treatment) revealed no significant effect of Cocaine Treatment ($F(1,28) = 2.06$) or Nalfurafine Pretreatment alone ($F(1,28) = 1.88$), however there was a significant Cocaine x Nalfurafine interaction ($F(1,24) = 5.22$, $p < 0.05$). Post-hoc Newman-Keuls analysis revealed significant difference between Saline/Cocaine and Nalfurafine/Cocaine (*p<0.05).

5.3.2 Effect of KOR agonists on cocaine self-administration after acquisition

Effects of these lower doses of U50,488 and nalfurafine were tested in a model of intravenous cocaine self-administration in mice as well. After 7 days of cocaine self-administration, at 0.5mg/kg/infusion for 2 hours on an FR1 schedule, mice were reliably self-administering cocaine at a mean dose of 12mg/kg over the 2 hour sessions (Figure 5.10). When mice were then immediately pretreated with a subcutaneous injection of 3mg/kg U50,488 or saline before self-administration sessions, the U50,488-treated mice increased cocaine intake (Figure 5.10). Similarly, a pretreatment of 10μg/kg nalfurafine caused an apparent increase in cocaine intake in the same paradigm. A 15 minute pretreatment with 3mg/kg of the antagonist LY2444296 before the nalfurafine injection blocked this effect, suggesting that it is KOR-mediated (Figure 5.11). Although the nalfurafine-treated group was only statistically significant compared to the LY/Saline control group on one day, this trend persisted over 7 consecutive days (Figure 5.11). In the same paradigm, pretreatment with a smaller dose of 3μg/kg nalfurafine alone had no effect on cocaine self-administration compared to saline, demonstrating a dose-dependent profile of this KOR agonist (Figure 5.12).

Figure 5.10. Effect of U50,488 on cocaine IVSA in mice, after acquisition. Mice intravenously self-administered 0.5mg/kg/infusion cocaine under an FR1 schedule for 2 hours daily until acquisition was stable (<20% variation across two consecutive days) and >70% of total nose pokes were in the active hole. Mice were injected with 3mg/kg U50,488 or saline immediately before IVSA sessions on pretreatment days. A. Daily cocaine intake. Two-way ANOVA (Treatment x Time), with repeated measures on Time, revealed a significant effect of Treatment ($F(1,12) = 5.84$, $p < 0.05$) and Time ($F(8,96) = 15.78$, $p < 0.0001$) but no interaction ($F(8,96) = 1.49$). Sidak's multiple comparison test for each day revealed a significant difference between Saline and U50,488-treated groups on Day 8 (*$p < 0.05$). B. Average cocaine intake during the pretreatment days (Days 8 and 9).

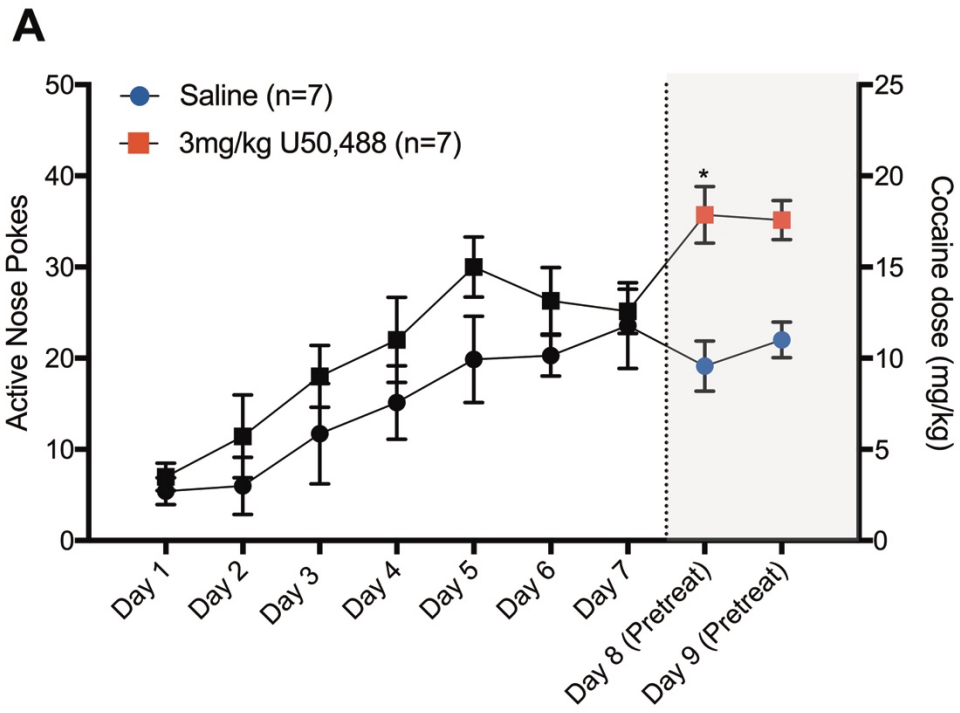
A
Saline (n=7)
3mg/kg U50,488 (n=7)
Active Nose Pokes
Cocaine dose (mg/kg)
*
Day 1
Day 2
Day 3
Day 4
Day 5
Day 6
Day 7
Day 8 (Pretreat)
Day 9 (Pretreat)

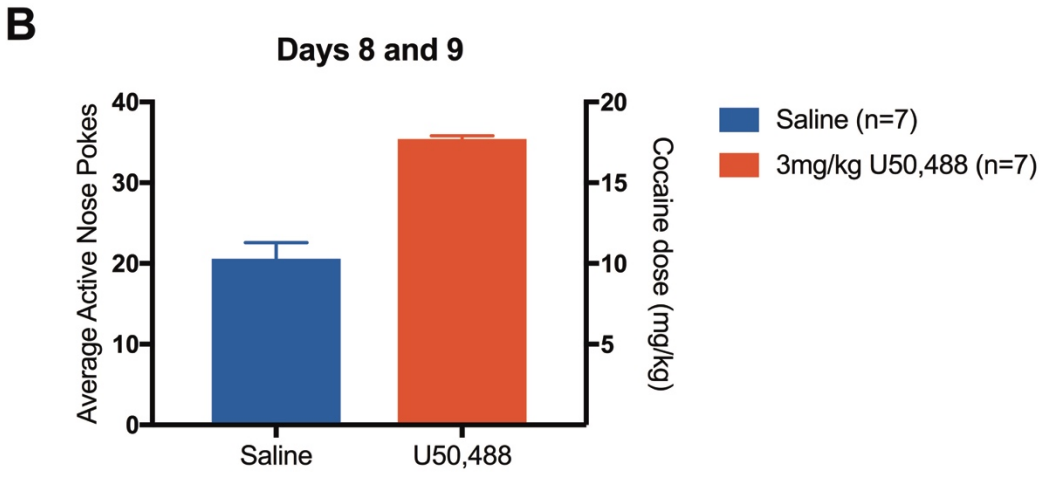
B
Days 8 and 9
Average Active Nose Pokes
Cocaine dose (mg/kg)
Saline
U50,488
Saline (n=7)
3mg/kg U50,488 (n=7)

Figure 5.11. Effect of 10μg/kg nalfurafine on cocaine IVSA in mice, after acquisition. Mice intravenously self-administered 0.5mg/kg/infusion cocaine under an FR1 schedule for 2 hours daily until acquisition was stable (<20% variation across two consecutive days) and >70% of total nose-pokes were in the active hole. Mice were injected with 3mg/kg LY2444296 or vehicle, and then 15 minutes later injected with 10μg/kg nalfurafine or saline immediately before IVSA sessions on pretreatment days. A. Daily cocaine intake. Two-way ANOVA (Overall treatment condition x Time), with repeated measures on Time, revealed no overall effect of Treatment ($F(3,24) = 0.75$), but a significant effect of both Time ($F(12,288) = 7.31$, $p < 0.0001$) and Treatment x Time Interaction ($F(36,288) = 1.63$, $p < 0.05$). Sidak's multiple comparisons test for each day revealed only a significant difference between Vehicle/Nalfurafine group and the LY/Saline group on Day 11 (*$p<0.05$). B. Average cocaine intake during the pretreatment days. Two-way ANOVA (LY Pretreatment x Nalfurafine Treatment) revealed no significant effect of LY244296 pretreatment alone ($F(1,24) = 1.67$), or nalfurafine treatment alone ($F(1,24) = 2.67$), however there was a significant interaction of LY2444296 x nalfurafine ($F(1,24) = 4.71$, $p < 0.05$). Newman-Keuls post-hoc analysis revealed a significant difference between Vehicle/Nalfurafine and LY/Saline groups (*$p < 0.05$).

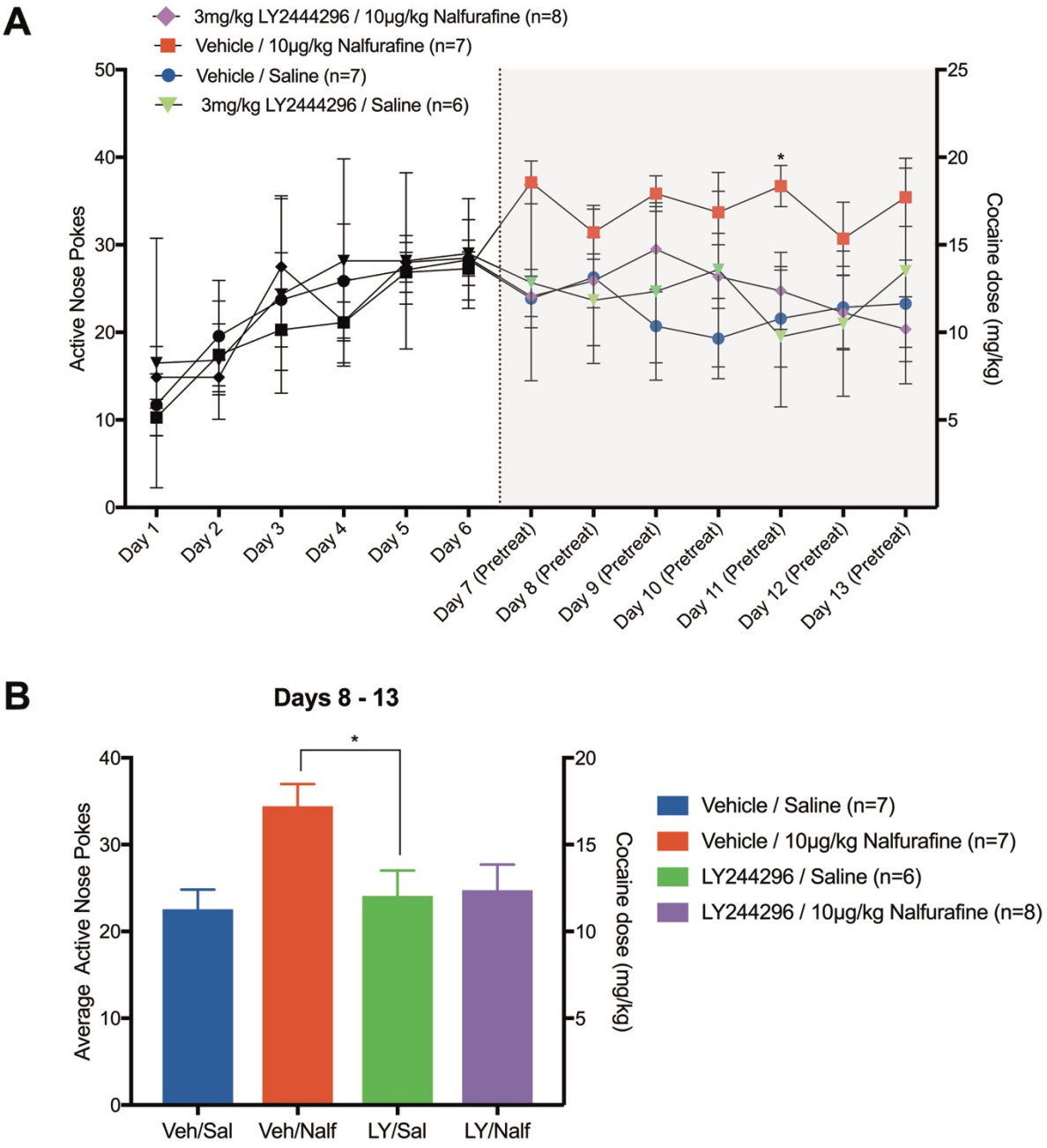
A
3mg/kg LY2444296 / 10µg/kg Nalfurafine (n=8)
Vehicle / 10µg/kg Nalfurafine (n=7)
Vehicle / Saline (n=7)
3mg/kg LY2444296 / Saline (n=6)
Active Nose Pokes
Cocaine dose (mg/kg)
0
10
20
30
40
50
5
10
15
20
25
*
Day 1
Day 2
Day 3
Day 4
Day 5
Day 6
Day 7 (Pretreat)
Day 8 (Pretreat)
Day 9 (Pretreat)
Day 10 (Pretreat)
Day 11 (Pretreat)
Day 12 (Pretreat)
Day 13 (Pretreat)
B
Days 8 - 13
Average Active Nose Pokes
Cocaine dose (mg/kg)
0
10
20
30
40
5
10
15
20
*
Veh/Sal
Veh/Nalf
LY/Sal
LY/Nalf
Vehicle / Saline (n=7)
Vehicle / 10µg/kg Nalfurafine (n=7)
LY244296 / Saline (n=6)
LY244296 / 10µg/kg Nalfurafine (n=8)

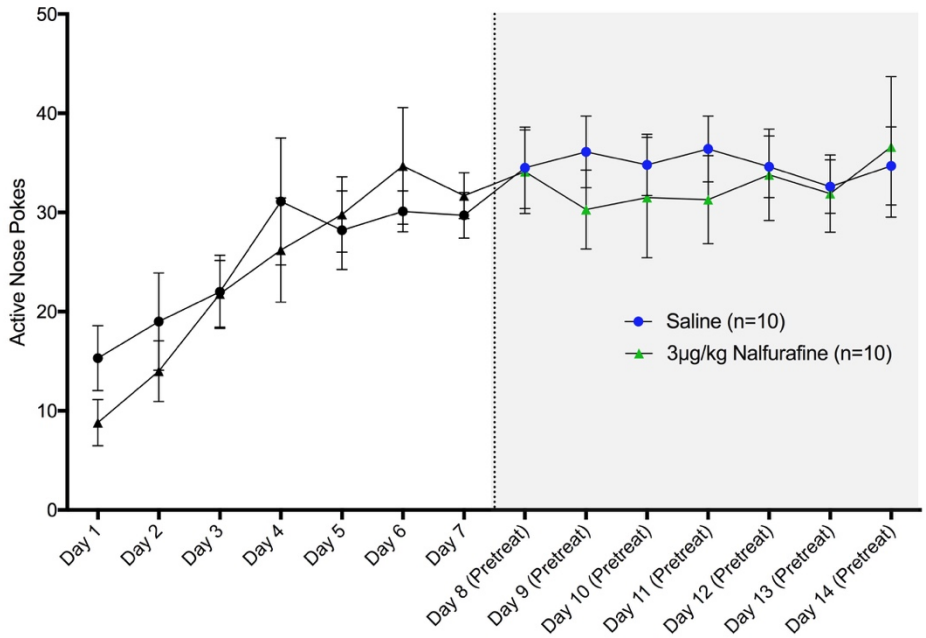

Figure 5.12. Effect of 3µg/kg nalfurafine on cocaine IVSA in mice, after acquisition. Mice intravenously self-administered 0.5mg/kg/infusion cocaine under an FR1 schedule for 2 hours daily until acquisition was stable (<20% variation across two consecutive days) and >70% of total nose-pokes were in the active hole. On pretreatment days (8-14), mice were injected with 3µg/kg nalfurafine or saline immediately before IVSA sessions. Two-way ANOVA (Treatment x Time), with repeated measures on Time, showed a significant effect of Time ($F(13,234) = 9.17$), but no effect of Treatment ($F(1,18) = 0.194$).

5.3.3 Effect of nalfurafine on acquisition of cocaine self-administration

In an additional experiment, mice were treated with 10μg/kg nalfurafine during the initial acquisition of cocaine self-administration. These mice immediately increased their intake of cocaine compared to saline-treated animals (Figure 5.13). This effect appeared to be temporary and reversible, as the nalfurafine-treated mice returned to saline-treatment levels when they received saline injections instead (Figure 5.13).

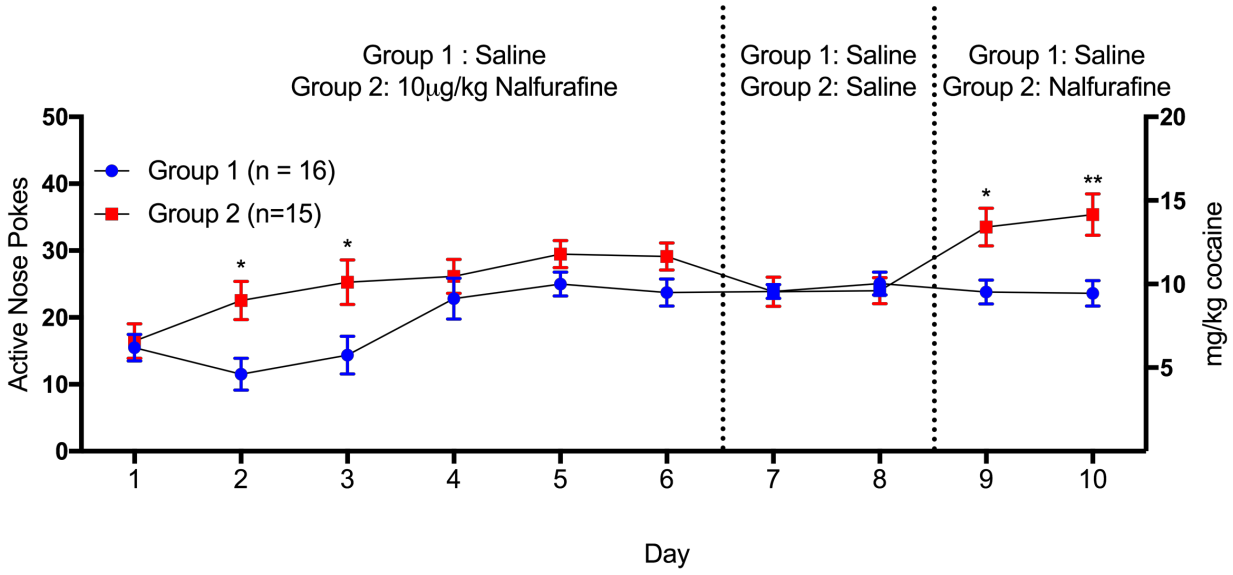

Figure 5.13. 10μg/kg nalfurafine on acquisition of cocaine IVSA in mice. Mice were given pretreatment injections of 10μg/kg nalfurafine or saline immediately before IVSA sessions for Days 1-6 and Days 9 and 10. All mice were given saline injections immediately before IVSA sessions on Days 7 and 8. IVSA sessions were 2 hours, on an FR1 schedule with 0.5mg/kg/infusion cocaine. Two-way ANOVA (Treatment x Time), with repeated measures on Time, revealed a significant effect of Treatment ($F(1,29) = 7.64$, $p<0.01$), Time ($F(9,261(=11.42$, $p<0.0001$), and interaction ($F(9,261)=3.01$, $p<0.005$). Sidak's multiple comparisons test for each day revealed significant differences between Group 1 and Group 2 (*$p<0.05$, **$p<0.005$).

5.3.4 Discussion

In these assays, both U50,488 and nalfurafine were able to modulate cocaine-related behaviors at doses that were not aversive and not sedative. The doses of 3μg/kg and 10μg/kg nalfurafine, for example, were not sedative in the rotarod assay (Figure 5.4 A and B) and did not cause aversion on their own (Figure 5.6), but were able to block cocaine-conditioned place preference (Figure 5.9). These doses of nalfurafine also caused significant prolactin release, demonstrating that nalfurafine still activated the KOR in mice at this dose (Figure 5.2 A and B). The dose of 3mg/kg of U50,488 was also able to block cocaine-induced CPP without causing aversion on its own (Figure 5.5 and Figure 5.8), suggesting that this beneficial therapeutic window, between modulation of cocaine-related behavior and aversion, may be a property of the KOR system in general and not unique to nalfurafine. This is in contrast to studies of the antinociceptive and antipruritic effects of nalfurafine and other KOR agonists, but consistent with previous CPP and self-administration studies demonstrating that anti-reward and aversive effects of KOR agonists can be uncoupled. The mechanism of this uncoupling could be related to different signaling mechanisms, as has been suggested for the uncoupling of therapeutic effects and sedation, however it is also possible that both anti-reward and aversion are mediated by dopamine inhibition downstream of the KOR and their uncoupling is a result of different thresholds.

Interestingly, both 3mg/kg U50,488 and 10μg/kg nalfurafine had opposing effects on cocaine-conditioned place preference and cocaine IVSA. At these doses, both compounds

blocked cocaine CPP, but caused significant potentiation of cocaine self-administration after mice had already acquired self-administration behavior (Figures 5.10 and 5.11). In the CPP assay, mice received a nalfurafine pre-treatment during the cocaine conditioning sessions, theoretically blunting the dopaminergic response to cocaine and the subsequent Pavlovian conditioning. In the initial self-administration experiment (Figure 5.11), mice had already learned the operant behavioral response to cocaine during the acquisition phase. When they then received KOR agonist injections, it is possible that they increased their self-administration behavior to overcome the blunting of the dopaminergic response to cocaine. We hypothesized that if mice were given KOR agonist injections during the initial acquisition phase, the effect would be similar to the CPP experiment in that the mice would not learn the operant behavioral response to cocaine.

In contrast, we found that mice treated with nalfurafine immediately prior to these initial sessions also increased their cocaine self-administration compared to saline-treated animals (Figure 5.13). Previous studies of KOR agonists like U50,488 have shown a potentiation of cocaine reward, both using CPP[18] as well as IVSA, at certain doses of cocaine. [118] Additionally, in a food vs cocaine-choice paradigm in rhesus monkeys, chronic U50,488 treatment increased responding for cocaine over food, even as it decreased responding rates overall.[119,120] This is consistent with the idea that activation of the KOR decreases the reinforcing effects of drugs of abuse like cocaine, and that increased self-administration behavior is observed as animals require additional drug administration to reach the same levels of reward and dopamine release.

The divergent effects of 3mg/kg U50,488 and 10ug/kg nalfurafine in cocaine CPP and cocaine IVSA highlight the differences between these assays. While both assays are commonly used to measure drug reward, studies have suggested that they do not measure the same reward

processes in the brain (reviewed in Bardo, 2000).[121] Certain classes of drugs, such as the hallucinogen lysergic acid diethylamide (LSD), cause CPP in rats but are not self-administered, and others, such as pentobarbitol, are self-administered but do not cause CPP. Additionally, pretreatment of animals with D2-receptor antagonists blocks the self-administration of cocaine, but not cocaine CPP, again suggesting that these behaviors involve different mechanisms.

A lower dose of 3μg/kg nalfurafine, however, blocked cocaine place preference (Figure 5.9 B) and did not cause any measurable change in cocaine self-administration (Figure 5.12). Very low doses of nalfurafine have also been effective in blocking alcohol intake in animal models, especially in combination with naltrexone, a mu opioid antagonist and kappa opioid G-protein biased partial agonist.[115] While additional experiments are necessary, these preliminary data, combined with the favorable post-marketing data from Japan, suggest that very low doses of nalfurafine could potentially be used to block drug reward. It is also possible that very low doses of U50,488 could have a similar effect, in light of the similar effects of 3mg/kg U50,488 and 10μg/kg nalfurafine. Overall, these data suggest that relatively low doses of potent KOR agonists, or possibly partial agonists, may be able to successfully modulate cocaine-related behaviors at doses that do not cause the side effects that have hampered the development of KOR agonists previously.

CHAPTER 6. CONCLUSIONS AND FUTURE DIRECTIONS

There has been a great deal of work done over the past 50 years to investigate the effects of KOR agonists both in human and animal models of diseases, including addictive diseases. Here, we have added to this work with investigations of structurally-diverse KOR agonists and their effects on different KOR signaling modalities and behaviors.

In **Chapter 3**, 21 structurally diverse KOR agonists were tested for their G-protein versus β-arrestin-2 bias using cell-based functional assays. Several compounds tested had notable bias profiles, including the relatively unbiased salvinorin compounds. The morphinan compounds were especially G-protein biased, with the exception of nalfurafine, which was among the only β-arrestin-biased compounds reported here or elsewhere in the literature. We found that using heterologous cell lines for measuring G-protein activity may not accurately reflect signaling in the disease-relevant tissue, and future studies of G-protein signaling in brain homogenate tissue will be important for accurately profiling different KOR agonists. In particular, the ligand bias of nalfurafine varies widely in the literature, depending on assay and cellular context, and measurements of signaling in the relevant tissue will be important for understanding its in vivo effects in the future.

Despite these caveats, we identified a significant correlation between in vitro β-arrestin-2 signaling, particularly the maximum efficacy in this signaling pathway, and the maximum sedative effect of KOR agonists in mice, measured by the rotarod assay. This supports previous studies that have suggested that arrestin recruitment is necessary for KOR-mediated sedation, and suggests that a G-protein biased KOR agonist may be beneficial for avoiding sedative side effects in therapeutic development. While studies in humans with non-selective G-protein biased

KOR agonists, like nalmefene and naltrexone, support this hypothesis, a KOR-selective G-protein biased agonist has not been tested in humans.

In **Chapter 4**, we investigated the effects of these diverse KOR agonists on two additional signaling pathways – ERK1/2 and mTOR. We did not find any evidence that either early G-protein or β-arrestin-2 signaling pathway directly or uniquely activated ERK1/2 or mTOR, suggesting that these pathways should be studied independently in the future. Future studies are also needed to further investigate the relationship between KOR-mediated behavior and ERK1/2 and mTOR signaling pathways. Additionally, we compared protein-receptor interactions at the KOR after activation by several different KOR ligands and found that ligand bias could affect these interactions. Future studies will focus on identifying the effect of different KOR agonists on other signaling pathways, such as 14-3-3 signaling, as well as the role of these pathways and proteins in KOR-mediated effects in vivo.

In **Chapter 5**, we examined the effects of pharmacologically distinct KOR agonists on behaviors in mice. In particular, we found that the extremely G-protein biased agonist BPHA was still able to cause aversion, but not sedation, at high doses. We also investigated the effects of nalfurafine – the only KOR-selective agonist to be used clinically in humans, albeit only in Japan currently. We found that nalfurafine could block cocaine-reward without causing aversion at very low doses (3μg/kg), and that slightly higher doses (10μg/kg) caused an increase in cocaine intake – likely as compensation for decreasing the reinforcing effects of cocaine. Similar results with a low dose of 3mg/kg U50,488 suggests that decreasing the reinforcing effects of cocaine may be a feature of KOR activation, and not unique to nalfurafine. These data suggest that a very low dose of a potent KOR agonist, or perhaps a partial agonist, could be effective for modulating cocaine reward without causing aversive or sedative side effects. Additional

experiments in preclinical models, and likely humans, are needed to determine how to translate this effect into a desirable therapeutic response.

KOR agonists have been shown previously to both block and potentiate the rewarding and reinforcing effects of drugs of abuse like cocaine. It is apparent that the KOR system is involved in drug-related behaviors and reward, however the side effects such as sedation, aversion and hallucinations have prevented KOR agonists from being tested in humans for this indication. While the psychotomimetic effects of KOR agonists can't be tested in animal models, our data suggest that some of these side effects could be avoided by very low doses of KOR agonists, or agonists with specific pharmacological profiles, while still affecting the rewarding properties of cocaine. It is also likely that future studies investigating the effects of other signaling pathways, such as ERK1/2, mTOR or 14-3-3, could help to further narrow down a pharmacological profile for a KOR agonist with fewer side effects. These data also support the idea, first proposed by the Kreek lab, that a KOR-selective partial agonist could be used for the treatment of cocaine addiction. The development of novel KOR agonists, including partial agonists, agonists with unique signaling profiles and very potent agonists, will be essential for testing these hypotheses in the future.

BIBLIOGRAPHY

1. Kreek, M. J., LaForge, K. S. & Butelman, E. Pharmacotherapy of addictions. *Nat. Rev. Drug Discov.* **1**, 710–726 (2002).
2. Pert, C. B. & Snyder, S. H. Opiate receptor: demonstration in nervous tissue. *Science* **179**, 1011–4 (1973).
3. Terenius, L. Characteristics of the "Receptor" for Narcotic Analgesics in Synaptic Plasma Membrane Fraction from Rat Brain. *Acta Pharmacol. Toxicol. (Copenh).* **33**, 377–384 (1973).
4. Simon, E. J., Hiller, J. M. & Edelman, I. Stereospecific binding of the potent narcotic analgesic (3H) Etorphine to rat-brain homogenate. *Proc. Natl. Acad. Sci. U. S. A.* **70**, 1947–9 (1973).
5. Portoghese, P. S. A New Concept on the Mode of Interaction of Narcotic Analgesics with Receptors. *J. Med. Chem.* **8**, 609–616 (1965).
6. Martin, W. R., Eades, C. G., Thompson, J. A., Huppler, R. E. & Gilbert, P. E. The effects of morphine- and nalorphine- like drugs in the nondependent and morphine-dependent chronic spinal dog. *J. Pharmacol. Exp. Ther.* **197**, 517–32 (1976).
7. Kosterlitz, H. W., Paterson, S. J. & Robson, L. E. Characterization of the k-subtype of the opiate receptor in the guinia pig brain. *Br. J. Pharmacol.* **73**, 939–949 (1981).
8. Lord, J. A., Waterfield, A. A., Hughes, J. & Kosterlitz, H. W. Endogenous opioid peptides: multiple agonists and receptors. *Nature* **267**, 495–9 (1977).
9. Evans, C., Keith, D., Morrison, H., Magendzo, K. & Edwards, R. Cloning of a delta opioid receptor by functional expression. *Science (80-.).* **258**, 1952–1955 (1992).
10. Kieffer, B. L., Befort, K., Gaveriaux-Ruff, C. & Hirth, C. G. The delta-opioid receptor: isolation of a cDNA by expression cloning and pharmacological characterization. *Proc. Natl. Acad. Sci.* **89**, 12048–12052 (1992).
11. Xie, G. X., Miyajima, A. & Goldstein, A. Expression cloning of cDNA encoding a seven-helix receptor from human placenta with affinity for opioid ligands. *Proc. Natl. Acad. Sci.* **89**, 4124–4128 (1992).
12. Chen, Y., Mestek, A., Liu, J., Hurley, J. A. & Yu, L. Molecular cloning and functional expression of a mu-opioid receptor from rat brain. *Mol. Pharmacol.* **44**, 8–12 (1993).
13. Wang, J. B. *et al.* mu opiate receptor: cDNA cloning and expression. *Proc. Natl. Acad. Sci.* **90**, 10230–10234 (1993).
14. Darcq, E. & Kieffer, B. L. Opioid receptors: drivers to addiction? *Nat. Rev. Neurosci.* **19**, 499–514 (2018).
15. Pradhan, A. A., Befort, K., Nozaki, C., Gavériaux-Ruff, C. & Kieffer, B. L. The delta opioid receptor: an evolving target for the treatment of brain disorders. *Trends Pharmacol. Sci.* **32**, 581–90 (2011).
16. Di Chiara, G. & Imperato, A. Opposite effects of mu and kappa opiate agonists on dopamine release in the nucleus accumbens and in the dorsal caudate of freely moving rats. *J. Pharmacol. Exp. Ther.* **244**, (1988).
17. Zhang, Y., Butelman, E. R., Schlussman, S. D., Ho, A. & Kreek, M. J. Effect of the endogenous κ opioid agonist dynorphin A(1-17) on cocaine-evoked increases in striatal dopamine levels and cocaine-induced place preference in C57BL/6J mice. *Psychopharmacology (Berl).* **172**, 422–429 (2004).
18. McLaughlin, J. P., Land, B. B., Li, S., Pintar, J. E. & Chavkin, C. Prior Activation of

Kappa Opioid Receptors by U50,488 Mimics Repeated Forced Swim Stress to Potentiate Cocaine Place Preference Conditioning. *Neuropsychopharmacology* **31**, 787–794 (2006).
19. McLaughlin, J. P., Marton-Popovici, M. & Chavkin, C. Kappa opioid receptor antagonism and prodynorphin gene disruption block stress-induced behavioral responses. *J. Neurosci.* **23**, 5674–83 (2003).
20. Wang, X.-M. *et al.* Acute intermittent morphine increases preprodynorphin and kappa opioid receptor mRNA levels in the rat brain. *Mol. Brain Res.* **66**, 184–187 (1999).
21. Spangler, R., Unterwald, E. M. & Kreek, M. J. 'Binge' cocaine administration induces a sustained increase of prodynorphin mRNA in rat caudate-putamen. *Mol. Brain Res.* **19**, 323–327 (1993).
22. Unterwald, E. M., Rubenfeld, J. M. & Kreek, M. J. Repeated cocaine administration upregulates kappa and mu, but not delta, opioid receptors. *Neuroreport* **5**, 1613–6 (1994).
23. Hurd, Y. L. & Herkenham, M. Molecular alterations in the neostriatum of human cocaine addicts. *Synapse* **13**, 357–69 (1993).
24. Banks, M. L. The Rise and Fall of Kappa-Opioid Receptors in Drug Abuse Research. *Handb. Exp. Pharmacol.* (2019). doi:10.1007/164_2019_268
25. Sperling, R. E., Gomes, S. M., Sypek, E. I., Carey, A. N. & McLaughlin, J. P. Endogenous kappa-opioid mediation of stress-induced potentiation of ethanol-conditioned place preference and self-administration. *Psychopharmacology (Berl).* **210**, 199–209 (2010).
26. Pande, A. C. *et al.* Analgesic efficacy of the kappa-receptor agonist, enadoline, in dental surgery pain. *Clin. Neuropharmacol.* **19**, 92–7 (1996).
27. Pande, A. C. *et al.* Analgesic Efficacy of Enadoline Versus Placebo or Morphine in Postsurgical Pain. *Clin. Neuropharmacol.* **19**, 451–456 (1996).
28. Wadenberg, M.-L. G. A review of the properties of spiradoline: a potent and selective kappa-opioid receptor agonist. *CNS Drug Rev.* **9**, 187–98 (2003).
29. Sheffler, D. J. & Roth, B. L. Salvinorin A: the 'magic mint' hallucinogen finds a molecular target in the kappa opioid receptor. *Trends Pharmacol. Sci.* **24**, 107–109 (2003).
30. Chavkin, C. *et al.* Salvinorin A, an active component of the hallucinogenic sage salvia divinorum is a highly efficacious kappa-opioid receptor agonist: structural and functional considerations. *J. Pharmacol. Exp. Ther.* **308**, 1197–203 (2004).
31. MacLean, K. A., Johnson, M. W., Reissig, C. J., Prisinzano, T. E. & Griffiths, R. R. Dose-related effects of salvinorin A in humans: dissociative, hallucinogenic, and memory effects. *Psychopharmacology (Berl).* **226**, 381–92 (2013).
32. Bart, G. *et al.* Nalmefene Induced Elevation in Serum Prolactin in Normal Human Volunteers: Partial Kappa Opioid Agonist Activity? *Neuropsychopharmacology* **30**, 2254–2262 (2005).
33. Windisch, K. A., Reed, B. & Kreek, M. J. Naltrexone and nalmefene attenuate cocaine place preference in male mice. *Neuropharmacology* **140**, 174–183 (2018).
34. Dunn, A. D., Reed, B., Erazo, J., Ben-Ezra, A. & Kreek, M. J. Signaling Properties of Structurally Diverse Kappa Opioid Receptor Ligands: Toward in Vitro Models of in Vivo Responses. *ACS Chem. Neurosci.* **10**, 3590–3600 (2019).
35. Schattauer, S. S., Kuhar, J. R., Song, A. & Chavkin, C. Nalfurafine is a G-protein biased agonist having significantly greater bias at the human than rodent form of the kappa opioid receptor. *Cell. Signal.* **32**, 59–65 (2017).
36. Liu, J. J. *et al.* Phosphoproteomic approach for agonist-specific signaling in mouse brains:

mTOR pathway is involved in κ opioid aversion. *Neuropsychopharmacology* **44**, 939–949 (2019).
37. Kozono, H., Yoshitani, H. & Nakano, R. Post-marketing surveillance study of the safety and efficacy of nalfurafine hydrochloride (Remitch® capsules 2.5 μg) in 3,762 hemodialysis patients with intractable pruritus. *Int. J. Nephrol. Renovasc. Dis.* **Volume 11**, 9–24 (2018).
38. Nakao, K. *et al.* Nalfurafine hydrochloride, a selective κ opioid receptor agonist, has no reinforcing effect on intravenous self-administration in rhesus monkeys. *J. Pharmacol. Sci.* **130**, 8–14 (2016).
39. Liu, J. J. *et al.* In vivo brain GPCR signaling elucidated by phosphoproteomics. *Science (80-.).* **360**, eaao4927 (2018).
40. Carroll, F. I., Carlezon, W. A. & Jr. Development of κ opioid receptor antagonists. *J. Med. Chem.* **56**, 2178–95 (2013).
41. Reed, B., Butelman, E. R., Fry, R. S., Kimani, R. & Kreek, M. J. Repeated Administration of Opra Kappa (LY2456302), a Novel, Short-Acting, Selective KOP-r Antagonist, in Persons with and without Cocaine Dependence. *Neuropsychopharmacology* **43**, 739–750 (2018).
42. Jones, J. D. *et al.* A randomized, double-blind, placebo-controlled study of the kappa opioid receptor antagonist, CERC-501, in a human laboratory model of smoking behavior. *Addict. Biol.* e12799 (2019). doi:10.1111/adb.12799
43. Kreek, M. J. Opiate and Cocaine Addictions: Challenge for Pharmacotherapies. *Pharmacol. Biochem. Behav.* **57**, 551–569 (1997).
44. Raehal, K. M., Walker, J. K. L. & Bohn, L. M. Morphine Side Effects in β-Arrestin 2 Knockout Mice. *J. Pharmacol. Exp. Ther.* **314**, 1195–1201 (2005).
45. Manglik, A. *et al.* Structure-based discovery of opioid analgesics with reduced side effects. *Nature* **537**, 185–190 (2016).
46. Schmid, C. L. *et al.* Bias Factor and Therapeutic Window Correlate to Predict Safer Opioid Analgesics. *Cell* **171**, 1165-1175.e13 (2017).
47. Groer, C. E. *et al.* An Opioid Agonist that Does Not Induce μ-Opioid Receptor—Arrestin Interactions or Receptor Internalization. *Mol. Pharmacol.* **71**, 549–557 (2007).
48. Singla, N. *et al.* A randomized, phase IIb study investigating oliceridine (TRV130), a novel μ-receptor G-protein pathway selective (μ-GPS) modulator, for the management of moderate to severe acute pain following abdominoplasty. *J. Pain Res.* **10**, 2413–2424 (2017).
49. Viscusi, E. R. *et al.* A randomized, phase 2 study investigating TRV130, a biased ligand of the -opioid receptor, for the intravenous treatment of acute pain. *Pain* **157**, 264–272 (2015).
50. Mores, K. L., Cummins, B. R., Cassell, R. J. & van Rijn, R. M. A Review of the Therapeutic Potential of Recently Developed G Protein-Biased Kappa Agonists. *Front. Pharmacol.* **10**, 407 (2019).
51. White, K. L. *et al.* The G Protein – Biased k -Opioid Receptor Agonist RB-64 Is Analgesic with a Unique Spectrum of Activities In Vivo. 98–109 (2015).
52. Brust, T. F. *et al.* Biased agonists of the kappa opioid receptor suppress pain and itch without causing sedation or dysphoria. *Sci. Signal.* **117**, 1–12 (2016).
53. Rives, M. L., Rossillo, M., Liu-Chen, L. Y. & Javitch, J. A. 6′-Guanidinonaltrindole (6′-GNTI) is a G protein-biased κ-opioid receptor agonist that inhibits arrestin recruitment. *J.*

Biol. Chem. **287**, 27050–27054 (2012).
54. DiMattio, K. M., Ehlert, F. J. & Liu-Chen, L.-Y. Intrinsic relative activities of κ opioid agonists in activating Gα proteins and internalizing receptor: Differences between human and mouse receptors. *Eur. J. Pharmacol.* **761**, 235–44 (2015).
55. Schattauer, S. S. *et al.* Ligand directed signaling differences between rodent and human κ-opioid receptors. *J. Biol. Chem.* **287**, 41595–607 (2012).
56. Kenakin, T., Watson, C., Muniz-Medina, V., Christopoulos, A. & Novick, S. A simple method for quantifying functional selectivity and agonist bias. *ACS Chem. Neurosci.* **3**, 193–203 (2012).
57. Black, J. W. & Leff, P. Operational Models of Pharmacological Agonism. *Proc. R. Soc. B Biol. Sci.* **220**, 141–162 (1983).
58. Bruchas, M. R. *et al.* Selective p38α MAPK deletion in serotonergic neurons produces stress resilience in models of depression and addiction. *Neuron* **71**, 498–511 (2011).
59. Ehrich, J. M. *et al.* Kappa Opioid Receptor-Induced Aversion Requires p38 MAPK Activation in VTA Dopamine Neurons. *J. Neurosci.* **35**, 12917–31 (2015).
60. Melief, E. J. *et al.* Duration of action of a broad range of selective κ-opioid receptor antagonists is positively correlated with c-Jun N-terminal kinase-1 activation. *Mol. Pharmacol.* **80**, 920–9 (2011).
61. Kivell, B. *et al.* Salvinorin A regulates dopamine transporter function via a kappa opioid receptor and ERK1/2-dependent mechanism. *Neuropharmacology* **86**, 228–40 (2014).
62. Lovell, K. M. *et al.* Structure-activity relationship studies of functionally selective kappa opioid receptor agonists that modulate ERK 1/2 phosphorylation while preserving G protein over βarrestin2 signaling bias. *ACS Chem. Neurosci.* **6**, 1411–9 (2015).
63. Stoeber, M. *et al.* A Genetically Encoded Biosensor Reveals Location Bias of Opioid Drug Action. *Neuron* **98**, 963-976.e5 (2018).
64. Spetea, M., Berzetei-Gurske, I. P., Guerrieri, E. & Schmidhammer, H. Discovery and Pharmacological Evaluation of a Diphenethylamine Derivative (HS665), a Highly Potent and Selective κ Opioid Receptor Agonist. *J. Med. Chem.* **55**, 10302–10306 (2012).
65. Bourgeois, C. *et al.* Synthesis and Pharmacological Evaluation of 5-Pyrrolidinylquinoxalines as a Novel Class of Peripherally Restricted κ-Opioid Receptor Agonists. *J. Med. Chem.* **57**, 6845–6860 (2014).
66. Bohn, L. M., Zhou, L. & Ho, J.-H. Approaches to Assess Functional Selectivity in GPCRs: Evaluating G Protein Signaling in an Endogenous Environment. *Methods Mol. Biol.* **1335**, 177–89 (2015).
67. Aksamitiene, E., Hoek, J. B., Kholodenko, B. & Kiyatkin, A. Multistrip Western blotting to increase quantitative data output. *Electrophoresis* **28**, 3163–73 (2007).
68. Ehlert, F. J. Analysis of Allosterism in Functional Assays. *J. Pharmacol. Exp. Ther.* **315**, 740–754 (2005).
69. Ehlert, F. J. On the analysis of ligand-directed signaling at G protein-coupled receptors. in *Naunyn-Schmiedeberg's Archives of Pharmacology* **377**, 549–577 (2008).
70. Kenakin, T. & Christopoulos, A. Signalling bias in new drug discovery: detection, quantification and therapeutic impact. *Nat. Rev. Drug Discov.* **12**, 205–16 (2013).
71. Stahl, E. L., Zhou, L., Ehlert, F. J. & Bohn, L. M. A novel method for analyzing extremely biased agonism at G protein-coupled receptors. *Mol. Pharmacol.* **87**, 866–77 (2015).
72. Shevchenko, A., Tomas, H., Havlis, J., Olsen, J. V & Mann, M. In-gel digestion for mass spectrometric characterization of proteins and proteomes. *Nat. Protoc.* **1**, 2856–2860

(2006).
73. Cox, J. & Mann, M. MaxQuant enables high peptide identification rates, individualized p.p.b.-range mass accuracies and proteome-wide protein quantification. *Nat. Biotechnol.* **26**, 1367–1372 (2008).
74. Rankovic, Z., Brust, T. F. & Bohn, L. M. Biased agonism: An emerging paradigm in GPCR drug discovery. *Bioorg. Med. Chem. Lett.* **26**, 241–250 (2016).
75. Jamshidi, R. J. *et al.* Functional selectivity of kappa opioid receptor agonists in peripheral sensory neurons. *J. Pharmacol. Exp. Ther.* **355**, 174–82 (2015).
76. Naqvi, T., Haq, W. & Mathur, K. B. Structure–activity relationship studies of dynorphin A and related peptides. *Peptides* **19**, 1277–1292 (1998).
77. Chavkin, C. Dynorphin-Still an Extraordinarily Potent Opioid Peptide. *Mol. Pharmacol.* **83**, 729–736 (2013).
78. Wang, Y. *et al.* Comparison of pharmacological activities of three distinct kappa ligands (Salvinorin A, TRK-820 and 3FLB) on kappa opioid receptors in vitro and their antipruritic and antinociceptive activities in vivo. *J. Pharmacol. Exp. Ther.* **312**, 220–30 (2005).
79. Simonson, B. *et al.* Pharmacology and anti-addiction effects of the novel κ opioid receptor agonist Mesyl Sal B, a potent and long-acting analogue of salvinorin A. *Br. J. Pharmacol.* **172**, 515–531 (2015).
80. Vonvoigtlander, P. F., Lahti, R. A. & Ludens, J. H. U-50,488: a selective and structurally novel non-Mu (kappa) opioid agonist. *J. Pharmacol. Exp. Ther.* **224**, (1983).
81. Bidlack, J. M. *et al.* In Vitro Pharmacological Characterization of Buprenorphine, Samidorphan, and Combinations Being Developed as an Adjunctive Treatment of Major Depressive Disorder. *J. Pharmacol. Exp. Ther.* **367**, 267–281 (2018).
82. Falcon, E. *et al.* Antidepressant-like Effects of Buprenorphine are Mediated by Kappa Opioid Receptors. *Neuropsychopharmacology* **41**, 2344–2351 (2016).
83. Béguin, C. *et al.* Differential signaling properties at the kappa opioid receptor of 12-epi-salvinorin A and its analogues. *Bioorg. Med. Chem. Lett.* **22**, 1023–6 (2012).
84. Bourgeois, C., Werfel, E., Schepmann, D. & Wünsch, B. Combination of cyclohexane and piperazine based κ-opioid receptor agonists: Synthesis and pharmacological evaluation of trans,trans-configured perhydroquinoxalines. *Bioorganic Med. Chem.* **22**, 3316–3324 (2014).
85. Erli, F. *et al.* Highly Potent and Selective New Diphenethylamines Interacting with the κ-Opioid Receptor: Synthesis, Pharmacology, and Structure-Activity Relationships. *J. Med. Chem.* **60**, 7579–7590 (2017).
86. Dunn, A. D. *et al.* Structurally related kappa opioid receptor agonists with substantial differential signaling bias: Neuroendocrine and behavioral effects in C57BL6 Mice. *Int. J. Neuropsychopharmacol.* **21**, 847–857 (2018).
87. Spetea, M. *et al.* Selective κ receptor partial agonist HS666 produces potent antinociception without inducing aversion after i.c.v. administration in mice. *Br. J. Pharmacol.* **174**, 2444–2456 (2017).
88. Lutz, P.-E. & Kieffer, B. L. Opioid receptors: distinct roles in mood disorders. *Trends Neurosci.* **36**, 195–206 (2013).
89. Nickolls, S. A., Humphreys, S., Clark, M. & McMurray, G. Co-Expression of GRK2 Reveals a Novel Conformational State of the μ-Opioid Receptor. *PLoS One* **8**, e83691 (2013).

90. Mason, B. J., Salvato, F. R., Williams, L. D., Ritvo, E. C. & Cutler, R. B. A Double-blind, Placebo-Controlled Study of Oral Nalmefene for Alcohol Dependence. *Arch. Gen. Psychiatry* **56**, 719 (1999).
91. Chiang, T., Sansuk, K. & van Rijn, R. M. β-Arrestin 2 dependence of δ opioid receptor agonists is correlated with alcohol intake. *Br. J. Pharmacol.* **173**, 332–43 (2016).
92. Bruchas, M. R. & Chavkin, C. Kinase cascades and ligand-directed signaling at the kappa opioid receptor. *Psychopharmacology* **209**, 137–147 (2010).
93. Lu, L., Koya, E., Zhai, H., Hope, B. T. & Shaham, Y. Role of ERK in cocaine addiction. *Trends Neurosci.* **29**, 695–703 (2006).
94. Lipton, J. O. & Sahin, M. The Neurology of mTOR. *Neuron* **84**, 275–291 (2014).
95. Kivell, B. *et al.* Kappa Opioid Receptor Agonist Mesyl Sal B Attenuates Behavioral Sensitization to Cocaine with Fewer Aversive Side-Effects than Salvinorin A in Rodents. *Molecules* **23**, 2602 (2018).
96. McLennan, G. P. *et al.* Kappa opioids promote the proliferation of astrocytes via Gβγ and β-arrestin 2-dependent MAPK-mediated pathways. *J. Neurochem.* **107**, 1753–1765 (2008).
97. Luttrell, L. M. *et al.* Manifold roles of β-arrestins in GPCR signaling elucidated with siRNA and CRISPR/Cas9. *Sci. Signal.* **11**, eaat7650 (2018).
98. Georgoussi, Z., Georganta, E.-M. & Milligan, G. The other side of opioid receptor signalling: regulation by protein-protein interaction. *Curr. Drug Targets* **13**, 80–102 (2012).
99. Mellacheruvu, D. *et al.* The CRAPome: a contaminant repository for affinity purification–mass spectrometry data. *Nat. Methods* **10**, 730–736 (2013).
100. Yuan, L. *et al.* 14-3-3 signal adaptor and scaffold proteins mediate GPCR trafficking. *Sci. Rep.* **9**, 11156 (2019).
101. Li, J.-G., Chen, C., Huang, P., Wang, Y. & Liu-Chen, L.-Y. 14-3-3 Protein Regulates Anterograde Transport of the Human κ-Opioid Receptor (hKOPR). *J. Biol. Chem.* **287**, 37778–37792 (2012).
102. Xiao, K. *et al.* Global phosphorylation analysis of beta-arrestin-mediated signaling downstream of a seven transmembrane receptor (7TMR). *Proc. Natl. Acad. Sci. U. S. A.* **107**, 15299–304 (2010).
103. Xiao, K. *et al.* Functional specialization of beta-arrestin interactions revealed by proteomic analysis. *Proc. Natl. Acad. Sci. U. S. A.* **104**, 12011–6 (2007).
104. Lobingier, B. T. *et al.* An Approach to Spatiotemporally Resolve Protein Interaction Networks in Living Cells. *Cell* **169**, 350-360.e12 (2017).
105. Zhang, J. & Zhou, Y. 14-3-3 Proteins in Glutamatergic Synapses. *Neural Plast.* **2018**, 8407609 (2018).
106. Torner, L. Actions of Prolactin in the Brain: From Physiological Adaptations to Stress and Neurogenesis to Psychopathology. *Front. Endocrinol. (Lausanne).* **7**, 25 (2016).
107. Petraglia, F., Vale, W. & Rivier, C. Beta-Endorphin and Dynorphin Participate in the Stress-Induced Release of Prolactin in the Rat. *Neuroendocrinology* **45**, 338–342 (1987).
108. Matton, A., Buydens, P., Finné, E., Govaerts, J. & Vanhaelst, L. Analysis of the receptor specificity of tolerance induction in stress versus opioid-related prolactin secretion in rats. *J. Endocrinol.* **128**, 281–285 (1991).
109. Bero, L. A., Lurie, S. N. & Kuhn, C. M. Early ontogeny of κ-opioid receptor regulation of prolactin secretion in the rat. *Dev. Brain Res.* **37**, 189–196 (1987).

110. Butelman, E. R. & Kreek, M. J. kappa-Opioid receptor agonist-induced prolactin release in primates is blocked by dopamine D(2)-like receptor agonists. *Eur. J. Pharmacol.* **423**, 243–9 (2001).
111. Butelman, E. R., Harris, T. J. & Kreek, M.-J. Apparent efficacy of κ-opioid receptor ligands on serum prolactin levels in rhesus monkeys. *Eur. J. Pharmacol.* **383**, 305–309 (1999).
112. Butelman, E. R. *et al.* Effects of Salvinorin A, a-Opioid Hallucinogen, on a Neuroendocrine Biomarker Assay in Nonhuman Primates with High-Receptor Homology to Humans. (2007). doi:10.1124/jpet.106.112417
113. Nagase, H. *et al.* Discovery of a structurally novel opioid kappa-agonist derived from 4,5-epoxymorphinan. *Chem. Pharm. Bull. (Tokyo).* **46**, 366–9 (1998).
114. Hasebe, K. *et al.* Possible Pharmacotherapy of the Opioid κ Receptor Agonist for Drug Dependence. *Ann. N. Y. Acad. Sci.* **1025**, 404–413 (2004).
115. Zhou, Y. & Kreek, M. J. Combination of Clinically Utilized Kappa-Opioid Receptor Agonist Nalfurafine With Low-Dose Naltrexone Reduces Excessive Alcohol Drinking in Male and Female Mice. *Alcohol. Clin. Exp. Res.* **43**, 1077–1090 (2019).
116. Townsend, E. A. *et al.* Effects of nalfurafine on the reinforcing, thermal antinociceptive, and respiratory-depressant effects of oxycodone: modeling an abuse-deterrent opioid analgesic in rats. *Psychopharmacology (Berl).* **234**, 2597–2605 (2017).
117. Mori, T., Nomura, M., Nagase, H., Narita, M. & Suzuki, T. Effects of a newly synthesized κ-opioid receptor agonist, TRK-820, on the discriminative stimulus and rewarding effects of cocaine in rats. *Psychopharmacology (Berl).* **161**, 17–22 (2002).
118. Kuzmin, A. V, Semenova, S., Gerrits, M. A. F. ., Zvartau, E. E. & Van Ree, J. M. κ-Opioid receptor agonist U50,488H modulates cocaine and morphine self-administration in drug-naive rats and mice. *Eur. J. Pharmacol.* **321**, 265–271 (1997).
119. Mello, N. K. & Negus, S. S. Effects of kappa opioid agonists on cocaine- and food-maintained responding by rhesus monkeys. *J. Pharmacol. Exp. Ther.* **286**, 812–24 (1998).
120. Stevens Negus, S. Effects of the kappa opioid agonist U50,488 and the kappa opioid antagonist nor-binaltorphimine on choice between cocaine and food in rhesus monkeys. *Psychopharmacology (Berl).* **176**, 204–213 (2004).
121. Bardo, M. T. & Bevins, R. A. Conditioned place preference: what does it add to our preclinical understanding of drug reward? *Psychopharmacology (Berl).* **153**, 31–43 (2000).